An Investigation of Drug Partitioning into Lipid Membranes using a Thickness Shear Mode Biosensor

By Matthew Reason

Thesis submitted in partial fulfilment of the requirements for the degree of Doctor of Philosophy at De Montfort University, Leicester

2003

ORIGINAL COPY TIGHTLY BOUND

PAGES 177-192 NOT

SCANNED AT THE

REQUEST OF THE

UNIVERSITY

ABSTRACT

Thickness shear mode (TSM) sensors are widely used by the electrochemical and biosensor communities for the investigation of thin films. The sensitivity of the TSM sensor to film mass and material properties has led to their use in a wide range of applications, including the study of partitioning processes. For example, Okahata et al.[1] used a simple mass-frequency relationship to successfully measure the partitioning of simple chemical molecules into phospholipid films. This project has advanced the application of TSM sensors in membrane studies by developing a novel TSM biosensor to investigate drug partitioning into the skin, while simultaneously monitoring the fluidity of the membrane. It is anticipated that this TSM biosensor will be a valuable in vitro technique for studying the interactions between the skin and drug molecules, and for investigating the mode of action of penetration modulators, such as Azone®.

Lipid films were deposited onto 8/9 MHz TSM sensors using two techniques, the first using a Langmuir-Blodgett technique and the second by spin coating. Initially, saturated fatty acids were used characterise the measurement system, later a matrix based on one developed by Moghimi et al[2] was used to mimic the intercellular lipid of the stratum corneum. Experimental frequency shifts of the coated lipid were determined from impedance spectra obtained from a Hewlett Packard E5100A network analyser. Theoretical predictions of the frequency shifts were calculated using the relationship proposed by Sauerbrey (1959)[3], which relates frequency shift to the mass loaded per unit area. Changes in the fluidity of the film are interpreted from changes in the shape of the biosensor impedance spectra.

Langmuir-Blodgett films demonstrated a linear relationship between frequency shift (mass) and the number of monolayers of lipid coated for both the arachidic acid and lipid matrix films. It was also apparent that more lipid was being coated onto the TSM sensor than expected. It is proposed that the reason for the difference was the underestimation of surface area caused by an assumption that the sensor was smooth when it actually possessed a microscopic surface roughness.

Spin coating deposited substantially more lipid onto the TSM sensor than the Langmuir-Blodgett technique, this enabled the fluidity of the film to be investigated in addition to mass. Results demonstrated that it was possible to measure an increase in membrane fluidity produced on hydration of the lipid films. A concentration dependant relationship between fluidity and the presence of the penetration enhancer Azone® was also demonstrated.

The frequency shift of the TSM sensor as ibuprofen partitioned into the lipid matrix from solution was investigated. The shift in frequency demonstrated that the membrane increased in mass with time, an indication that ibuprofen was partitioning into the lipid film.

While the results from these studies indicate that the TSM biosensor can be used to investigate the partitioning of drugs into lipid membranes and to monitor changes in the fluidity of the films, additional development is required to improve the robustness of the technique. In particular, the stability of the lipid membranes on the TSM sensor surface and the design of the flow cell require improvement.

ACKNOWLEDGEMENTS

TABLE OF CONTENTS

LIST OF FIGURES

LIST OF TABLES

LIST OF SYMBOLS

A	Area (cm^2)
c	Concentration (g cm^{-3})
c_A	Equilibrium concentration in solvent A (g cm^{-3})
c_B	Equilibrium concentration in solvent B (g cm^{-3})
C_0	Capacitor of the static arm of the BVD circuit (with capacitance C_0, F)
C_q	Static capacitance of quartz (F)
C_r	Parasitic capacitance (F)
C	Capacitor of the motional arm of the BVD circuit (with capacitance C, F)
C_1	Capacitor of the motional arm of the unloaded BVD circuit (with capacitance C_1, F)
C_2	Capacitor of the motional arm of the loaded BVD circuit (with capacitance C_2, F)
D	Diffusion coefficient (cm^{-2} s^{-1})
η_L	Viscosity of liquid (poise)
η_F	Viscosity of film (poise)
Δf	Shift in resonant frequency (Hz)
f_0	Resonant frequency of unloaded TSM sensor (Hz)
f_S	Series resonant frequency (Hz)
f_P	Parallel resonant frequency (Hz)
i	Imaginary vector
J	Flux (g cm^{-2} s^{-1})
K	Equilibrium constant
K_{em}	Electromechanical coupling factor of AT cut quartz = 0.0880 (dimensionless)
L	Inductor of the motional arm of the BVD circuit (with inductance l, H)
L_1	Inductor of the motional arm of the unloaded BVD circuit (with inductance l_1, H)
L_2	Inductor of the motional arm of the unloaded BVD circuit (with inductance l_2, H)

μ_Q — Shear modulus of AT cut quartz $= 2.947 \times 10^{11}$ dyn cm^{-2}

Δm — Change in mass per unit area (g cm^{-2})

N — Harmonic number (dimensionless)

ω — Angular frequency of resonance (Hz)

Q — Quantity of drug (g)

R — Resistor of the motional arm of the BVD circuit (with resistance R, Ω)

R_1 — Resistor of the motional arm of the unloaded BVD circuit (with resistance R_1, Ω)

R_2 — Resistor of the motional arm of the loaded BVD circuit (with resistance R_2, Ω)

ρ_L — Density of liquid (g mL^{-1})

ρ_F — Density of film (g mL^{-1})

ρ_Q — Density of AT cut quartz $= 2.651$ g cm^{-3}

t — Time (s)

x — Distance (cm)

Z — Electrical impedance (Ω)

1 INTRODUCTION

Modern medicine relies heavily on the use of drugs, developed by the pharmaceutical industry, to alleviate or counteract disease conditions. The pharmaceutical industry, in an attempt to provide the best possible products, invests large amounts of money in ensuring the drugs that it provides are efficacious.

The efficacious delivery of any drug into the body requires the breach of one or more of the biological membranes that protect the body from the environment. Such breaches are commonly achieved in one of two ways: invasive methods (e.g. injections), which bypass the barriers, or non-invasive techniques (e.g. tablets and transdermal patches) that rely on transporting the drug across the biological barrier. While invasive techniques offer fast and reproducible dosage delivery, their use is limited by patient acceptance and the difficulty of self-administration. Non-invasive techniques are the preferred dosage delivery technique for the majority of medicines.

A number of different biological barriers are targeted in the non-invasive delivery of drug molecules; commonest are the gastro-intestinal tract, lung, and skin. Of these barriers the skin is the most convenient in terms of accessibility and has the considerable benefit of avoiding passage through the hostile environment of the gastro-intestinal tract. Despite this benefits and its relative accessibility to research, drug delivery across the skin still holds a number of secrets[4]. There is scope therefore for the development of methods that provide a means for the prediction of drug passage through the skin and the investigation of dermal membrane properties.

A thickness shear mode (TSM) biosensor would allow some of these issues to be addressed. The sensitivity of TSM sensors to mass loading makes them very suitable for biosensor

applications. Sensitivity is an essential attribute for most biosensor techniques since the responses monitored are typically very small. The TSM sensor is a unique device, which enables both the determination of nanogram quantities of rigidly loaded mass and the characterisation of the material properties of viscoelastic and liquid systems[5]. These qualities would allow the measurement of very small changes in lipid membrane mass, such as those caused by the partitioning of a drug molecule, and the monitoring of changes in membrane fluidity, such as those caused by chemical penetration enhancers.

1.1 Transdermal drug delivery

1.1.1 The skin

The skin is a specialised biological membrane that performs functions vital to the survival of all mammals. One of the primary functions of skin is the protection of the body from external influences, including the exclusion of foreign chemical entities. In this regard the skin has evolved as a robust barrier system that prevents molecules entering and leaving the body. It is, therefore, a particularly difficult route by which to deliver drugs. While drug delivery across the skin presents a sizeable challenge to the formulation scientist, it does offer certain benefits if these challenges can be overcome. One notable benefit of transdermal drug delivery is that this route bypasses the 'first pass-metabolism' of the liver. First pass-metabolism refers to the absorption of a drug from the intestine whereby it enters the systemic circulation via the hepatic portal vein. From the hepatic portal vein it is transported to the liver where it immediately undergoes metabolism and sometimes inactivation. Transdermal drug delivery offers a method of avoiding this metabolic stage by delivering a drug into the systemic blood stream away from the liver.

The skin differs in composition and function from most other biological organs. The skin comprises three distinct regions: the dermis, the epidermis, and the subcutaneous tissue. The epidermis is further split into the stratum germinativum, the stratum granulosum, the stratum lucidum and the stratum corneum (Figure 1.1). It is the stratum corneum that is widely considered as the primary barrier to the transdermal delivery of most drugs[6, 7]. An understanding of the properties of this structure is therefore important in-order to predict drug penetration through the skin.
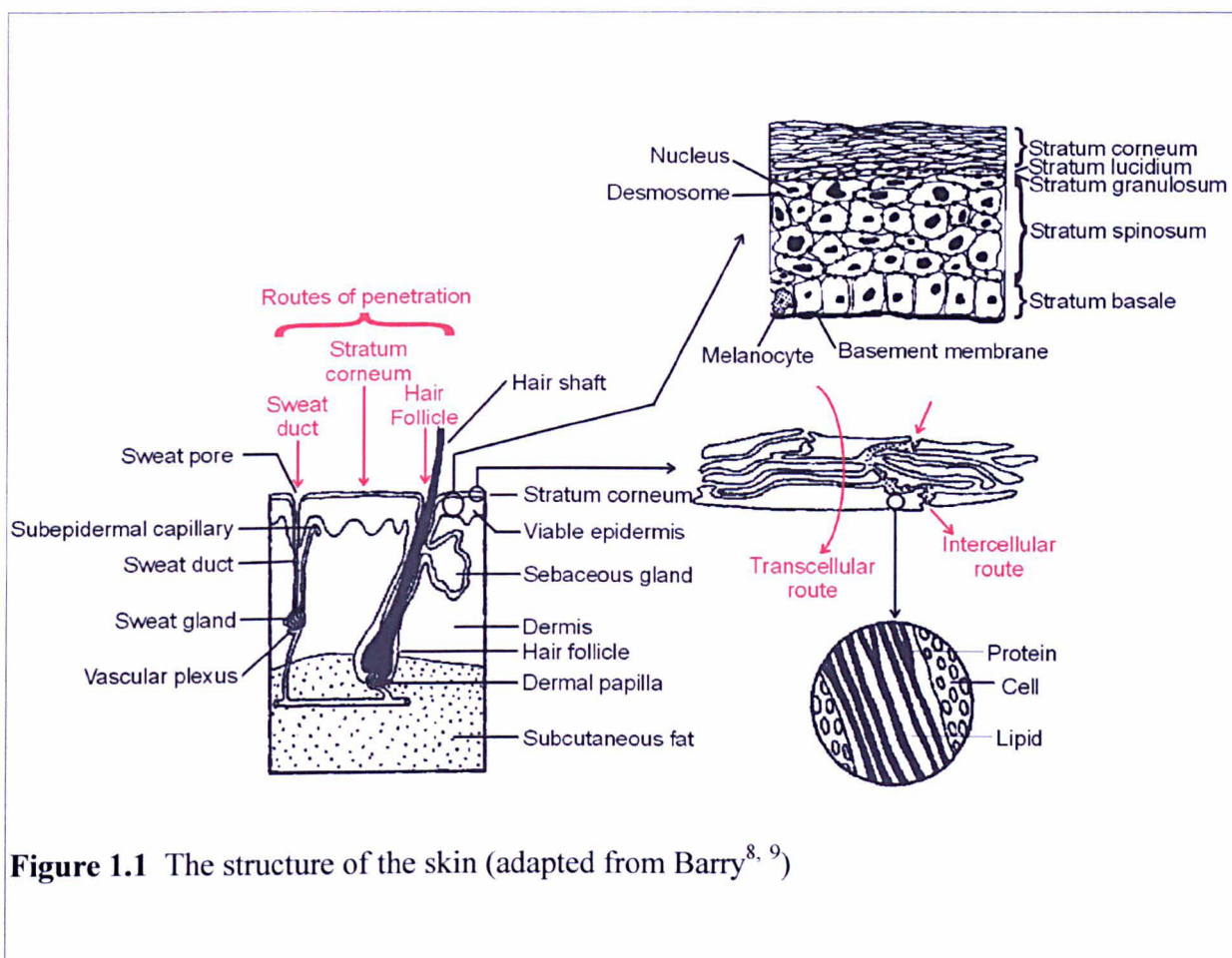
Figure 1.1 The structure of the skin (adapted from Barry[8, 9])

1.1.2 Routes of transdermal permeation

There are several potential routes by which a molecule can cross the stratum corneum and therefore breach the skin barrier (Figure 1.1), these are[8]:

1. Via skin appendages, such as the hair follicles and sweat glands. This route breaches the skin barrier by offering a route that bypasses the stratum corneum.

2. By crossing the stratum corneum, either transcellularly or intercellularly.

Of these possible routes, it is generally accepted that the intercellular route is probably the most important[10].

While the appendageal routes offer an attractive breach of the stratum corneum, allowing molecules to bypass the tortuous lipid membrane, the skin appendages occupy only approximately 0.1% of the total human skin surface[11]. The relative scarcity of the skin appendages therefore limits the amount of drug that can be delivered through them. However, in certain cases the delivery of drug molecules via the appendageal route can be significant e.g. during electroporation at medium voltages[12].

The stratum corneum therefore needs to be crossed if a steady drug flux across the skin is to be achieved. There are thought to be two possible routes of drug penetration through the stratum corneum, the intercellular route and the transcellular (intracellular) route (Figure 1.1). If a drug is to cross the stratum corneum by the transcellular route it must penetrate through both the corneocyte cells and the lipid matrix that is located between them. This route is unfavourable for most drug molecules, as it involves the migration between polar and non-polar phases. The intercellular route, though more tortuous, is believed to be the more favourable route, as the drug has only to diffuse through the intercellular lipid. It is believed that the intercellular route is the dominant method of crossing the stratum corneum for most drug molecules; some scientific evidence supports this[4].

1.1.3 Stratum corneum

The stratum corneum is an almost impermeable layer of 10-15 flattened, keratinised, dead cells (known as corneocytes) that are arranged in a highly organised, stacked formation. The cells lay tangential to the surface of the skin with their edges overlapping to form cohesive layers. Within the cells are the products of epidermal metabolism (i.e. sebaceous and sweat gland secretions). In the interstitial spaces between the corneocytes is a neutral, lipid enriched domain (called the intercellular domain) that results from the secretion of distinctive bodies in the viable epidermis (i.e. the lamellar bodies[13, 14]). The general structure of the stratum corneum has lead to it being described as a "bricks and mortar" arrangement[6], with the cells forming the bricks and the lipid forming the mortar.

Lamellar bodies are ovoid, secretary organelles that fuse with the membrane of the epithelial cell and secrete their contents prior to differentiation of the cell into a keratinocyte. The secretary vesicle contains polar lipids, proteins, and hydrolytic enzymes all of which are important in determining the final composition of the intercellular lipid. By the time the lipid mixture reaches the stratum corneum the lipids have been hydrolysed, by the action of enzymes, to a mixture of neutral lipids with abundant free sterols. In contrast to most other lipid membranes of the body the stratum corneum contains almost no phospholipid. This is unusual as phospholipids are usually present in high concentrations and are a major factor in the formation of the bilayer structure, characteristic of most of these membranes[15].

The major fractions of the stratum corneum intercellular lipid are as follows: 78% neutral lipids, 18% sphingolipids, and 4% of other lipids, including a small amount of polar lipid[16]. These lipids can be classified further into the categories: cholesterol, ceramides, free fatty acids, glycolipids, cholesteryl esters, and cholesteryl sulphate[17] (Table 1.1). Examples of

selected lipid structures are illustrated in Appendix 2. Variations in the stratum corneum do occur and are influenced by the hydration, lipid composition, and confirmation of the aliphatic chains as a function of anatomical site[7, 18].

Table 1.1 Stratum corneum lipid composition of human skin[5].

Stratum corneum lipid	Percentage composition (human skin)
Cholesteryl esters	10.0
Fatty acids	9.1
Cholesterol	26.9
Ceramide 1	3.2
Ceramide 2	8.9
Ceramide 3	4.9
Ceramide 4	6.1
Ceramide 5	5.7
Ceramide 6	12.3
Cholesteryl sulphate	1.9
Other	11.1

The arrangement of these lipids in the stratum corneum is complex. *In vivo*, most lipid membranes require phospholipid to allow the formation of a bilayer structure. However, in the case of the stratum corneum, the constituent lipids arrange themselves into multiple lamellar structures[19, 20, 21, 22], despite the almost complete absence of phospholipid. Non-polar lipid mixtures, of similar composition to stratum corneum lipids, have been shown to be capable of forming stable bilayers *in vitro*[23, 24, 25]. It is the combination of amphiphilic lipids (e.g. ceramides) and amphipathic lipids (e.g. cholesterol sulphate) in stratum corneum that allow this structure to be formed[11, 26].

The importance of the stratum corneum in transdermal drug delivery has meant that a considerable amount of work has been done to ascertain the structure and arrangement of the intercellular lipids. A range of different forms of lipid packing has been reported, demonstrating the complexity of the lipid arrangement in the stratum corneum. Two main lamellar phases have been identified in the stratum corneum with periodicities of 6 and 13nm[27, 28, 29, 30, 31] though other reflections have been reported[32]. Several different types of lipid chain packing have been reported within the stratum corneum including orthorhombic (crystalline),

hexagonal (gel) phases, and possibly a fluid phase[33, 28, 26, 34, 35, 36]. A domain mosaic model has been proposed to explain the different lipid phase present in the stratum corneum[37].

It is not only the composition and arrangement of the intercellular lipids that is important to the barrier function of the stratum corneum. Water is also an important constituent of the membrane, as the level of stratum corneum hydration has considerable influence on the permeability of skin[38].

1.1.4 Transdermal penetration enhancement

The skin, in particular the stratum corneum, is an excellent barrier to the egress of water from the body and the ingress of exogenous substances from the environment. Unfortunately, in-order to deliver a drug molecule to the systemic circulation via a transdermal route this barrier must be breached. Often enhancement of drug penetration through the skin is required, in order to achieve the desired drug flux.

A wide variety of different techniques have been investigated as a means to increase the penetration of drugs through the stratum corneum. Barry's (2001)[38] review considers some of the possible techniques for optimising this process, including: drug vehicle interactions, vesicles, particles, disruption of the stratum corneum, removal or bypassing the stratum corneum, and electrical techniques. The technique that is of most interest to this project is the modification of the stratum corneum using chemical penetration enhancers.

When a drug molecule partitions into a lipid membrane, it is almost certainly the case that the membrane is affected in some way. The inclusion of the drug molecule into the membrane has effects on the membrane structure and therefore the properties of the membrane. Chemical penetration enhancers are deliberately added to transdermal delivery formulations in order to

increase the flux of drug molecules across the skin. Barry describes them as 'substances temporarily diminishing the barrier of the skin[38].

The mechanisms by which individual enhancers work are still under investigation but can be broadly split into three groups according to the mode of action; lipid modifying, protein modifying, and partition promoting[39, 40, 41, 42].

Lipid modifying penetration enhancers function by disrupting the lipid organisation of the stratum corneum. This increases the permeability of the stratum corneum by making more free volume available for drug diffusion[38]. Alterations in the phase structure of the intercellular lipid can result in conformational changes to the lipid hydrocarbon chains, and the formation of membrane defects that increase the fluidity of the membrane and increase drug flux[11]. An increase in the number of phase boundaries between lipid domains has also been suggested as a mechanism by which drug flux can be increased, e.g. the facilitation of piroxicam by oleic acid[43]. Examples of enhancers that act by effecting the lipid packing of the stratum corneum include: water, Azone[®44], terpenes[45], fatty acids[46], DMSO, and alcohols[47].

In-order to alter the packing of the intercellular lipid, an enhancer can interact with either the polar head group or the hydrocarbon chain. Water increases the permeation of drug molecules through the stratum corneum by its action on the polar head groups[11]. Oleic acid is an example of a penetration enhancer that has its action by affecting the packing of the hydrocarbon chains of the lipid bilayers. Azone[®] is thought to affect both the packing of the polar headgroups and the hydrocarbon chains by assuming a 'soupspoon' configuration in the lipid bilayers[44].

Some enhancers interact with the keratin in the corneocytes of the stratum corneum, opening up the protein structures and therefore making them more permeable. Although the intercellular route is not normally a significant route for drug permeation, this could make it a

much more favourable permeation pathway[38]. An example of penetration enhancement that effects the keratin structures of the stratum corneum is the use of linoleic acid/ethanol and iontophoresis in the delivery of luteinizing hormone releasing factor[48].

Solvents entering the stratum corneum will alter the solvating properties of membranes; this may increase the partitioning of a second molecule into the layer. Water, ethanol, and propylene glycol are often used for this purpose[38], though some evidence suggest that other modes of action may also be important[49]. Good correlation between enhancement of solubility and permeation of 5-flurouracil has been demonstrated using a range of terpenes[50], some of this enhancement effect was also attributed to the formation of complexes.

While the mechanisms of action of penetration enhancers have been split into three separate groups, most enhancers act by a combination of effects. For example, DMSO at high concentrations will disturb the lipid bilayers, extract lipids, interact with keratin, and facilitate partioning[38].

1.1.5 Penetration enhancement using Azone®

Azone® (Figure 1.2) has been shown to increase the flux of a range of drugs through the stratum corneum including: metronidazole[61], naproxen[51], sotalol[62], and propanolol[62].
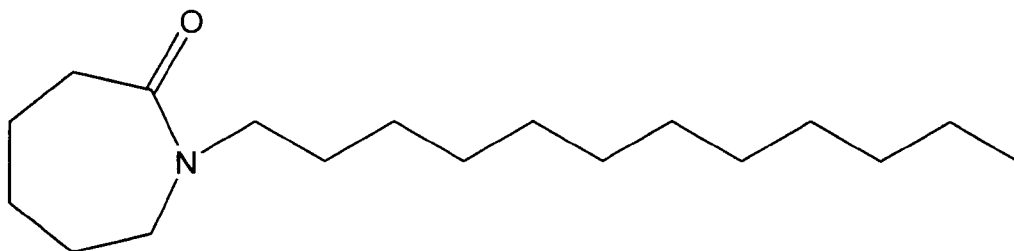
Figure 1.2 The structure of 1-dodecyl-azacycloheptan-2-one (Azone®).

The mode by which Azone® increases the penetration of these drugs, is widely considered to be by increasing the fluidity of the stratum corneum intercellular lipid, thereby decreasing its diffusional resistance to drug passage. Evidence for the increase in membrane fluidity has been demonstrated by a range of different techniques:

1. Langmuir-Blodgett monolayer studies have shown that the incorporation of Azone® into lipid monolayers resembling the stratum corneum affects the compressibility of the lipid mixture, indicating an increase in the film fluidity[52, 53]. The expansion of phospholipid monolayers by Azone® has also been reported[61]. The Langmuir-Blodgett isotherm for Azone® is shown in the work of Engbolm and Engström[54].

2. Thermal analysis of lipid systems has demonstrated that the incorporation of Azone® into bilayers reduces the phase transition temperature of those systems, indicating that it disorders the system[61]. In some cases Azone® can disrupt the lipid structure to such an extent as to make some transitions undetectable[55].

3. Fluorescence studies have shown a concentration dependant relationship between Azone® and the anisotropy of fluorescence markers, indicating a decrease in the lipid

packing order in the hydrophobic tail region of the model stratum corneum bilayers studied[62].

4. Attenuated Fourier transform infra-red (ATR-FTIR) spectroscopy has been used to investigate the method by which Azone® enhance drug passage through the stratum corneum[56]. This study showed that Azone® had only a minimal effect on the solubility of the drug in the membrane, but effected the diffusion through the membrane to a much greater extent. This evidence supports the theory that Azone® has its mode of action on the fluidity of the stratum corneum.

5. Fourier transform infra-red (FTIR) spectroscopy has provided evidence that Azone® is evenly distributed homogenously throughout the stratum corneum lipids and does not form separate phases. These studies have also provided evidence for an increase in the fluidity of the hydrocarbon region of the lipid bilayers[63].

6. Nuclear magnetic resonance studies (NMR) have also lent support to the increase in fluidity of stratum corneum lipids after the addition of Azone®.

A number of mechanisms by which Azone® could increase membrane fluidity have been suggested: It was originally hypothesised that Azone® inserted itself into the bilayers of the lipid intercellular lipid membrane in a 'soup spoon' configuration (Figure 1.3)[61], thereby disrupting the packing of the lipid[54], making it less dense and therefore more permeable to drug molecules. More recently it was suggested that the action of Azone® is due to its effects on the hydrogen bonding between lipid molecules in the stratum corneum[61]. Investigation of stratum corneum lipid organisation using x-ray microanalysis demonstrated that some changes in the stratum corneum lipids may occur on the addition of Azone®[57].
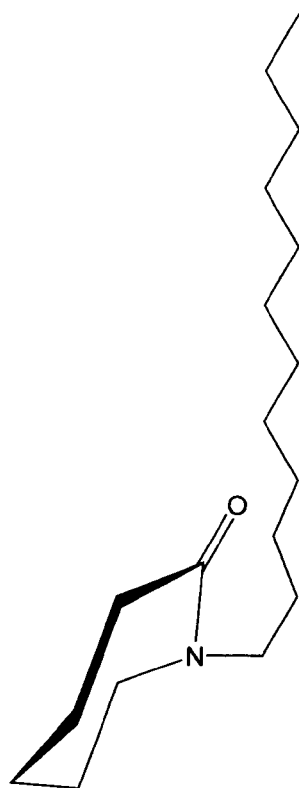
Figure 1.3 A representation of the 'soup spoon' conformation of Azone[®61].

The length of the hydrocarbon chain of the Azone[®] molecule has been shown to be critical to its action as a penetration enhancer. Analogues of Azone[®] with varying chain lengths have been investigated using differential scanning calorimetry (DSC). The data obtained indicate that the analogue with shorter chain lengths have less (or no) effect on the order of lipid membranes[61].

The increase in stratum corneum lipid fluidity that is associated with Azone[®] enhanced drug flux through the dermal membrane demonstrates the importance of membrane fluidity in

prediction of drug penetration. It is therefore important that a range of scientific techniques are available to measure membrane fluidity.

1.1.6 Membrane fluidity

The fluidity of lipid membranes can conventionally be measured by a number of different methods including:

1. Electron paramagnetic resonance (EPR) or electron spin resonance (ESR) can be used to measure the molecular dynamics of lipid membranes[58] and lipoidal delivery systems[59]. The technique measures the resonance of an unpaired electron when a magnetic field is applied to it using a microwave detector. Lipid molecules which don't contain an unpaired electron, e.g. cholesterol, can be monitored by bonding them to a chemically stable free radical. A direct relationship can be established between the spin movement and the viscosity in the area around the label[60], by altering the position of the label the fluidity of individual regions of the lipid membrane can be investigated e.g. the headgroup region[59].

2. Thermal analysis techniques e.g. differential scanning calorimetry (DSC)[55], are regularly used to measure the phase transition temperatures of lipid mixtures. Changes in the phase transition temperatures of lipid membranes can be used to infer differences in the membrane properties e.g. a change in fluidity[44], and to investigate the roles of individual membrane components.

3. Fluorescence allows the investigation of membrane fluidity using labelled markers that are introduced into the lipid system under investigation[76, 61, 62]. The probes are excited

using a spectroflurometer and the emissions measured at the maxima, changes in the emissions can be related to the fluidity of the membrane.

4. Fourier transform infrared (FT-IR) and attenuated total reflectance-Fourier transform infrared (ATR-FTIR) spectroscopy have been used to monitor the organisation and rate of motion of the lipid acyl chains of the stratum corneum[63, 64]. Changes in the frequency and bandwidth of the $C-H_2$ stretch of the IR spectrum has been used to investigate the fluidity of the stratum corneum lipids and investigate the interaction of penetration enhancers with the membrane lipids using both normal enhancers and perdeuterated analogues. The degree of membrane hydration can also be investigated using FT-IR by measuring the degree of hydrogen bonding present[65], this is also one disadvantage of FT-IR as samples with a high hydration may be difficult to measure.

5. Raman spectroscopy is a light scattering technique used to investigate lipid membrane fluidity without the need to include probes in the membrane[66] and in many ways the technique is complementary to FT-IR[67]. Conformationally dependant bands in the Raman spectrum indicate the ordered structure of the hydrocarbon chains without the water interference problems that can occur for FT-IR[68, 69].

6. ^2H NMR has been used to study the fluidity of stratum corneum lipids[70] and has also been used to investigate the mode of action of penetration enhancers[71]. The lipid or enhancer under investigation needs to be deuterated.

7. The packing and, therefore, fluidity of a monolayer can be investigated using a Langmuir-Blodgett trough [53, 72]. The Langmuir-Blodgett trough allows the measurement of the area per molecule for a monolayer and therefore the effect that individual membrane components have on the membranes packing can be

investigated[52]. This technique while useful for investigating interactions between different lipids/drugs is limited because it doesn't resemble a biological membrane.

These methods are often used in combination with each other. Other methods are also used to indirectly measure changes in the properties of the barrier e.g. transepidermal water loss (TEWL)[73], where a measurement of the skin barrier function is made by the amount of water loss. High values for TEWL usually mean that the barrier has been perturbed. Magnetic resonance microscopy has been used to measure water distribution and diffusion coefficients in the skin[74], as have colorimetric methods[57]. Techniques such as transmission electron microscopy, and freeze fracture microscopy are also used to gather information on the structure of lipid membranes, but these techniques are destructive (to the sample) and sample preparation can itself influence the data obtained.

1.1.7 Prediction of transdermal permeation

The theoretical prediction of the permeation of drugs through the skin is an important tool in the development of transdermal delivery devices. In the pharmaceutical industry, preformulation studies use models predicting permeation of drug molecules through the skin to evaluate the best candidates for transdermal delivery. In academic studies the correct model can be used to reveal a wide range of information about the skin, including the potential routes for drug passage[10].

Several different processes must be accounted for when considering a drug molecule crossing the skin. Two processes; i.e. partitioning of the molecule into the membrane and diffusion of the molecule through the membrane, control the passage of most molecules through skin[50]. In addition, drug metabolism in the viable tissue, or binding to skin constituents may also occur and affect the rate of permeation.

Since the underlying transport process is usually considered to be controlled by simple passive diffusion[Error! Bookmark not defined.], then Fick's laws of diffusion are normally used to analyse permeation data. A simple statement of Fick's first law of diffusion is that the flux (J) of a drug is proportional to the concentration gradient ($\delta c / \delta x$):

$$J = -D \frac{\delta c}{\delta x}$$

Equation 1.1

where D is the diffusion coefficient (cm^2 sec^{-1}), c is the concentration (g cm^{-3}), and x the distance diffused. The flux is defined as the quantity of drug (Q, g) flowing through a unit area (A, cm^2) of membrane in a unit time (t, s).

$$J = \frac{\delta Q}{A \delta t}$$

Equation 1.2

Fick's first law is concerned with steady state diffusion, when the rate of drug flux does not change. Steady state conditions occur for transdermal delivery after the lag phase, when the drug is partitioning into the membrane and equilibrating through it (Figure 1.4).
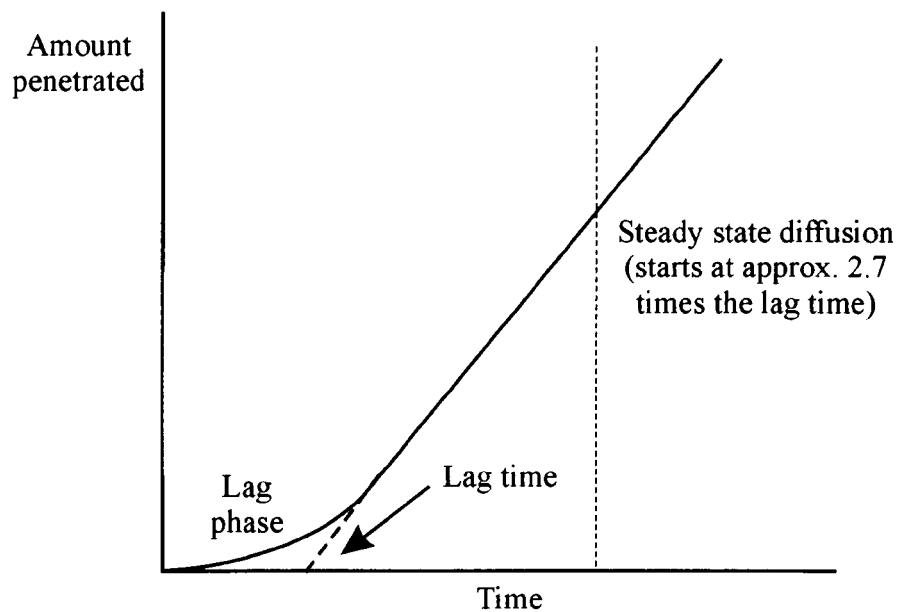
Figure 1.4 A typical profile for the penetration of a drug molecule across the skin.

However, because of the impermeable nature of the stratum corneum steady state conditions are unlikely to be established in normal therapeutic or cosmetic applications[75]. For non-steady state conditions solutions to Fick's second law of diffusion (Equation 1.3) must be obtained.

$$\frac{\delta c}{\delta t} = D \frac{\delta^2 c}{\delta x^2}$$

Equation 1.3

Solutions to Fick's second law, with boundary conditions relevant to the experiment, are often used to describe diffusion in vivo.

When the membrane is the sole or major source of diffusional resistance (e.g. in transdermal delivery) the partition coefficient of a molecule can be very important in establishing a high

flux[8]. The partition coefficient is the equilibrium constant of a drug distributed between two solvent phases (e.g. a donor compartment and the intercellular lipid of the stratum corneum) and is defined mathematically as:

$$\frac{c_A}{c_B} = K_B^A$$

Equation 1.4

where c_A is the equilibrium concentration in solvent A, c_B the equilibrium concentration in solvent B, and K_B^A the equilibrium constant. Choice of the correct solvents that mimic the system under observation, can tailor the technique to be an accurate predictor of the penetration.

The use of combinations of predicative factors such as Fick's diffusion laws, partition coefficients, and the solubility of the drug (among others), allows the prediction of transdermal penetration rates to be made. This process can be vital in saving both time and money for the pharmaceutical industry and is therefore very important. However these methods of prediction are complicated and can involve large numbers of variables.

Traditionally, oil/water partition coefficients have been used extensively in preformulation studies as a method for assessing the ability of a drug to enter a biological membrane. The oil/water partition coefficient measures the equilibrium concentrations of a drug between polar and non-polar solvents and produces an indicator of the lipophilicity of the drug. Oil/water partition coefficients can, however, be inaccurate due to the differences between the oil used (often n-octanol) and the stratum corneum lipid matrix[76]. Recently, methods involving the measurement of partitioning between an aqueous phase and lipid vesicles have been used to

determine drug partition coeffiecients[76]. The disadvantage of these types of method are that they require the extraction and assay of one of the phases.

Another method frequently used to predict the penetration of a drug through the skin is the Franz type diffusion cell. Franz diffusion cells use a supported membrane (often of cultured cells or excised whole membrane) between two reservoirs of buffer; drug penetration through the membrane is monitored allowing a prediction of the drugs *in-vivo* behaviour. Unfortunately these experiments are time consuming and have a high degree of variability. In addition, this type of in-vitro experiment do not allow specific information to be obtained about the role of skin lipids, as the stratum corneum also contains proteins[76].

The physical characteristics of a drug molecule are important in predicting the penetration of a drug molecule across the skin. The solubility, size, charge, pKa, and chemical reactivity of a molecule all have an effect on the penetration of a drug molecule through the stratum corneum. These parameters are usually determined by simple physical tests early on in the development process.

1.2 Current gap in knowledge

Two areas of investigation have been identified for consideration during this research project:

1. The development of an inexpensive and effective, *in vitro* method for the high throughput screening of drug molecules for transdermal drug delivery.

2. The development of a scientific instrument to investigate the micro-fluidity of the lipid matrix. Specifically the effect of penetration enhancing chemicals on the fluidity of the stratum corneum membrane lipids and the implications that this has on their mode of action.

1.3 Aim

This aim of this project was to initiate the development of a high throughput biosensor capable of measuring a drug partitioning into a model biological membrane that mimics the stratum corneum. The biosensor (based on a thickness shear mode quartz resonator) will be able to give accurate measurements of the drug partition coefficient into the membrane, and will also be able to monitor changes in the physical properties (fluidity) of the membrane enabling it to be used in novel scientific work on transdermal penetration enhancement.

1.4 Project outline

1.4.1 Biosensor development

Thickness shear mode (TSM) sensors are highly sensitive to changes in the mass and material properties of thin films and as such should make an ideal method for the investigation of drug partitioning into lipid membranes. Initially Langmuir-Blodgett films will be used to characterise the response of the TSM sensor to the deposition of simple lipid films e.g. the fatty acids: stearic acid, arachidic acid, and behenic acid. Langmuir-Blodgett coating of fatty acids films on to gold substrates, such as the sensing electrodes of the TSM sensor, results in the controlled deposition of lipid overlayers and will therefore allow the characterisation of the TSM sensor response. Interpretation of the film's mass will be made using a Sauerbrey type relationship, while the impedance spectrum of the TSM sensor will be used to investigate changes in film fluidity.

After the initial characterisation of the TSM sensor response with the simple lipid films more complex matrices will be coated on to the sensor to better mimic the stratum corneum. A

mixture of fatty acids, and cholesterol will be spin coated on to the TSM sensor and the sensor response investigated.

1.4.2 Studies on the fluidity of the stratum corneum membrane

After characterisation of the lipid matrix film on the TSM sensor it will be possible to investigate the fluidity of the lipid membrane using the TSM sensor response. By investigation of the impedance spectrum of the TSM sensor, and in particular changes in the resistance, it will be possible to elucidate trends in the fluidity of the membrane.

One area of investigation which should have particular attention paid to it is the fluidity of the fatty acid membranes. Previous studies of drug membrane interactions have used the frequency shift of the sensor to quantify the amount of drug that has partitioned into the membrane. This method assumes that the membrane properties remain the same during the partitioning process. This assumption is probably incorrect, as chemical molecules have been shown to affect the properties of the lipid membranes, e.g. chemical penetration enhancers[77].

The technique will then be used to investigate the effect of transdermal penetration enhancers e.g. Azone® and water on the fluidity of the lipid membrane. Careful control of the experimental temperature will also allow the investigation of the phase behaviour of the lipid membranes.

The potential advantages of TSM sensor approach to membrane fluidity determination are:

- The lipids do not have to be modified in order to measure the fluidity i.e. deuterated labels are not required.

- The fluidity of the whole membrane is measured and not individual components.

- It is a direct measure of fluidity and does not need to be inferred from a change in phase transition or membrane density.

- TSM measurements are related to an established mechanical property i.e. the shear modulus of the film.

In order to assess the ability of the biosensor to measure changes in membrane fluidity, the lipid matrix film will be measured with the inclusion of varying amounts of the penetration enhancer Azone®.

1.4.3 Studies on drug partitioning into the stratum corneum membrane

Measurement of the shift in resonant frequency of the TSM sensors on exposure to ibuprofen in a custom built flow cell will allow the monitoring of the membrane properties as the drug partitions in to it. This approach should allow the measurement of the drug partition coefficient, an important indicator as to whether a drug may be suitable for transdermal drug delivery.

2 DEVELOPMENT OF A TSM SENSOR MEASUREMENT SYSTEM

This chapter records the construction and characterisation of the TSM sensor measurement system. The experimental set-up is described, and a brief overview of the custom written software, used to control the measurements, is given. A comparison of the new TSM measurement system against an independently constructed TSM sensor set-up is described, and demonstrates the validity of the new experimental equipment. Experiments investigating the effect of temperature on TSM measurements, in air and liquids, are presented and form the groundwork for experiments later in the thesis.

2.1 Theory

TSM sensors consist of a thin wafer of quartz crystal, sandwiched between two metal electrodes (usually gold or platinum), which are linked to an external electrical source via sprung wire connectors (Figure 2.1). The piezoelectric nature of quartz means that when an oscillating electrical voltage is applied across the electrode, a mechanical oscillation is set up within the crystal at a particular frequency, this oscillation can be transformed into a resonant mode oscillation. The frequency at which this resonance occurs can be measured using a feed back loop amplifier and a standard frequency meter or a network analyser.

Figure 2.1 Schematic and photograph of a thickness shear mode sensor.
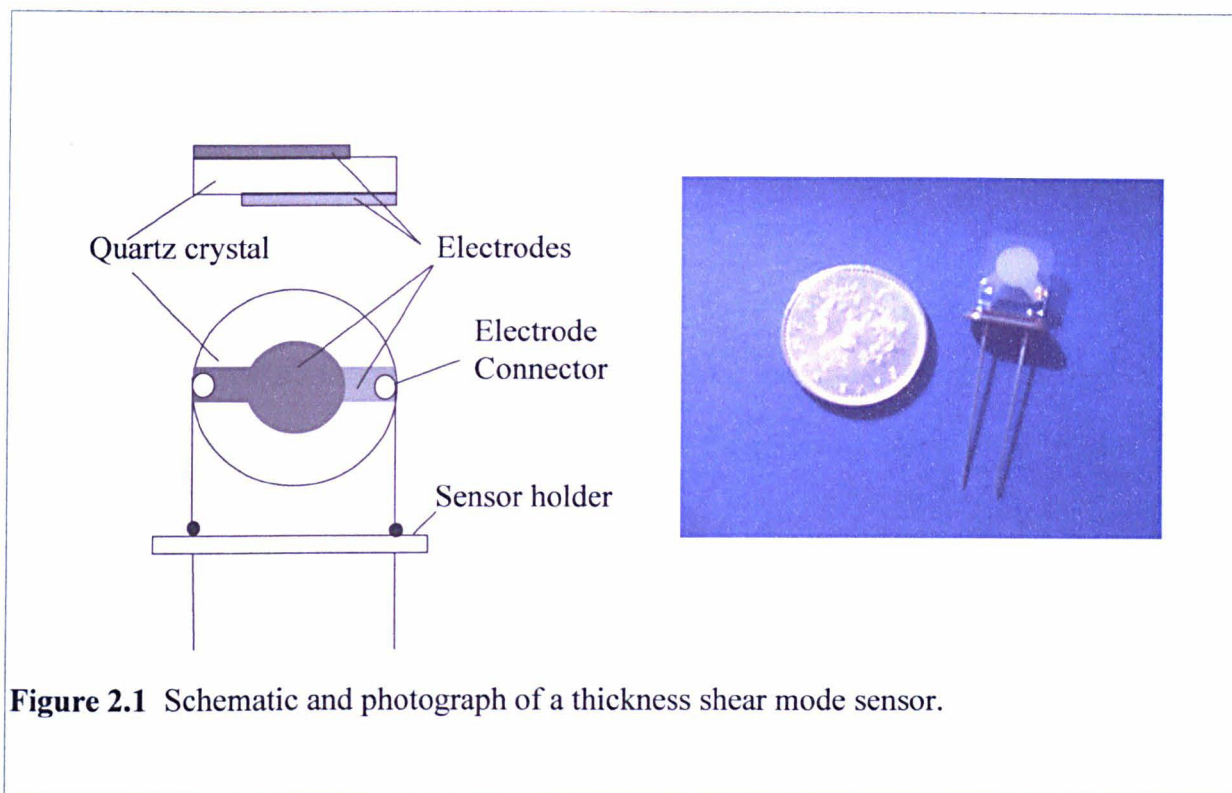
The use of TSM sensors in biosensor applications has become widespread recently as advances in TSM sensor design and theory have allowed the application of the technique to biological systems. TSM sensors have developed from their concept as devices used solely in the study of thin rigid films, to devices capable of the study of both Newtonian liquids and non-Newtonian films. Some applications of TSM devices include studies of antibody binding[78], drug/substrate interactions[79, 80], DNA hybridisation[81] and binding kinetics[82], protein absorption[83], whole cell interactions[84], and particle gel rheology[85], as well as the more established study of polymers[86]and metal films[87].

Lipid coated TSM biosensors have been used in a wide variety of different studies, of most relevance are the studies of partitioning processes and the characterisation of the membrane systems. These subject areas are reviewed briefly in Chapters 3 and 6.

2.1.1 Thickness shear mode sensors

The discovery of the piezoelectric nature of anisotropic crystals, by Pierre and Jacque Currie in 1880, paved the way for the use of quartz crystals in acoustic wave measurements. The Curries discovered that the application of a current across certain types of crystal resulted in mechanical distortion of the crystal lattice. Sauerbrey[3] used this principle, in 1959, to perform acoustic wave measurements of 'foreign layers' in vacuum, and thereby developed a relationship, which described the change in resonant frequency of the sensor with mass loaded onto the sensor surface.

Sauerbrey proposed that the change in frequency at which the crystal resonates was proportional to the mass of the "foreign layer" on the crystal surface, according to the following relationship:

$$\Delta f = -\frac{2 f_0^2 \Delta m}{(\mu_q \rho_q)^{\frac{1}{2}}}$$

Equation 2.1

where Δf is the frequency shift (Hz), f_0 is the native resonant frequency of the unloaded quartz sensor (Hz), Δm is the mass change per unit area (g cm^{-2}), μ_q is the shear modulus on the quartz (g cm^{-2}) and ρ_q is the density of the quartz (g cm^{-3}). However, the Sauerbrey relationship does have restrictions imposed on it, by the assumptions used in its derivation. These limitations mean that under certain conditions Equation 2.1 is no longer valid, and that the mass of the film can no longer be calculated from the frequency shift alone. Most important is the assumption that the film is an extension of the quartz (having the same density and stiffness as quartz) and has negligible thickness. This assumption holds true for thin solid

films, at a solid/gas interface, but becomes inaccurate if the film or medium is viscoelastic or liquid. Despite this limitation, TSM sensors experiments are still reported where the Sauerbrey relationship is used to interpret 'non-solid' results. The review by Thompson *et al.*[88] goes into greater depth on this topic.

Since Sauerbrey's publication, the mathematical models of TSM sensor loading with mass layers (at the solid/gas interface) have been refined by a number of workers. Stockbridge[89] used the Rayleigh perturbation theory to derive the relationship between frequency shift and a uniformly deposited mass. The relationship is appropriate for very thin films. Behrndt[90] showed that a period measurement technique is accurate for a larger mass range than the frequency method. Miller and Bolef[91, 92] applied a continuous-wave acoustic analysis to the problem and produced a relationship more suited to uniform films of defined thickness. Both the Stockbridge and Miller and Bolef approaches yield the same mass–frequency relationship as Sauerbrey for the addition of small masses[93].

Lu and Lewis[94] investigated the models of Stockbridge, Behrndt, Miller, and Boelef when loaded with large masses. They discovered that for frequency measurements to be reasonably accurate (using the Sauerbrey relationship, Equation 2.1) then the frequency shift of the resonator must be less than 2%. Lu and Lewis showed the superiority of the period measurement technique and the Miller and Bolef model over the Sauerbrey method, and could demonstrate accuracy in mass determination up to and beyond 15% mass loading.

2.1.1.1 TSM sensors in liquid environments

TSM sensor measurements in liquid environments were originally considered impossible due to the effects of viscous damping on the resonating crystal[95]. However, in 1979, Glassford[96] studied a liquid deposit using a quartz crystal microbalance and in 1980, Konash and

Bastiaans[97] and Nomura and Minimura[98] produced stable crystal oscillation in a liquid environment. This dispelled the previous misconception, though it was still recognised that liquid environments impaired the ability of the crystal to oscillate[99].

Konash and Bastiaans, and Nomura and Minimura[97, 98], both reported that changes in liquid density had an effect on the frequency at which the crystal oscillated. Despite this sensitivity of the TSM device to the liquid environment in which it was placed, both groups were still able to detect and quantify the absorption of the molecules under investigation. Nomura also noted the effect of the specific conductivity of the solution and proposed an empirical formula to correct for this[100].

The effect of the density and conductivity of the liquid medium was subsequently investigated by Nomura and Okuhra[101]. They investigated the frequency shift of TSM sensors on immersion in a range of organic liquids. Their studies showed that for non-electrolytes, the frequency shift of the sensor depends on the density and viscosity of the solvent. A new empirical relationship was proposed that incorporated the density and viscosity of the (non-electrolyte) solvent. Yao and Zhou[102] investigated the accuracy of Nomura and Okuhra's relationship on a wider range of liquids. They found that for the liquids investigated, the correlation was variable. This observation led them to propose a new empirical relationship which included density, viscosity, dielectric constant, and specific conductance.

Following the publication of these empirical relationships, Kanasawa and Gordon[95, 103] proposed a more robust relationship in 1985. Kanasawa and Gordon's mathematical treatment determined the behaviour of the system by examining the coupling of the elastic shear waves in the crystal to the viscous shear wave in the liquid. Equation 2.2 resulted:

$$\Delta f = -f_0^{\frac{3}{2}} \left(\frac{\mu_L \rho_L}{\pi \mu_Q \rho_Q} \right)^{\frac{1}{2}}$$

Equation 2.2

where Δf is a shift in frequency from the resonant frequency of the unperturbed crystal f_0, μ_L and ρ_L are the viscosity and density of the liquid respectively, and μ_Q and ρ_Q are the density and shear modulus of the quartz.

Bruckenstein and Shay[104] independently developed a relationship comparable to Kanazwa and Gordon's in the same year. They considered a layer of liquid, the thickness of which is calculated using a diffusion layer approach (which incorporates the viscosity and density of the liquid and the frequency of the crystal). Further, *in situ*, changes in mass (by electrodeposition) were interpreted using the Sauerbrey relationship.

Lee and Huang achieved good correlation between theoretical and experimental results by considering the effects of both compressional and shear wave in the liquid layer[105].

While liquid density and viscosity are major factors effecting the operation of TSM sensors in the liquid phase (as indicated by the Bruckenstein and Shay, and Kanazawa and Gordon relationships) other factors also have to be taken into account for a fuller understanding of how these acoustic devices[106] operate in the liquid phase. In addition to the consideration of specific conductivity by Nomura[100] other factors have been found to effect TSM operation in liquids. Important factors to consider[106] include; chemical reactions, surface free energy, interfacial viscosity, and diffusion on the crystal surface. Of particular importance to the sensor response are factors that effect the coupling of the film to the electrode. Some of these factors affecting TSM operation in liquids are briefly reviewed here.

Sauerbrey[88] originally investigated the sensitivity of TSM sensors operating with adsorbed solid films in gaseous environments, and demonstrated that the sensor had a radial mass sensitivity which diminished to zero beyond the edge of the electrode. Studies by Ward and Delawski[107] investigated this radial mass sensitivity, in liquid media, by metal deposition in a polymer film. These experiments demonstrated the importance of a uniform film in the liquid environment, in addition to the discovery of a significant mass sensitivity beyond the electrode boundary. These findings indicate that it is vital that films are coated uniformly onto the sensor.

Schumacher et al.[108, 109, 110] demonstrated the importance of surface roughness on the response of the TSM sensor. In a series of studies using metal films, they showed that 80% of an observed frequency shift could be due to changes in surface roughness. Since Schumacher et al., the importance of the surface roughness of the sensor has been investigated by a number of other groups[111, 112, 113]. Bruckenstein et al.[114] found their data to be inconsistent with a model where liquid was solely trapped by surface roughness, suggesting that part of the effect is due to hydrodynamic coupling of liquid trapped in and external to surface features. Urbakh and Daikhin[115, 116, 117] used perturbation theory and an approach based on the Brinkman equation to produce models for the behaviour of smooth and rough surfaces with a variety of different media. The model allowed them to predict the roughness induced frequency shift for viscous liquids. The profound effect that surface roughness has on TSM measurements means that many groups now use polished quartz sensors with a negligible surface roughness.

Changes to the surface energies of rough sensors have been found to influence the frequency shift of the sensor in liquid environments. Martin et al.[113] measured the frequency shift for liquids using sensors with different contact angles. These findings showed that contact angle had virtually no effect for 'smooth' crystals but significantly decreased the response of 'rough'

crystals. The authors attributed these results to a combination of changes in the surface energy and the surface roughness of the sensor[113, 118]. Martin *et al.*'s theory is that the surface energy affects the manner in which the fluid layer is trapped by the surface roughness. It was proposed that a sensor with a low contact angle (hydrophilic surface) would trap water (or another polar solvent) in the surface aberrations. A sensor with a high contact area (hydrophobic surface) will restrict the penetration of water causing an air pocket to be trapped, the trapped air will effect the sensor frequency reading. Thompson *et al.*[119, 106, 120, 121, 122] have investigated the effect that surface energy has on the response of TSM sensors in liquids. These studies, which included modification of the electrode surface energy by the use different films and electrode materials, have led the authors to propose a different theory to that of Martin *et al.* Thompson *et al.* suggest that the anomalous frequency shifts are due to changes in the interfacial slip between the sensor/liquid. Most models of TSM sensor loading (with liquids) assume that there is no slip between the sensor surface and the liquid. Thompson *et al.* suggest that slip does occur at the interface and that the amount of slip is dependant on the energy of the surface. For example, at a hydophilic surface a polar liquid will have a stronger binding to the surface of the sensor than at a hydrophobic one. Recently, Thompson *et al.*[122] have presented a paper that casts doubt on the importance of surface roughness to this process, thereby adding weight to their theory. Whichever theory is correct, surface energy is important in TSM sensor measurement, as changes in the energy of the sensor electrodes will effect the data (frequency shifts) that are obtained.

Stress effects and their origins have been discussed by EerNisse[123] and include films coated on to the sensor surface, film processes (such as chemical reactions and nucleation processes), sputtering, and pressure differences across the faces of the crystal. Heusler *et al.*[124] investigated surface stress at one electrode by altering the pressure exerted by the electrolyte on to the crystal surface: the authors found that a pressure change of approximately 3 kPa caused a

frequency shift in the crystal of approximately 70 Hz. The most significant surface stresses in our experiments are likely to come from the crystal holders and flow cell. Minimising these effects will be an important factor in the experimental set-up.

The potential for film resonance in viscoelastic films has been described by Lucklum *et al.*[125], in an attempt to explain unexpected changes in frequency and impedance spectra for TSM sensors. Recently, Martin *et al.*[126] provided a theoretical examination of the subject using a new equivalence model to describe the conditions at film resonance. Martin *et al.*'s finding, though yet to be proven experimentally, predicts a dampening of the sensor admittance at film resonance or even the appearance of a double peak when the quartz and film resonance converge.

Several reviews have been written on TSM devices and the interfacial properties that effect their operation, for more information the reader is referred to these[106, 112, 121].

While the factors mentioned above are of considerable importance, perhaps one of the most important factors to be considered is not directly related to the crystal but to the film. One of the most significant factors affecting the resonant frequency of a TSM sensor is the material properties of the film. If a film behaves non-rigidly (e.g. a liquid or viscoelastic film), then the Sauerbrey relationship Equation 2.1 is no longer valid. The breakdown in the Sauerbrey relationship is due to acoustic losses in the film[5]. Changes in the material properties of a coated film cause a shift in frequency similar to that for a mass change. This can make it very difficult to interpret changes in resonator frequency for a viscoelastic film and care must be taken not to confuse a change in film properties with a change in film mass. Many factors can cause a change in the material properties of a film. Some examples are:

- *Conformational changes.* Höök *et al.* demonstrated binding of egg-phosphatidylcholine to TSM sensors (in the liquid phase) and switching of the bound lipid structure from vesicles to bilayers[127]. Su and Thompson have used a TSM biosensor to detected changes in the coil structure of DNA when it is placed in different strengths of electrolyte solution[128].

- *Electrochemical reactions.* Numerous papers have demonstrated electrochemical changes in polymer films. Etchenique and Calvo demonstrated changes in shear modulus for a redox polymer film by simultaneously measuring the film by a TSM sensor and cyclic voltammetry[129]. Bandey *et al.*[130] performed a similar study on the electrodeposition of conducting poly(2,2'-bithiophene) polymer films. The combination of cyclic voltammetry and a TSM sensor is known as an electrochemical quartz crystal microbalance (EQCM).

- *Polymer binding and hydration.* Reason *et al.*[131] have demonstrated that the hydration of low crystalline cellulose (LCC) polymer films results in a change in the viscoelastic properties of the films. They also showed that the binding of a mucin layer to the LCC film resulted in changes in the film material properties.

In order to interpret changes in the mass and material properties of a film (in a gaseous or liquid environment) it is necessary to move away from the frequency and period techniques of TSM sensor measurement and use the more sophisticated technique of impedance measurement.

2.1.1.2 Impedance measurement

The reason that the Sauerbrey equation is inaccurate for non-rigid films results from the dampening of the sensor by the viscous losses in the film. As described earlier, a TSM sensor detects the film coated onto it by measuring an alteration in the frequency at which it oscillates. In order to quantify the relationship between frequency and mass, Sauerbrey made a number of assumptions in his derivation, one of importance is that the film is an extension of the sensor surface. For this assumption to be true then the density and acoustic properties of the film must be the same as for quartz. In practice the Sauerbrey equation can be used to measure thin rigid films, because the mechanical oscillation of the quartz simply propagates into the film as

an acoustic wave with little loss of energy. However, in a non-rigid film the acoustic wave is dampened (Figure 2.2), this loss mechanism means that a smaller frequency decrease occurs, than predicted by the Sauerbrey equation.

Figure 2.2 Propagating acoustic waves into a film. Red line illustrates the dampened acoustic wave in a viscoelastic film or liquid. Blue line illustrates the undampened acoustic wave in a rigid film.
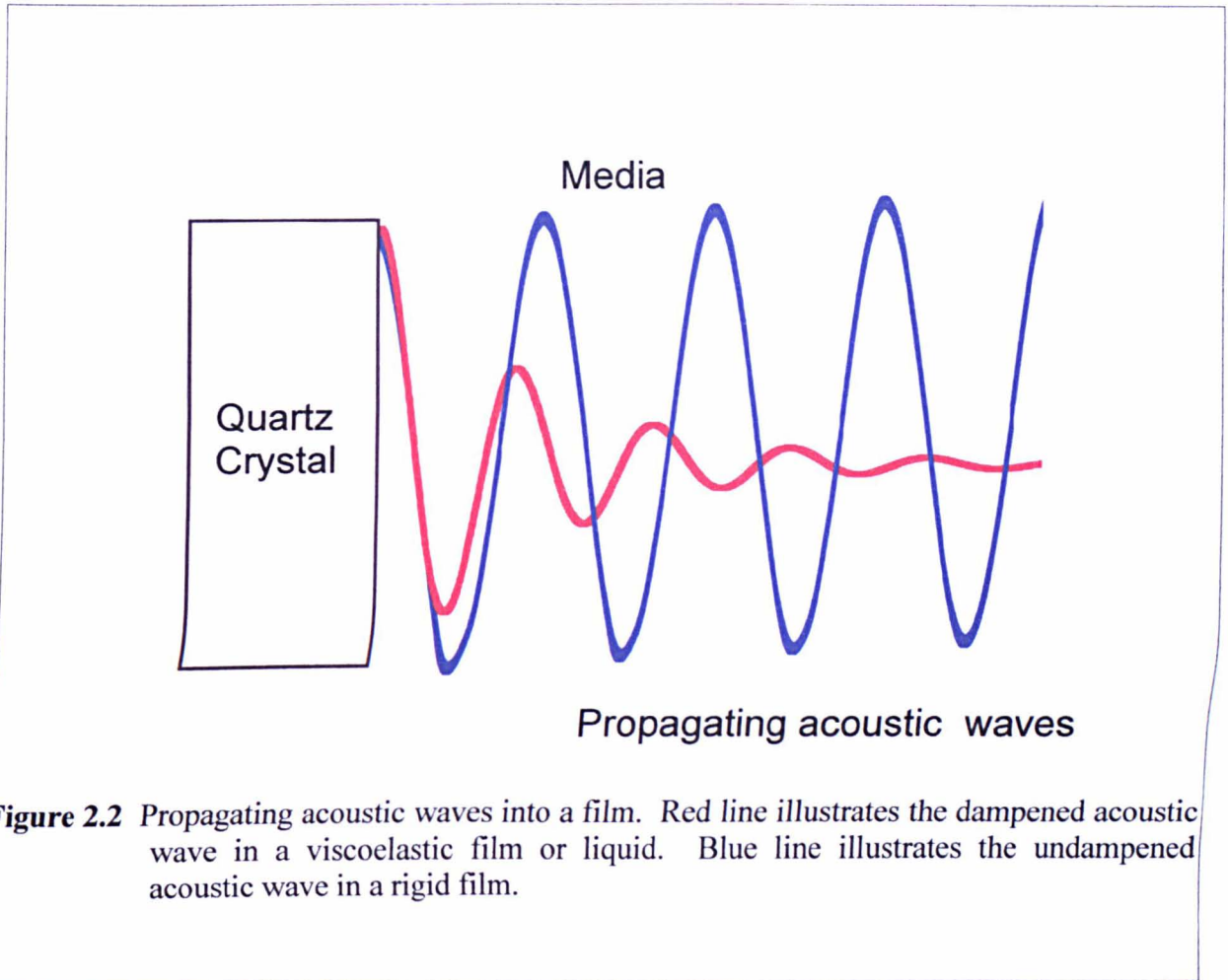
Crane and Fisher[132] were the first people to perform impedance measurements on a TSM sensor coated with a viscoelastic film. Crane and Fisher investigated lossy Carbowax films using the impedance of the sensor to demonstrate changes in the viscoelasticity of the film as the temperature was increased. Since that study, several approaches based on impedance measurements have been proposed for viscoelastic film systems.

Approaches based on both quantitative and qualitative impedance measurements have been used to assess changes in the material properties of the films investigated in this Thesis. These approaches are described in the following Sections.

Qualitative measurement

Qualitative changes in the physical nature of the film can be observed from changes in the shape of the impedance spectrum of the coated resonator (Figure 2.3). A resonator, coated with a film that is coupled as a rigid solid to the resonator surface, will give rise to a narrow resonant peak (similar to that of the uncoated resonator). At the other extreme, a resonator coated with a lossy film such as a viscoelastic mass or a liquid will give rise to a broad resonant peak.
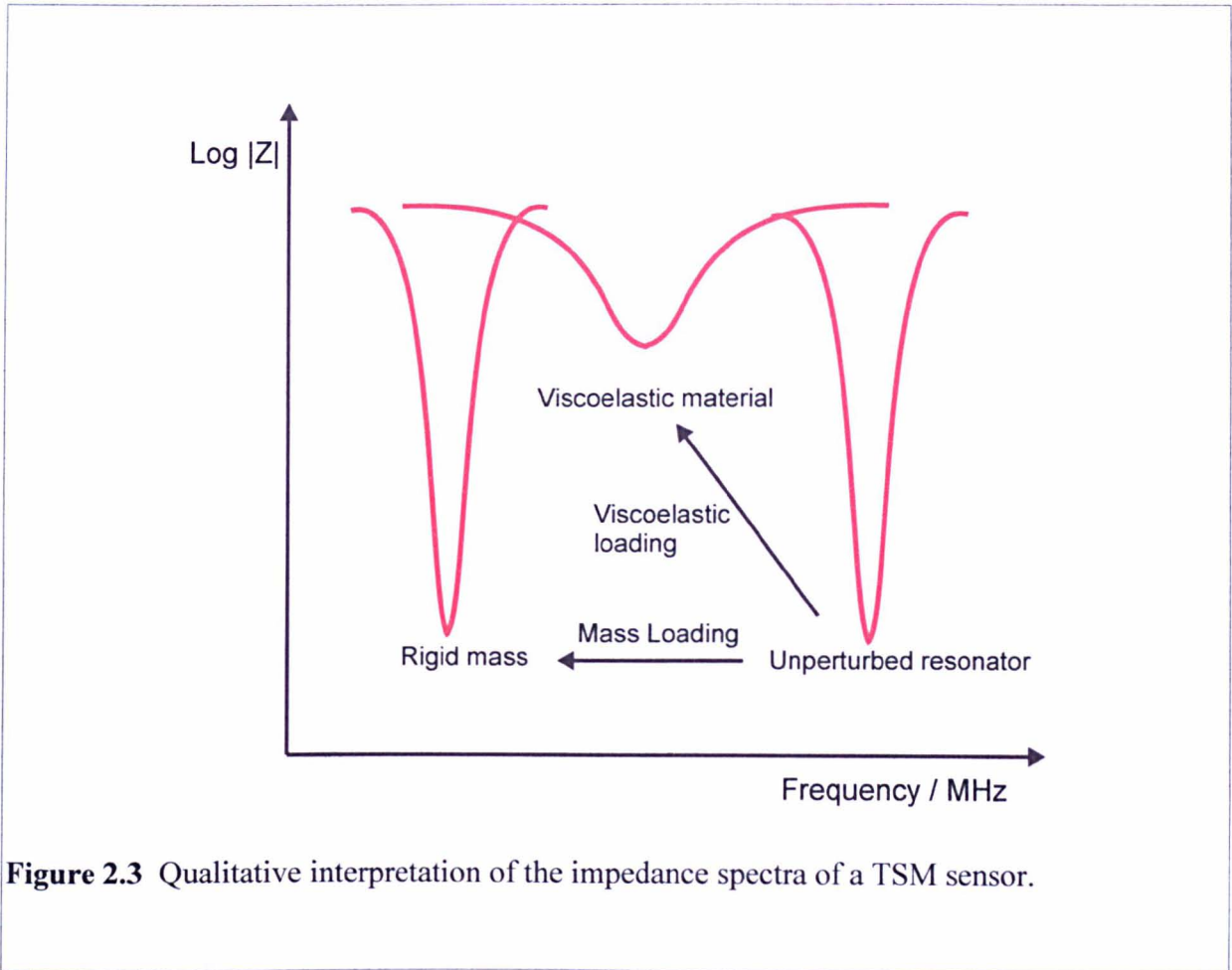
Figure 2.3 Qualitative interpretation of the impedance spectra of a TSM sensor.

Quantitative measurement

Quantitative models of TSM sensor impedance are usually based on electrical equivalent circuits and the application of acoustic wave theory. An electrical equivalent circuit is an electrical representation of a physical system. Several electrical representations for the piezoelectric resonator have been used, of these the Butterworth van Dyke (BVD) and Mason transmission line models (both methods are described by Rosenbaum[133]) are most common, though other methods such as finite element analysis based on Mindlim plate theory have also been considered[134]. Bandey *et al.*[130] also gave a good description of the two electrical equivalent models, and further proposed a method by which the theory can be applied to TSM sensors in order to reveal the shear moduli of the film, i.e. the model described by Bandey *et al.*

provides a method of quantifying material properties of viscoelastic films. A brief description of the BVD model is given here to help the understanding of the measurements made during this project.

Before the discovery of the piezoelectric resonator, Dye[135] and Butterworth[136] showed that an electrical circuit could be used to represent a mechanically vibrating system driven by an electromagnetic field, i.e. an electromechanical transducer. Following the discovery of the piezoelectric resonator Van Dyke[137] developed a model for an electrostatic transducer (Figure 2.). This electrical model of the piezoelectric resonator became known as the Butterworth van Dyke equivalent circuit (the BVD circuit).

The BVD equivalence circuit has two arms, the motional arm and the static arm. The piezoelectric current (a current component is discussed later in this section) is modelled by the motional arm, which contains a resistor (R), an inductor (I), and a capacitor (C) in series (Figure 2.4). The motional arm of the circuit models the resonant oscillation of the TSM sensor. In parallel to the motional arm is coupled a capacitor (C_0), which forms the static arm. This capacitor is a simplification of what are two separate capacitors in parallel C_q, the static capacitance of the quartz between the electrodes and C_r, the parasitic capacitance of the

fixture, where $C_0 = C_r + C_q$. This capacitor accounts for the other two current types (dielectric displacement and Maxwell displacement current components, discussed later in this section) and dominates the impedance spectrum away from the resonant frequency. The motional arm of the BVD circuit (R, C, and L) represents the piezoelectric displacement current.
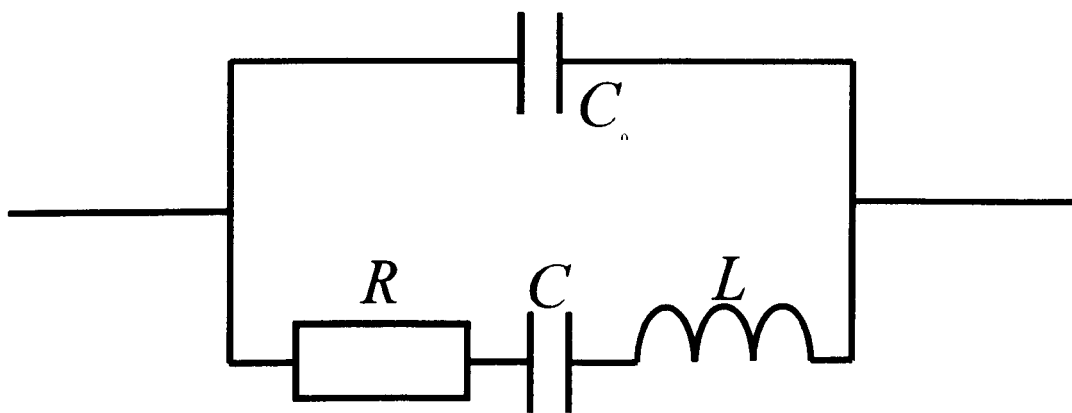
Figure 2.4 Equivalent model for an electrostatic transducer.

Typical values for a 9 MHz TSM sensor are shown in Table 2.1.

Table 2.1 Approximate values for BVD circuit components (9 MHz AT cut quartz crystal).

Circuit element	Typical value for circuit component
C_0	5×10^{-12} F
C	5×10^{-14} F
R	$20 \, \Omega$
L	6×10^{-3} H

The BVD circuit was developed from a consideration of the electrical current that flows in a piezoelectric oscillator when a voltage is applied across it. The quartz crystal resonator behaves in part as a parallel plate capacitor, with a quartz plate sandwiched as the dielectric

between the two electrode plates. When an alternating voltage is applied across the capacitor plates, an alternating current flows that comprises three parts[138]:

1. The Maxwell displacement current.

2. The dielectric polarisation current.

3. The piezoelectric displacement current.

The Maxwell displacement current results (solely) from the charge per unit area that builds up on the plates of the capacitor. It is worth noting that if the dielectric were a vacuum, and not quartz, then the Maxwell current would be the sole current component.

The dielectric polarisation can be thought of as positive and negative charges with limited freedom of movement relative to each other (Figure 2.5), and is the result of the migration of electronic charge. The dipole moment is the product of the magnitude of the displaced charge and the distance between them. N.B. If the material forming the dielectric were not piezoelectric (e.g. glass) then the total current would comprise the Maxwell and dielectric currents. However when the dielectric is piezoelectric (e.g. quartz) then a third current component exists, the piezoelectric polarisation current.
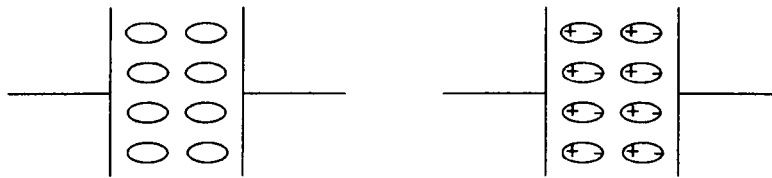
Figure 2.5 A representation of the dielectric displacement current, showing the rest state (left) and the induced charge dipoles when a voltage is applied (right).

Piezoelectric polarisation is associated with the displacement of ionic charge in the crystal lattice (Figure 2.6). The result is a macroscopic dipole moment, which can be modelled by the capacitor C in the motional arm of the BVD circuit. The relocation of the ionic charge centres (i.e. atoms in the crystal lattice) differentiates this polarisation current from that of the dielectric polarisation. It is the relocation of ionic charge centres that results in the induced strain in the crystal lattice that forms the physical distortion ('oscillation') of the TSM sensor. In the case of AT–cut quartz the relocation of charge causes a shear deformation in the quartz. The strain in the crystal manifests as an inertial 'element' that opposes the piezoelectric current and increases in proportion to the rate of distortion of the charge centres. In electrical terms, this mechanical restoring force is manifest as an inductive element in series with the capacitance representing the piezoelectric polarisation current.
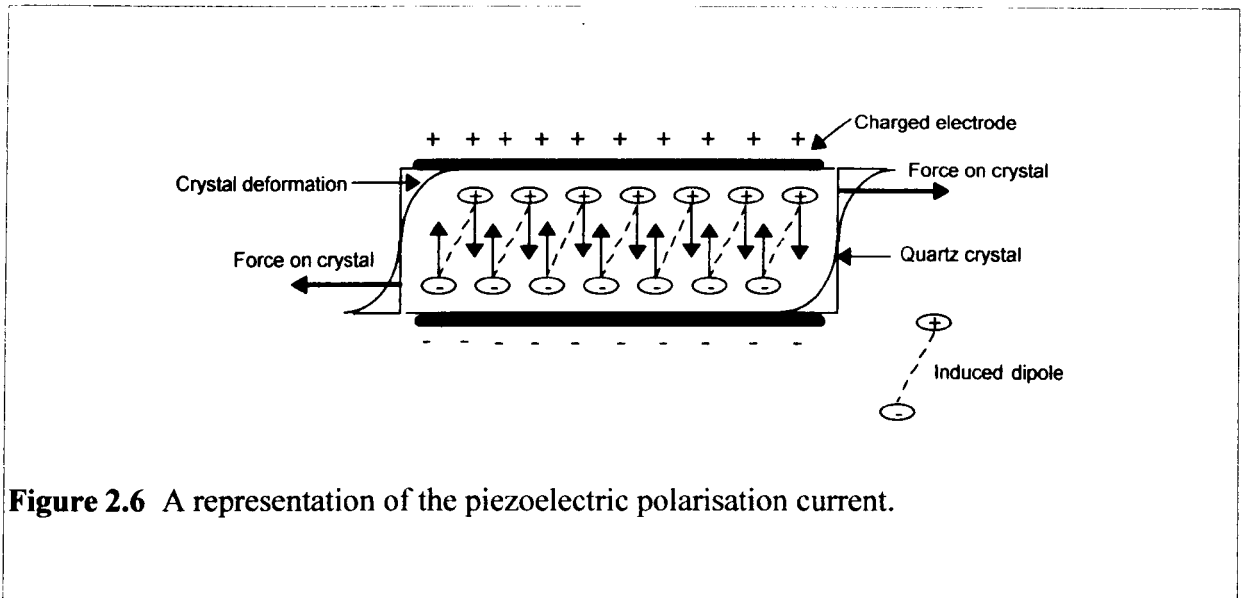
Figure 2.6 A representation of the piezoelectric polarisation current.

It is the piezoelectric polarisation current that underpins the use of a quartz crystal as a microbalance.

At frequencies away from the resonant frequency, the TSM sensor will behave as a simple capacitor (C_0, with capacitance C_0), the impedance (Z) of which is given by:

$$Z = -\frac{i}{\omega C_0}$$

Equation 2.3

where i is the imaginary vector, and ω is the angular frequency $2\pi f$. The current is leading the voltage by 90°.

At frequencies approaching the resonant frequency of the TSM sensor the piezoelectric displacement current becomes increasingly significant and the total current becomes the vector sum of the three component parts. The piezoelectric displacement current can lead or lag the

applied voltage depending on whether the frequency is above or below the resonant frequency. At frequencies below the resonant frequency the current leads the voltage and the device, and is represented by the capacitor (C, with capacitance C) of the motional arm.

$$\mathbf{Z} = -i\frac{1}{\omega C}$$

Equation 2.4

At frequencies above the resonant frequency the current lags the voltage and is modelled by the inductor (L, with inductance L) in the motional arm.

$$\mathbf{Z} = +i\omega L$$

Equation 2.5

When the applied frequency is the resonant frequency the current is in phase with the voltage and the impedance of the motional arm is represented by the resister (R, with resistance R).

$$\omega L = -1/\omega C$$

Equation 2.6

Considering Ohms law, we can see that the impedance of the motional arm of the BVD circuit will be the sum of the individual components:

$$\mathbf{Z} = R + i\omega L - i\frac{1}{\omega C}$$

Equation 2.7

If we now add the capacitance of the static arm of the BVD circuit to Equation 2.7 an equation that describes the impedance of the BVD circuit (and therefore the TSM sensor) is obtained:

$$Z = \frac{R_1 + i(\omega L - \frac{1}{\omega C})}{1 - \omega^2 L\ C_0 + \frac{C_0}{C} + i\omega R\ C_0}$$

Equation 2.8

If the impedance is set to zero in Equation 2.8, then two solutions can be found for the resonant frequency.

$$f_S = \frac{1}{2\pi} \sqrt{\frac{1}{L\ C}}$$

Equation 2.9

$$f_P = \frac{1}{2\pi} \sqrt{\frac{1}{L\ C} + \frac{1}{L\ C_0}}$$

Equation 2.10

The first frequency (f_s) is the result of the inductor and capacitor of the motional arm of the BVD circuit and is termed the series resonant frequency. The second frequency (f_p) results from the inductor of the motional arm and the capacitor of the static arm and is termed the parallel resonant frequency. Figure 2.7 shows a typical impedance spectrum for a 9 MHz TSM sensor oscillating in air the two resonant frequencies are indicated.
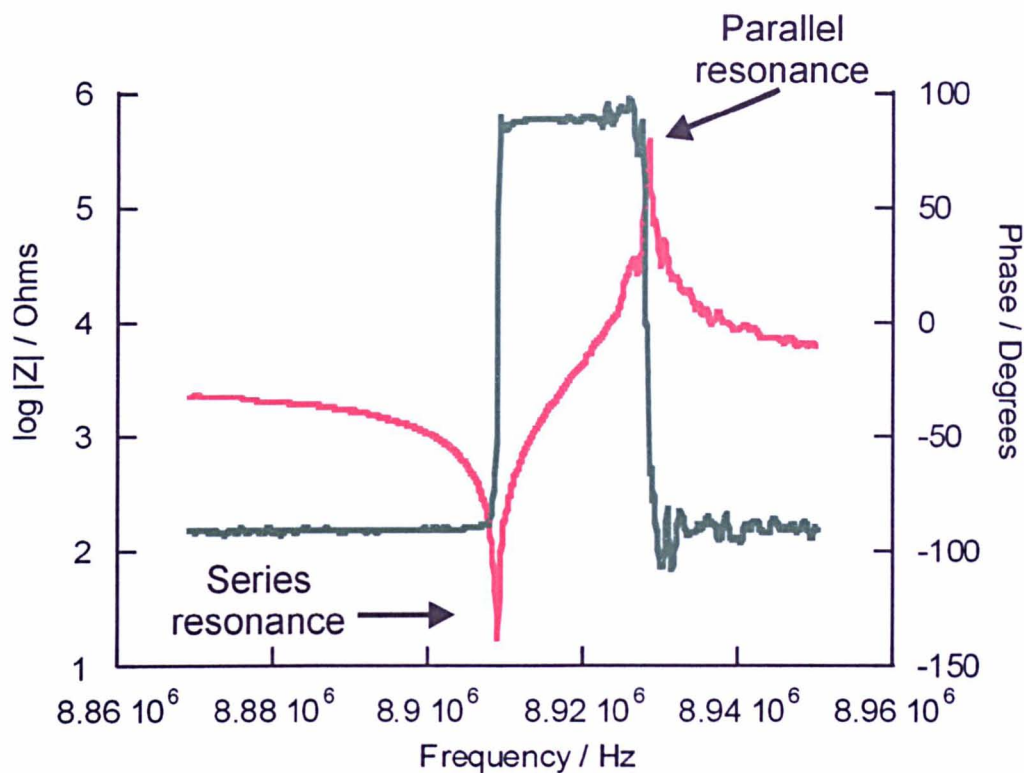
Figure 2.7 A typical impedance spectra for a 9 MHz TSM sensor with the series and parallel resonant frequency indicated.

Therefore the BVD circuit can be used to model the behaviour of an uncoated TSM sensor. The electrical components can be related to the mechanical oscillation of the TSM sensor using acoustic wave theory, and the mechanical properties of the resonator determined from the electrical impedance spectrum fitted to a BVD model[130]. If a film is coated onto the TSM sensor, then the mechanical properties of that film (i.e. density, viscosity, and shear modulus) can also be determined using models based on the BVD circuit. A film coated onto the TSM sensor can be represented as two additional electrical components added to the circuit, i.e. a resistor and inductor in series with the motional arm (Figure 2.8). The resister (R_2) represents the dampening of the TSM sensor oscillation caused by the film, while the inductor (L_2)

represents the inertia imparted to the TSM sensor by the mass that has been added to its surface.
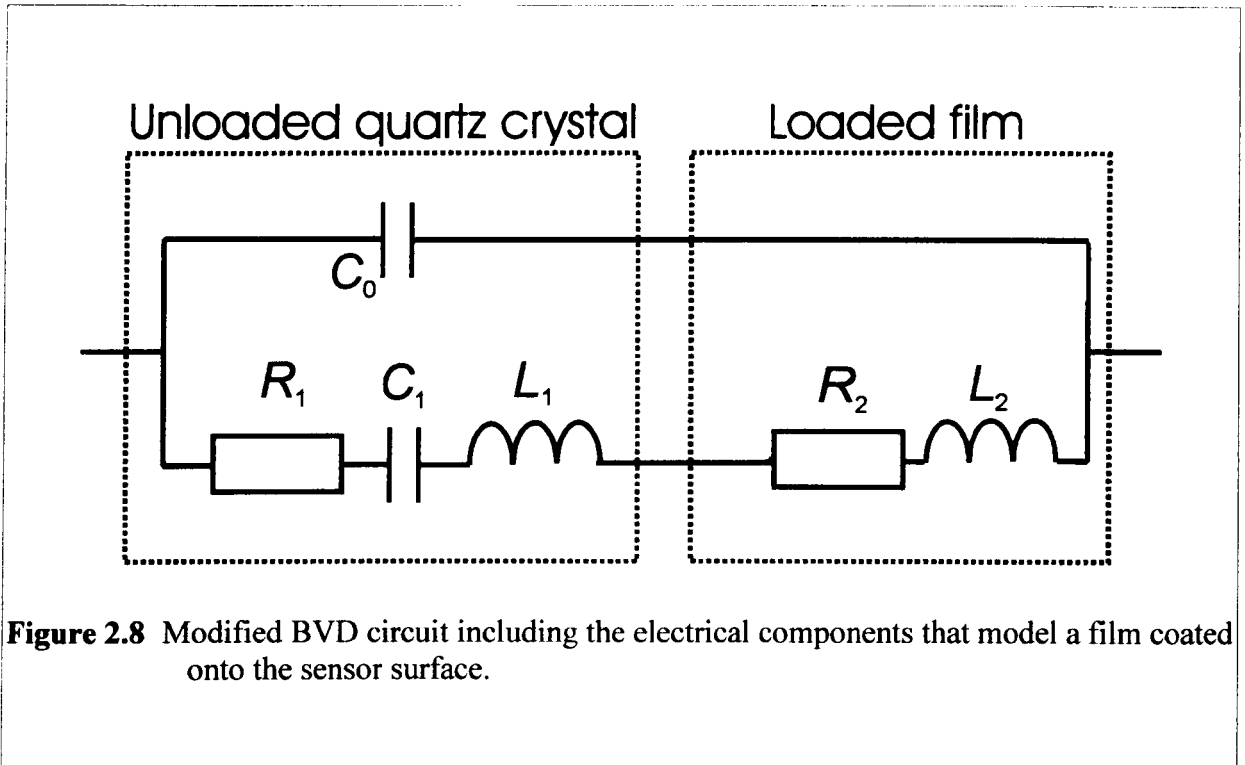
Figure 2.8 Modified BVD circuit including the electrical components that model a film coated onto the sensor surface.

Since these two components (R_2 and L_2) are in series to the unloaded resistor (R_1) and inductor (L_1) then the equivalent circuit for the TSM sensor and film (Figure 2.8) can be simplified to a circuit that looks exactly the same as the BVD circuit except that:

$$R = R_1 + R_2$$

Equation 2.11

and

$$L = L_1 + L_2$$

Equation 2.12

The above model was used in this project to quantify changes to the impedance spectrum of the TSM sensor. Physically the inductance represents the effect of the film on the inertial mass of the quartz sensor and the resistance the dissipation of electrical energy due to the dampening of the shear vibration[85]. Measurements of the resistance of the TSM sensor at the series resonance frequency before (R_1) and after (R) loading of the TSM sensor with a film are obtained by fitting the impedance spectrum to the BVD circuit. Equation 2.11 is then used to calculate the shift in resistance (R_2). Changes in the value R_2 are used in this project to demonstrate that a change in the material properties of a film, are occurring. For example an increase in the value R_2 indicates that the film is dampening the oscillation of the TSM sensor and therefore is not behaving rigidly[139]. Approaches similar to this is have been used previously to investigate the influence of film viscoelasticity on TSM sensor measurements[5]. This has been demonstrated mathematically by Martin *et al.*[113] who have shown for a rigid film that:

$$R_2 = 0$$

Equation 2.13

and

$$L_2 = \frac{N\pi}{4K_{em}^2 \omega^{3/2} C_0} \left(\frac{\rho_F \eta_F}{2\mu_q \rho_q} \right)^{1/2}$$

Equation 2.14

but for a Newtonian liquid:

$$R_2 = \frac{N\pi}{4K_{em}^2 C_0} \left(\frac{\rho_L \eta_L}{2\omega_s \mu_q \rho_q} \right)^{1/2}$$

<div align="right">**Equation 2.15**</div>

and

$$L_2 = \frac{N\pi}{4K_{em}\omega^{1/2}C_0}\left(\frac{\rho_L\eta_L}{2\mu_q\rho_q}\right)^{1/2}$$

<div align="right">**Equation 2.16**</div>

where N is the harmonic number (1), $\rho_{L/F}$ is the density of the liquid/film, d_L is the thickness of the film, K_{em} is the electromagnetic coupling coefficient, ω is the angular frequency of series resonance, μ_q is the shear modulus of quartz, ρ_q is the density of quartz, and $\eta_{L/F}$ is the viscosity of the liquid/film.

Quantification of the material properties of more complex films coated onto TSM sensors can be achieved by adapting the electrical model used. This approach, while outside the remit of this project, has been used successfully[139,130].

Though most of the literature methods for quantifying TSM measurement of viscoelastic films have been based on ac impedance analysis, the only system that is commercially available is based on a fundamentally different method[127, 140, 141]. The QCM-D technique (as it is known) switches on and off the unit driving the crystal, and measures the decay of the crystal oscillation. From the decay curve the viscoelastic properties of the film can be inferred or calculated[83].

2.2 Development of the TSM measurement system

Two different types of AT-cut quartz resonators were used in the TSM measurement system. Unpolished TSM sensors, which had a nominal resonant frequency of 9 MHz and an electrode

area of 0.19 cm^2 were obtained from EG & G (Wokingham, Berks). Polished TSM sensors with a nominal resonant frequency of 8 MHz and an electrode area of 0.4 cm^2 were obtained from two sources; International Crystal Manufacturing (Oklahoma, USA) and Ieuan Jenkins Ltd (Mid Glamorgan, Wales).
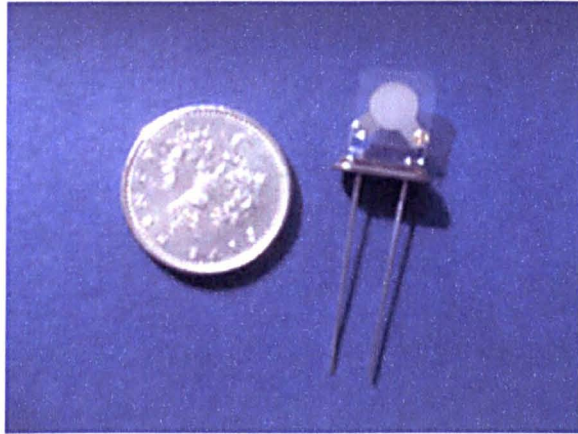
Figure 2.9 A photograph of a TSM sensor with a five pence coin.

Throughout this project a passive measurement technique is used to monitor the response of the TSM sensor as it is exposed to different experimental conditions. In a passive measurement system, a network analyser measures the impedance of the TSM sensor. The network analyser provides an alternating voltage across the electrodes of the TSM sensor at a specific frequency and measures the magnitude and phase shift of the reflected voltage, from which the impedance of the sensor is determined. The measurement is repeated at a range of different frequencies around the resonant frequency of the crystal that are specified by the operator and an impedance spectrum produced. The impedance spectrum is then be used to monitor the mass and fluidity changes in the film via shifts in the resonant frequency (f) and resistance (R_2) of the film coated resonantor.

The passive measurement system used throughout this project is shown diagrammatically in Figure 2.10.
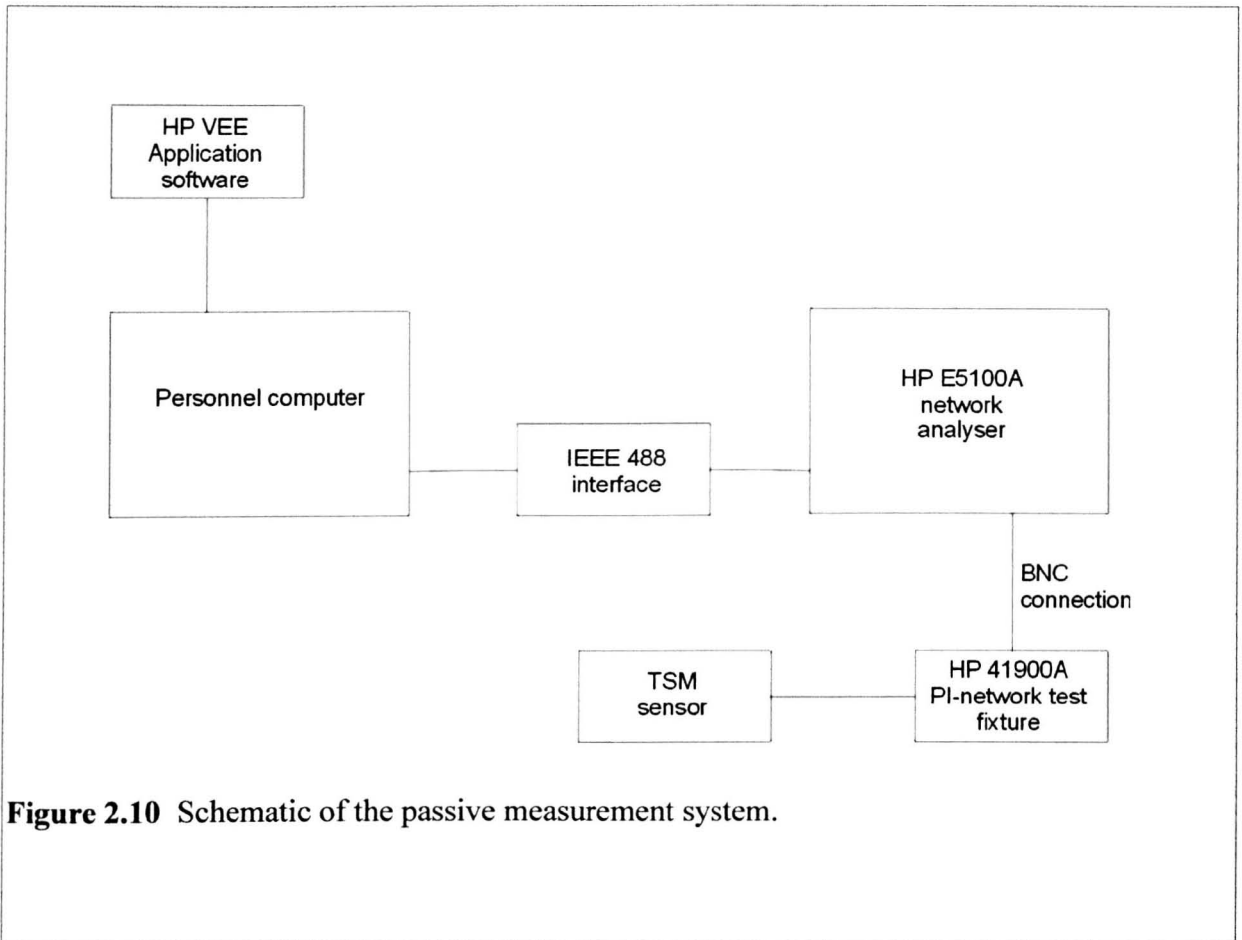
Figure 2.10 Schematic of the passive measurement system.

The measurement system consists of a Hewlett Packard E5100A network analyser connected to a Hewlett Packard 41900A PI-network test fixture. A personal computer is used to control the network analyser, via an IEEE 488 connection, using a custom built instrument driver constructed in the Hewlett Packard visual engineering environment (HPVEE).
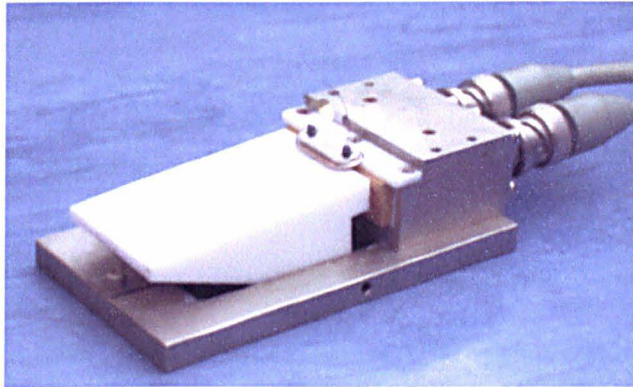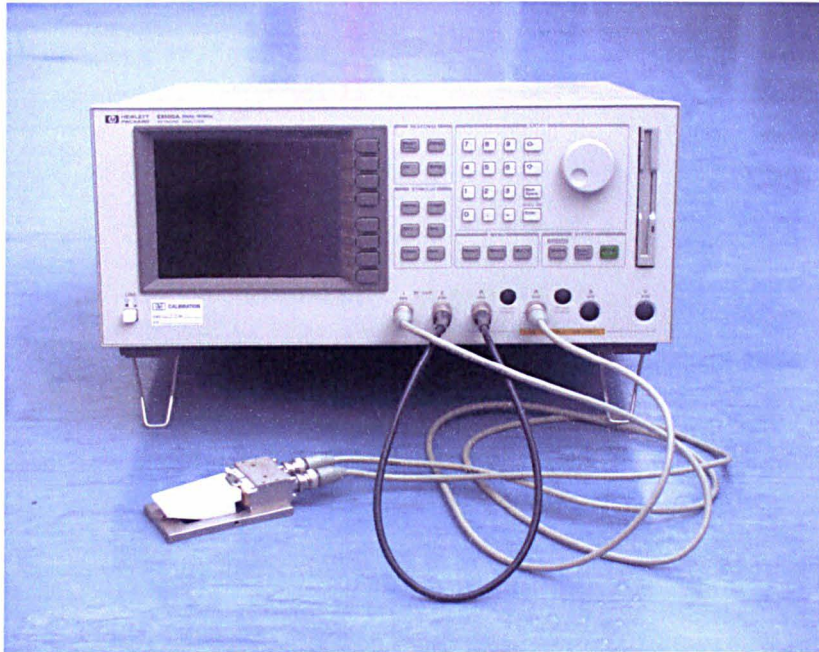
Figure 2.11 Photographs of the network analyser and PI network test fixture.

Liquid measurements were performed using a commercially sourced flow cell (International Crystal Manufacturing, Oklahoma USA) that is purpose made for TSM sensor measurements. The flow cell consists of two sections that are clamped to either side of the TSM sensor using two bolts and O-rings. The flow cell was been manufactured so that when the two sides are clamped onto the TSM sensor an even, constant, and reproducible force is applied to the

crystal. One side of the flow cell is constructed to act as a static flow cell in which 1 mL of liquid can be placed onto the sensor surface, while the other side contains a chamber through which liquid can be flowed. When either the static or flow system are being used, the other side of the TSM sensor is left exposed to air.
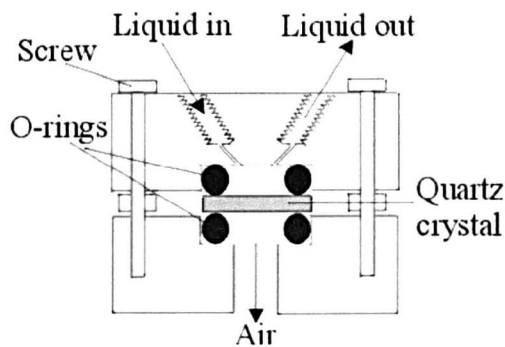
Figure 2.12 Schematic representation of the flow cell, showing the flow system of use.

2.2.1 Software development

The Hewlett Packard Visual Engineering Environment (HP VEE) is a visual programming language allowing the remote operation of an instrument via a computer interface. The user controls the instrument, via a computer, by sending a series of commands that are recognised by the instrument and then 'asks' for a reply. In this way, an instrument may be instructed to perform an operation and then asked for a response, e.g. to return the data that it has generated. In addition, HP VEE also allows the use of a number of pre-programmed (or user programmable) functions that control operations such as saving to file, data analysis, and plotting graphs. The final product is a Microsoft Windows™ based system that is controlled from a front panel consisting of mouse, or keyboard operated boxes, switches and/or menus.

A block diagram showing the key steps of the program is shown in Figure 2.13. The HP VEE program commands the network analyser to perform a number of pre-programmed functions in the correct order, at an interval determined by the operator and then to return the data that is generated to the PC for storage and analysis. Initially the analyser is re-set and a calibration function is performed to remove systematic errors from the analyser, test fixture and connections. A three term calibration is used which involves measurement of the circuit open, shorted, and with a 50 Ω resistor inserted. Following calibration a broad-band impedance sweep is initiated in order to locate the approximate position of the TSM sensor resonant frequency. This is followed by a narrower impedance sweep in order to determine the series resonance frequency of the sensor. The reason for the broader impedance sweep is to ensure that the resonance peak of the sensor is not missed, while the narrower sweep guarantees that sufficient data points are taken at and around the series resonance peak for later analysis. Only one broad impedance sweep is completed during the program, after this initial sweep the series resonance frequency of the previous narrow impedance sweep is used to predict the next. The interval between impedance sweeps of the TSM sensor is determined by the operator.

Calibration:
1. Open circuit.
2. Shorted circuit.
3. 50Ω resister.

Nominal resonant frequency. Number of data points.

Broad impedance sweep centred on the nominal resonant frequency.

Actual resonant frequency

Narrow impedance sweep

Impedance data

TSM sensor impedance data fitted to a 4-component BVD circuit.

Impedance data

Data split and saved in individual files on a PC.

Resonant frequency. Impedance data. Resistance data.

Figure 2.13 A block diagram illustrating the key steps in the network analyser program. Red type is a data input and blue text a data output.

After each sweep has been completed and the impedance spectra of the TSM sensor has been recorded the network analyser is used to fit a standard four component BVD circuit model to the data. The impedance spectra, the fitted values for the components of the BVD circuit, and the series resonance frequency of the sensor are then returned to the PC for collation and storage. The large number of individual commands and processes in the program make it impractical to discuss them individually, for further information the reader is referred to the HP VEE help program and the E5100A network analyser programming manual.

2.3 Validation of the measurement system

In order to validate the passive sensor system a comparison between the series resonance frequency recorded by the network analyser and an independently constructed active oscillator system was performed.

In an active oscillator system, the TSM sensor is part of an oscillator circuit. The sensor is connected to an amplifier, which causes it to oscillate at the resonant frequency of the sensor. This frequency is then recorded using a frequency counter. Changes in the resonant frequency of the sensor can be used to interpret changes in the mass at the sensor surface according to Sauerbrey, however changes in the material properties of the film cannot be interpreted as they are in the passive method.

The measurement equipment used in this study was based on an active measurement system designed by Bruckenstein[104].

In order to compare the two techniques lipid films were deposited on to the TSM sensors and the films measured using both the active and passive technique. The technique used to coated

the lipid films was the Langmuir-Blodgett technique, this method was also used in later studies and is discussed in greater detail in Section 3.1.

2.3.1 Method

Lipid films of two fatty acids were coated onto TSM sensors using a Langmuir-Blodgett trough. 1 mg mL^{-1} solutions of stearic and arachidic acid were made in chloroform. Approximately 40 μL of the fatty acid solution was dropped on to a zinc sulphate subphase using a syringe. The lipid film was compressed at a rate of 20 cm^2 min^{-1} and the TSM sensor then dipped through the compressed monolayer at a rate of 10 mm min^{-1}. The sensor was then removed and allowed to dry in air for approximately 5 mins or until excess water had disappeared from the surface. The frequency of the TSM sensor was measured blank and then at odd numbers of fatty acid monolayer using both the active and passive measurement system. The shift in resonant frequency, determined using the two measurement techniques, was plotted and a fitted using a linear regression function in KaleidaGraph™. Gradients and coefficients of determination were obtained from the linear regression.

2.3.2 Results and discussion

Figure 2.14 shows the correlation between the active (oscillator circuit) and passive (network analyser) measurement systems on loading of a TSM sensor with fatty acid films. Two short chain, unsaturated fatty acid films, arachidic acid (c 14) and stearic acid (c 12), are presented.
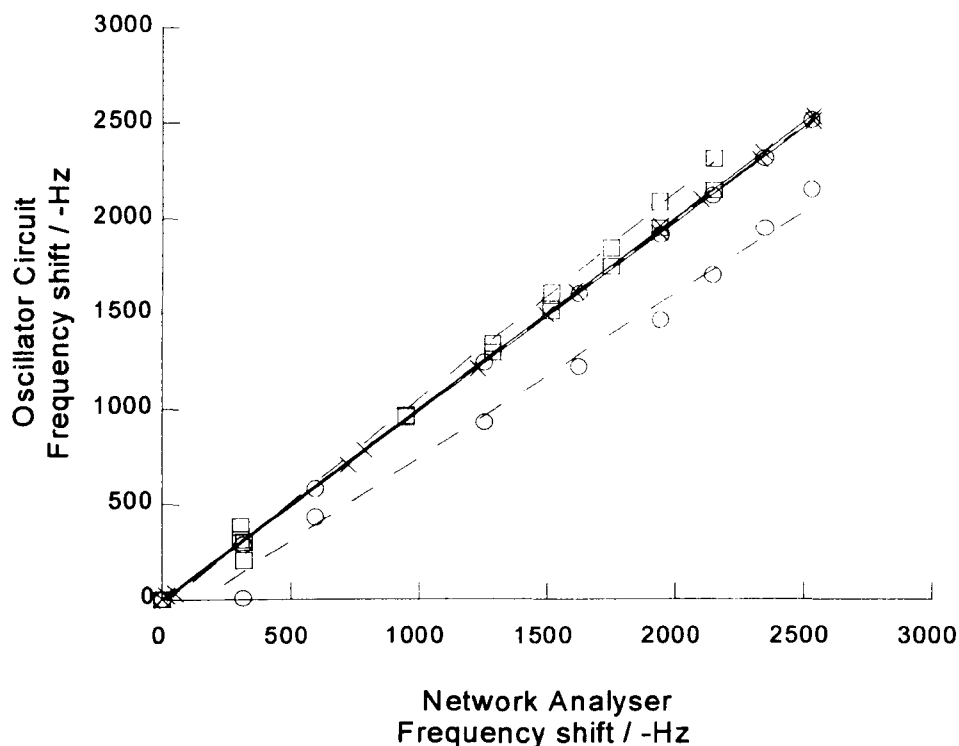
Figure 2.14 Correlation between TSM sensor frequency shifts measured using either an oscillator or network analyser technique. Unbroken lines represent the stearic acid films, the broken lines represent arachidic acid films, and each symbol represents a replicate (n=3).

Three replicates of each fatty acid film are plotted and each has been fitted with a straight line, the gradients of which are shown in Table 2.2. The coefficients of determination (R^2) for the lines (0.9885-0.9999) indicate that the linear regression fits the data points well (an R^2 of 1 indicating a perfect fit).

Table 2.2 Gradients of the fitted lines for three TSM sensors coated with fatty acid films. R^2 is the coefficient of determination.

Curve fit	Gradient	R^2
Arachidic acid (1)	1.00	0.9999
Arachidic acid (2)	1.00	0.9999
Arachidic acid (3)	1.00	0.9999
Stearic acid (1)	0.99	0.9998
Stearic acid (2)	0.87	0.9885
Stearic acid (3)	1.08	0.9960

The results (Figure 2.14 and Table 2.2) show that the TSM sensor frequency shift measured using the network analyser and oscillator circuit techniques correlate well. The gradients, from the straight line fits, are all close to 1 (0.87-1.08) showing that the relationship between the two methods is direct i.e. a frequency shift measured by one method is the same magnitude as the frequency shift measured by the other.

The direct correlation between the measurements made using the network analyser and oscillator circuit indicates that the analyser and the measurement software are functioning correctly. The network analyser can therefore be used reliably to perform TSM measurements.

2.4 Environmental studies

The temperature at which TSM sensor measurements are operated, can be critical to the interpretation of the results. The resonant frequency of oscillation of a TSM quartz sensor, is not only sensitive to changes in the properties of the films to which it is exposed but will also shift as a result of changes in the environmental temperature.

In order to limit the effect of the thermal environment on the TSM sensor a specific type of quartz crystal (AT cut) is usually used in the construction of TSM sensors. The AT cut is used primarily because it has a favourable temperature profile at close to room temperature. AT cuts of quartz exhibit a stable area in frequency at temperatures of approximately 0 to 60°C (Figure 2.15) compared with other cuts of quartz.
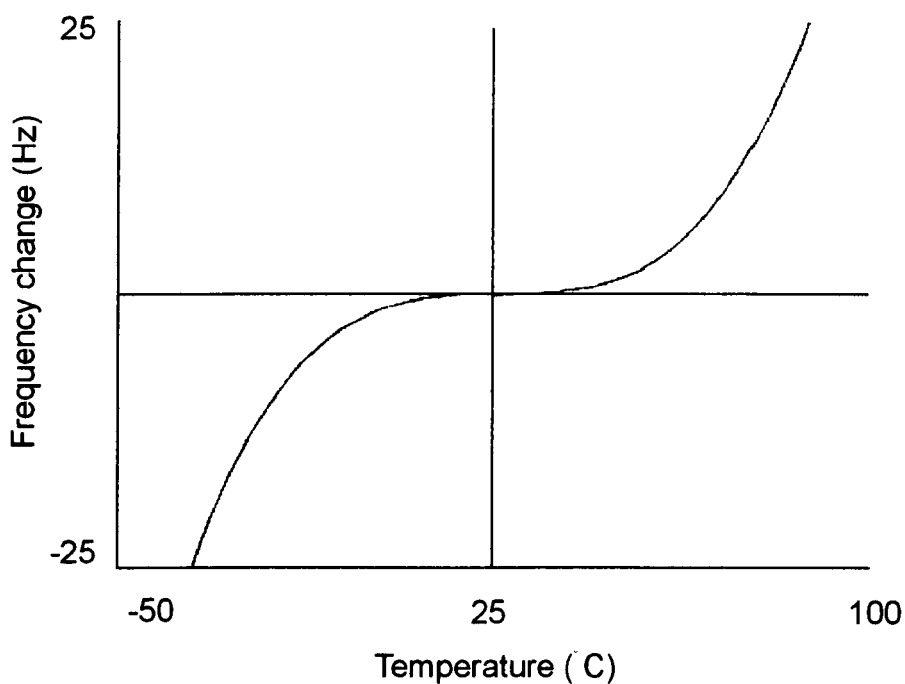
Figure 2.15 Temperature/frequency dependency of an AT cut quartz crystal. Adapted from Crystal devices data book[142].

An investigation of the temperature related frequency shift was completed on the TSM sensors used in this project. Evaluation of the temperature sensitivity of the TSM sensor in air and liquid were used to indicate what precautions, if any, are required to ensure stable measurements in subsequent experiments.

In order to obtain the shift in the resonant frequency of the TSM sensor in air, the sensor can simply be cooled and heated in a controlled humidity environment. Any fluctuations in the resonant frequency of the TSM sensor under these conditions will be a direct result of the temperature. In a liquid, however, it will be important to take into account the effect of changes in the density and viscosity of the liquid on the TSM sensor surface.

2.4.1 Methods

TSM sensors were cleaned by dipping it in piranha solution (1 part of 40% vol. hydrogen peroxide to 3 parts conc. sulphuric acid) for at least two minutes, followed by a rinse in acetone and then methanol for at least two minutes in each solvent. Between each set of cleaning processes, and at the end of the process, the crystal was rinsed with purified water (Nanopure, resistivity >17 MΩ cm^{-1}). Finally the crystal was air-dried for 30 mins or until all surface water had been removed.

2.4.1.1 Measurements in air

Cleaned sensors were placed in the network analyser measurement fixture. The fixture was then sealed inside a watertight plastic container and placed in a water bath. The container also contained dried, self-indicating silica gel to reduce the chance of condensation effecting the measurements. Impedance measurements were taken at a selection of discrete temperatures between −12.5°C and +80°C (at approximately 2°C intervals). The air temperature in the chamber was recorded using a LogIT™ temperature probe. The results were analysed using KaleidaGraph™ graphics program, via a 3rd order polynomial.

2.4.1.2 Measurements in liquid

Cleaned sensors were placed in to the liquid flow cell and connected to the PI network fixture. Purified water (Nanopure, >17 MΩ cm^{-1}) was placed in the static side of the flow cell along with a temperature probe (LogIT measurement system). The sensor was then placed in to a temperature controlled chamber and impedance measurements taken at a range of discrete temperatures between 20°C and 60°C (approximately 5°C intervals). The chamber was constructed from a copper cylinder with copper pipe wrapped around it. The copper pipe was

connected to a water bath to provide the temperature control. The results were analysed using

KaleidaGraph™ graphics program.

2.4.2 Results and discussion

2.4.2.1 Measurements in air

The temperature/frequency dependency of the TSM sensor investigated (Figure 2.16) is largely

as expected for AT cut crystal in air (Figure 2.15). The frequency shift of the sensor is small at

a broad range of temperatures at around room temperature (0-55°C), but large and significant

frequency shifts occurred at temperatures below 0°C and above 55°C. Bellow 0°C a very fast

drop in the frequency of the TSM sensor occurs.
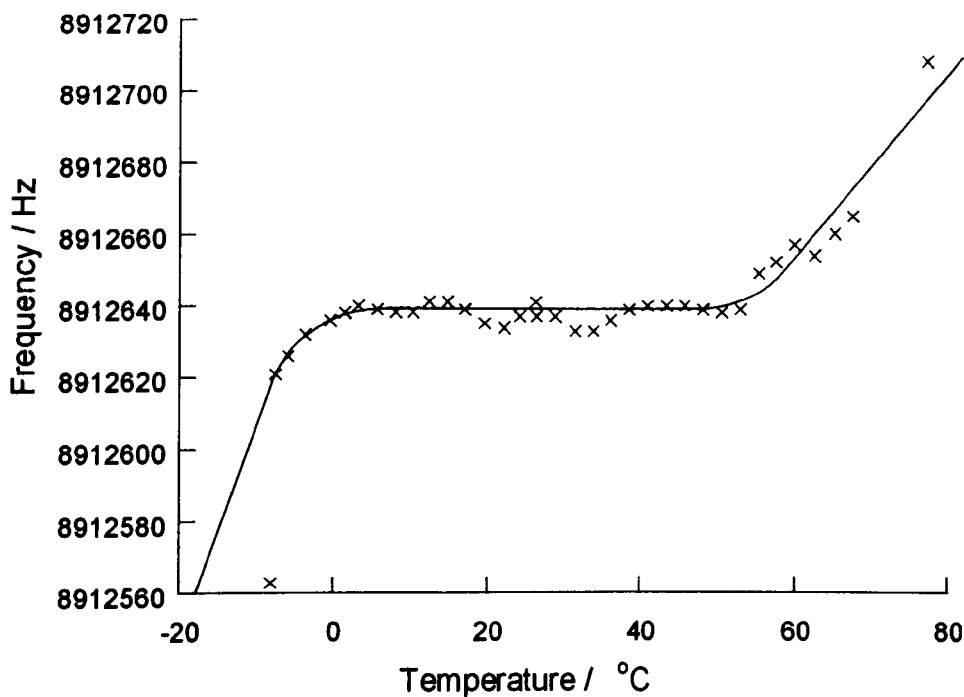
Figure 2.16 The temperature dependency of frequency for an AT cut TSM sensor.

The frequency/temperature profile (Figure 2.16) of the TSM sensor highlights the need for care in controlling the temperature of the experiments. It is imperative that all experiments are performed in the plateau region of the temperature profile and that large changes in experimental temperature are avoided. If experiments are performed outside of the plateau region, a reference sensor will be required to allow adjustment of the frequency shifts with reference to a baseline. However, within the plateau region, the measurements made using the TSM sensor are reasonably insensitive to changes in the environmental temperature and therefore measurements can be made using the system at room temperature.

Below 0°C a very fast drop in the frequency shift of the TSM sensor occurs, it is likely that this is due, in part, to experimental conditions. Despite the desiccant in the chamber it is likely that some condensation of water vapour occurred on the crystal electrodes at very low temperatures, this water would cause a decrease in the sensor frequency in addition to that caused by the temperature decrease. Special care must therefore be taken at low temperatures to ensure that condensation cannot occur during TSM sensor studies.

2.4.2.2 Measurements in liquid

The frequency/temperature profile of TSM sensors in a liquid environment (in this case water) is shown in Figure 2.17. The frequency of the TSM senor has been expressed as the frequency shift (using the first data point as the zero frequency) rather than as the absolute frequency as in Figure 2.16. The temperature range in this experiment has been reduced to between 20°C and 60°C; this temperature range is more representative of the experimental conditions that will be used in later investigations.

As TSM sensors are sensitive to both the mass and material properties of any film coated on to its surface any change in the density and viscosity of the liquid will affect the frequency and

resistance of the TSM sensor. The equation suggested by Kanazawa and Gordon[95] (Equation 2.2, Appendix 1) demonstrates this relationship. As the density viscosity product of the Newtonian liquid under investigation decreases (as it does with increasing temperature) it is expected that the frequency of the TSM sensor to increase. The theoretical effect of density and viscosity on frequency over the temperature range under investigation is plotted in Figure 2.17. For a change in temperature from 20°C to 60°C the difference in the predicted frequency shift is 466 Hz, or 11.7 Hz °C^{-1}. This demonstrates the importance of controlling temperature when TSM sensor measurements are made in a liquid environment.
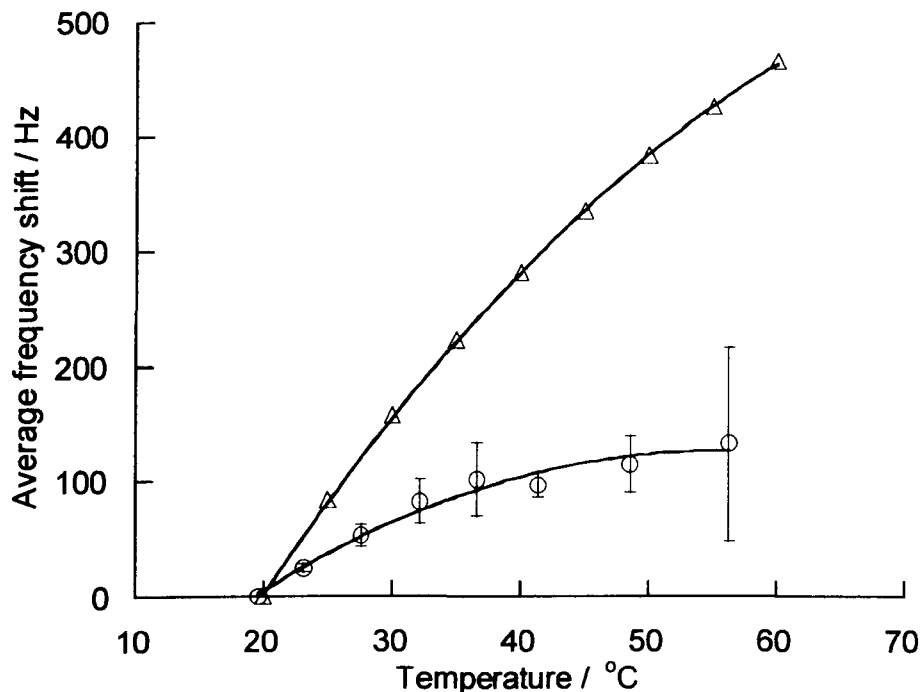
Figure 2.17 Change in frequency with temperature for TSM sensors in water (n=3). Circles are experimental data, while triangle represent the theoretical calculations based on the change in density and viscosity of water.

The change in temperature of a TSM sensor in liquid (Figure 2.17) is much greater than that for a TSM sensor in air (Figure 2.16). This increased shift is due to the greater sensitivity of the sensor response to temperature dependant changes in the density and viscosity of the liquid compared to the temperature dependant changes in the properties of quartz.

When the experimental frequency shift is compared to the theoretical it is possible to see that it is smaller than predicted. The relationship between the frequency shift and temperature also appears to be slightly different from the theoretical. Initially (20 to 37 °C) the experimental results follow the same trends as the theoretical but with a reduced magnitude. Above 37 °C the experimental results appear to level off, a trend that is not exhibited by the theoretical results. It is therefore likely that two different processes are responsible for the discrepancies seen between the two sets of data.

Initially (20 to 37 °C) the discrepancy between the magnitude of the theoretical and experimental data is probably due to the lack of calibration of the system. Simple assumptions used in the Kanazawa equation when calculating the theoretical data could account for this. The calibration of the TSM sensor system will be addressed in the next Chapter, when a Langmuir-Blodgett transfer system will be used to deposit characterised films on the sensor surface.

The reason for the discrepancy above 37 °C could be either due to experimental or theoretical reasons. The Kanazawa relationship does not appear to adequately describe the physical relationship between frequency and the density viscosity product at these higher temperatures for our system. This divergence is probably an artefact associated with the experimental set-up possibly caused by the formation of gas bubbles on the sensor surface as the temperature is increased.

Since that material properties of the film coated on the TSM sensor are being altered in this experiment it is not only the frequency of the TSM sensor impedance spectrum that will be affected, the shape of the spectrum will also change. Figure 2.18 shows the effect that the change in temperature has on the resistance of the TSM sensor at resonance. This is expressed as the shift in resistance using the initial resistance at 20°C as the zero. Theoretical calculations of resistance were made using Equation 2.15 (Appendix 1)
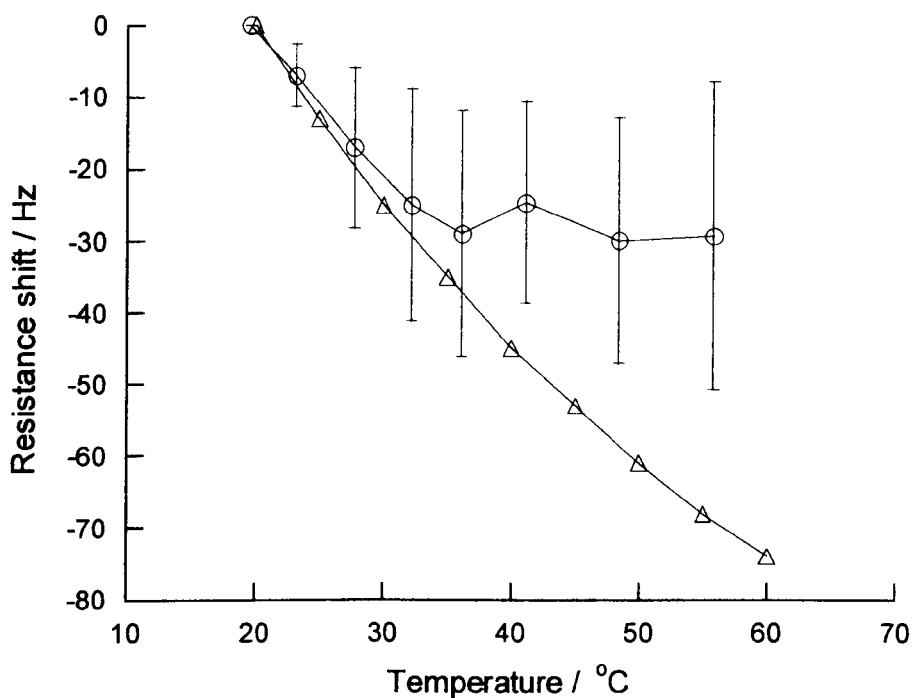
Figure 2.18 Change in resistance with temperature for TSM sensors in water. Circles are experimental data, while triangle represent the theoretical calculations based on the change in density and viscosity of water.

Figure 2.18 demonstrates that as the temperature of the liquid increases (i.e. the viscosity density product decreases) the resistance measurement for the TSM decreases. This change in

the resistance is a result of a change in the dampening of the TSM sensor by the liquid. As the liquid become less viscous and dense the oscillation of the TSM sensor, is dampened less and therefore the resistance is reduced.

The data in Figure 2.18 demonstrates a similar trend to the frequency results shown in Figure 2.17. Between temperatures of between 20 and 37 °C the experimental resistance shifts closely mimic the theoretical, however, above 37 °C the experimental shift levels off and differs from the theoretical.

For TSM sensor measurements in liquids it is therefore important to take into account the liquid that is under investigation and make a decision as to whether the temperature of the measurement system needs to be controlled or the effects of density and viscosity need to be taken into account. For measurements where the temperature of the TSM sensor is deliberately changed to elicit an effect from a film, e.g. an investigation of the phase behaviour of a lipid film, then the changes in environment especially for liquids must be taken into account.

2.5 Summary

This chapter is concerned with the development of the TSM sensor system, including its validation and the effect of the environments on the measurements:

- Validation of the TSM sensor and control software was made by comparison of film mass measurements with an independently constructed device. Data obtained using the two devices possessed a high degree of correlation.

- The effect of temperature on TSM sensor measurements made in air was investigated. As expected a sigmoidal type relationship was demonstrated for the AT cut TSM

sensors used in this project. Frequency measurements were found to have changed little between 0 to 55 °C giving a good stable region in which experiments could be completed.

- Investigations into the effect of temperature on TSM sensor measurements in liquid environments demonstrated the importance of the environment on these types of measurements. Clear shifts in both frequency and resistance were measured over the temperature range investigated. This experiment demonstrates the importance of control measurements in this type of study.

3 COATING STUDIES OF LIPID FILMS

This chapter is concerned with investigations into the deposition of lipid films onto TSM sensors. Different coating methods, types of sensor, and lipids were investigated to produce a well-characterised system that could be used as a model for the stratum corneum. The resulting TSM biosensor will be used to investigate the partitioning of drug molecules into, and the fluidity of, lipid membranes (Chapters 4 and 6).

Previous studies have demonstrated that it is possible to deposit lipid films onto the measurement electrodes of TSM sensors using a wide variety of different techniques. Langmuir-Blodgett technique has been utilised to coat film forming amphiphiles, such as oleic acid[143] and phospholipids[144] onto sensors. Films of polyion complexes[145] and phospholipids[146] have been cast onto TSM sensors to form bilayer model lipid membranes. Membranes have also been formed from liposome solutions[140], by pre-treating the surface of the sensor with chemical spacers[147], and self-assembled monolayers have been investigated using TSM sensors[148, 149]. The membranes used in these studies usually do not constitute more than one or two film forming amphiphiles. In order to develop a model for biological membranes, such as the skin, it will be necessary to deposit a more complicated lipid mixture.

Two methods have been used, in this investigation, to deposit lipid films onto TSM sensors; these are the Langmuir-Blodgett technique (Section 3.1) and a spin coating method (Section 3.2). The Langmuir-Blodgett technique was chosen in this study, as the films it produces are well documented, and reproducible and therefore facilitate the characterisation of the biosensor system. Use of the Langmuir-Blodgett technique will also provide additional information on the quality of the films that are under investigation. Unfortunately Langmuir-Blodgett films are not a good mimic for most naturally occurring lipid membranes as they produce very close

packed and well ordered bilayer systems. In order to addresses this, a spin coating technique was also employed. Spin coated lipid bilayers have a greater degree of tortuosity and therefore this system should provide a better mimic of naturally occurring membranes.

In order to better understand the systems that we are working with, several different membranes, possessing different degrees of complexity, have been investigated. Initially alkanoic acid (commonly referred to as fatty acids) membranes, were investigated as they are widely available and easily coated onto the gold substrates using the LB technique. Later in the investigation, a more complex mixture of fatty acids and cholesterol was used as this is a closer mimic for the stratum corneum.

Initial coating studies were performed on three fatty acid films: stearic acid, arachidic acid, and behenic acid (Figure 3.1). Stearic acid, arachidic acid, and behenic acid are long chain, saturated carboxylic acids with a carbon chain length of between 18 and 22 atoms. They tend to adopt a fully extended confirmation (not shown in Figure 3.1) as this minimises steric repulsions between neighbouring methylene groups. Saturated fatty acid pack efficiently into crystal structures with van der Waal bonding between the fatty acid chains.
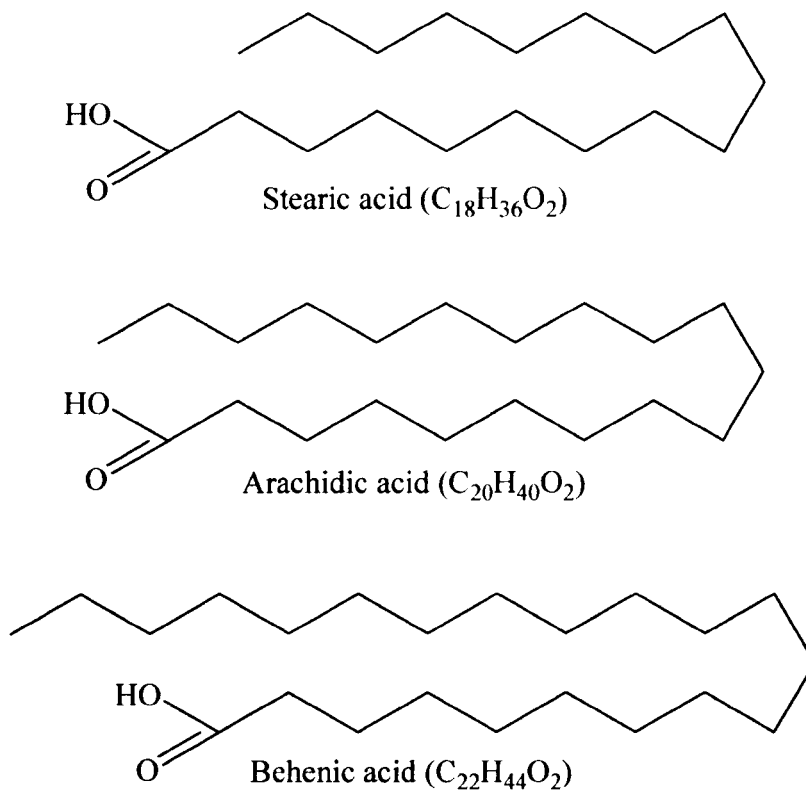
Figure 3.1 The chemical arrangement of stearic, arachidic acid, and behenic acid.

While fatty acids are a major constituent of the stratum corneum lipids (making up around 10 %w/w of the total amount. Table 1.1), other major classes of lipid are also present. In order to better mimic the composition of the stratum corneum lipids, a lipid matrix designed used by Moghimi *et al.*[2] has been adopted. The lipid matrix comprises a mixture of saturated and unsaturated fatty acid molecules, cholesterol, and antioxidants (Table 3.1).

Table 3.1 Composition of lipid matrix.

Component	Source	Purity (quoted)	% weight in matrix
Stearic acid	Sigma	Approx. 99 %	7.2
Palmitic acid	Sigma	Min.99 %	27.1
Myristic acid	Sigma	99-100 %	2.8
Oleic acid	Sigma	Approx. 99 %	24.4
Linoleic acid	Sigma	Min. 99 %	9.2
Palmitoleic acid	Sigma	Approx. 99 %	2.7
Cholesterol	Sigma	99 +%	26.7
Butylated hydroxyanisole	Sigma	Min.99 %	0.01
Butylated hydroxytoluene	Sigma	Min. 99.0%	0.01

The structure of these lipids is shown in Figure 3.2.
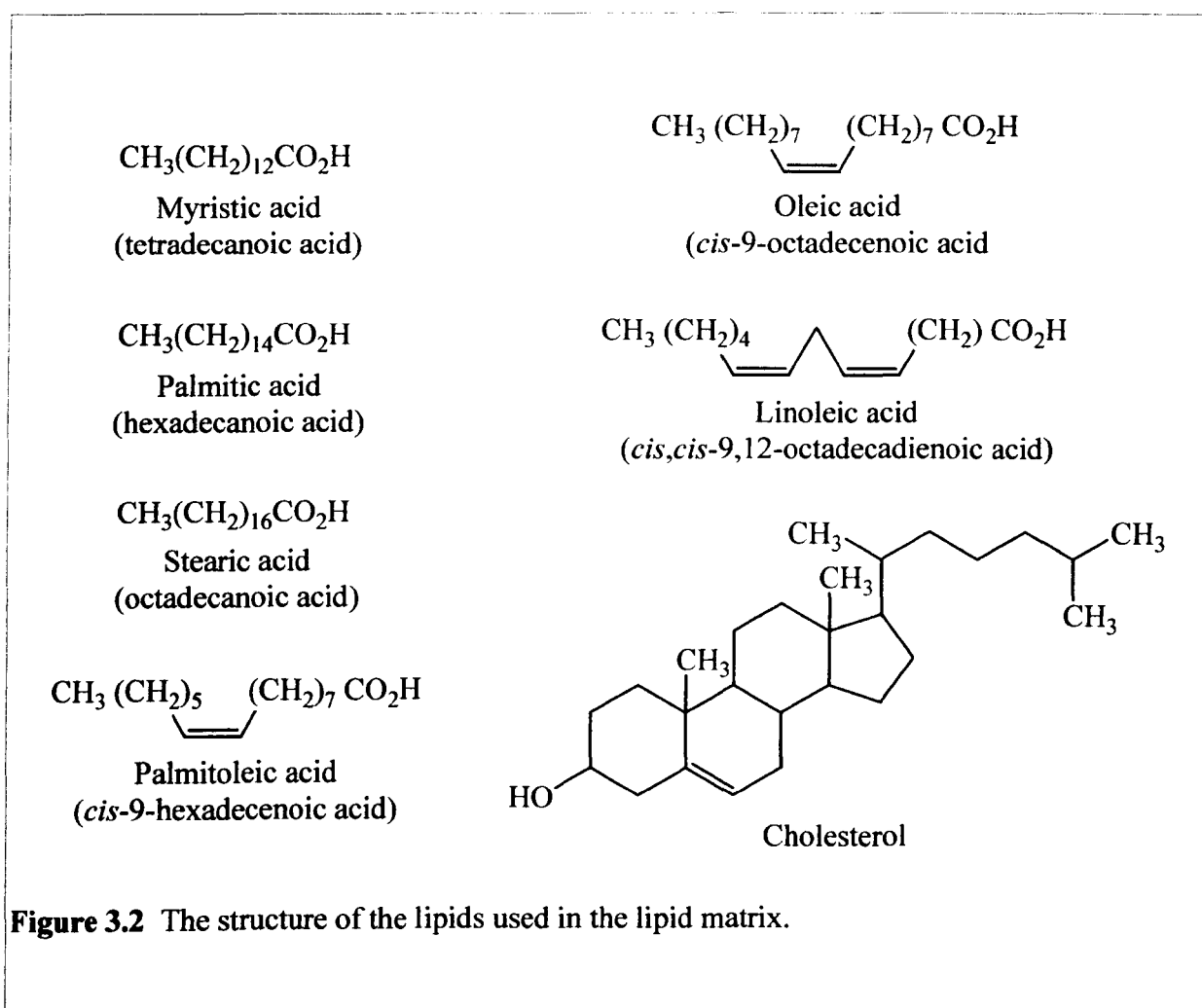
Figure 3.2 The structure of the lipids used in the lipid matrix.

The fatty acid fraction of the lipid matrix consists of both saturated (e.g. myristic, palmitic, and stearic acids) and unsaturated (e.g. palmitoleic, oleic, and linoleic acids) molecules. The

unsaturated fatty acids will add a degree of disorder to the membrane because unlike the saturated fatty acid they have 'kink' in the carbon chain, caused by the '*cis*' configuration of the double bond. The unsaturated fatty acids will tend to reduce the packing density of the membrane. The incorporation of fatty acids into membranes can increase and decrease the rigidity of the membrane depending on the fatty acid chosen.

Cholesterol is present in almost all animal tissues, its inclusion in the lipid matrix is therefore important. In phospholipid membranes cholesterol has important functions in the formation of domain structures and in the ordering of the membranes. The rigid structure of cholesterol reduces the movement of the first 10 to 12 carbons in the alkyl chain of the phospholipid molecules while increasing the movement of the lower part of the chain due to the increased space available, these effects are dependant on the cholesterol concentration and temperature[150]. In the skin cholesterol interacts with ceramide moieties in a similar way to phospholipids. However the smaller headgroup of the ceramide molecules means that the disruptive effect of cholesterol is expected to be bigger[150]. The disruptive effect that cholesterol has on the mainly fatty acid lipid matrix can therefore be expected to be quite large.

One major lipid component of the stratum corneum is missing from the lipid matrix model, the ceramides. Ceramides are an important constituent of the stratum corneum membrane, replacing the phospholipid component of other membranes. In this project they have been left out of the model membrane to simplify the initial development and characterisation of the biosensor. A more complex mimic for the stratum corneum is planned once the technique has been developed.

Initially the Langmuir-Blodgett technique will be used to coat the lipid films onto the TSM sensor for characterisation.

3.1 Langmuir-Blodgett film deposition

The Langmuir-Blodgett (LB) method was pioneered by Katherine Blodgett under the supervision of Irving Langmuir in the 1900's and later become known as the Langmuir-Blodgett technique. While the Langmuir-Blodgett technique was first used by Langmuir and Blodgett, the idea of studying monolayer films had been around for a while, the study of the spreading of oil on water being recorded by the Babylonians in the 18th century BC[151]. It was Lord Rayleigh though who really initiated this branch of physical chemistry.

A 'trough' containing a monolayer of lipid molecules spread onto a liquid sub-phase is used to produce LB films. A barrier on the surface of the sub-phase is used to compress the monolayer of lipid, until a confluent film of lipid is produced. The substrate is then dipped through the lipid film, thereby allowing transfer of lipid from the trough to the substrate. This process is monitored by means of a sensitive device that measures the surface pressure of the lipid layer on the sub-phase.

Surface pressure measurement

Surface tension measurements of the monolayer are made in order to monitor the formation of the monolayer and the coating process. The tensiometer used to perform the surface pressure measurements consists of an accurate balance and a strip of PTFE filter paper known as a Wilhelmy plate (Figure 3.3). The Wilhelmy plate is attached to the balance and the tip submerged in the sub-phase of the LB trough. It is possible to calculate the surface tension of the liquid from the force exerted, and the dimensions and weight of the plate.
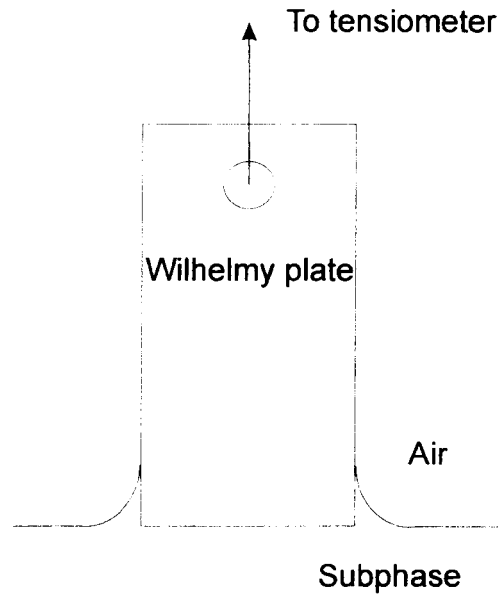
Figure 3.3 Wilhelmy plate, used for surface tension measurements.

By monitoring the surface tension in relation to the position of the trough barrier (and therefore the surface area of the film) it is possible to determine important information about the lipid film.

Isotherms

An isotherm (Figure 3.4) is the plot of the surface tension/pressure on the originate verses the molecular area of the film, as measured from the barrier position, on the abscissa. It is possible to characterise the compression of the lipid monolayer from the characterisation of the isotherm plot and observe the changes in lipid phase that occur as the molecules are compressed.
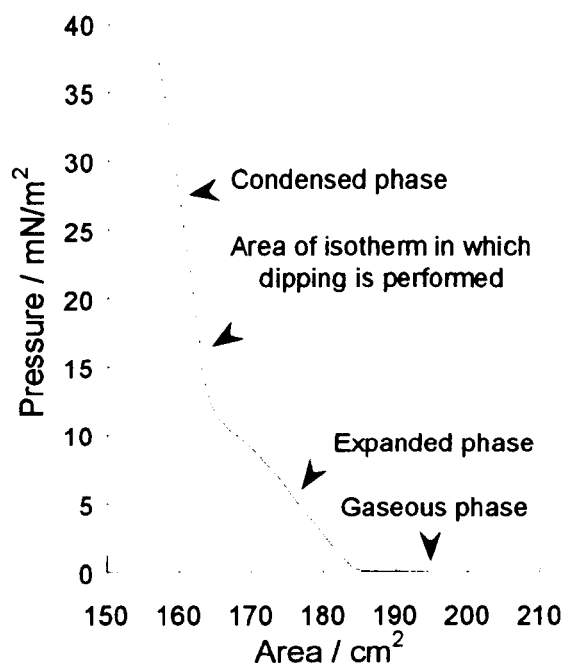
Figure 3.4 A typical isotherm measured for arachidic acid.

Figure 3.4 shows the typical behaviour of a lipid monolayer as it is compressed. The various phases result from the increased interaction of lipid molecules as they are forced closer together. The gaseous phase occurs when the lipid molecules are spread over a large surface area and do not interact with each other, rather like a gas. As the monolayer is compressed, a phase change occurs and the surface pressure starts to increase as the monolayer is compressed. At this stage, short-range molecular interactions begin to have an effect, and the monolayer behaves in a manner similar to that of a liquid. The monolayer is then said to be in the expanded or liquid phase. The final phase change is from the expanded phase to the solid, or condensed phase. The change from the expanded phase to the condensed phase is characterised by a change in the gradient of the isotherm and results from the consolidation of molecules into an orderly (regular) 2 dimensional array (very much like that exhibited by a 3

dimensional solid). For fully saturated fatty acids, such as stearic acid and arachidic acid, the molecules pack very closely together with the hydrocarbon chain positioned vertically from the surface of the sub-phase.

Lipid deposition

Three different types of lipid deposition are possible, which are termed arbitrarily X, Y, and Z (Figure 3.5). Most lipids deposit in the Y type mode with head groups associating with head groups and tail groups with tail groups. This type of deposition is the one that most closely resembles the lipid membranes of the body. X and Z type deposition occur when the head group of one-molecule associates with the tail of another, thereby resulting in multilayers with all molecules orientated in the same direction. X deposition is when the tail fixes to the substrate and Z deposition when the head group fixes to the substrate. Care must be taken when the film appears to deposit in an X or Z fashion, as it is often simply due to patchy film adhesion. In this case cleaning methods should be reviewed.

Y type deposition   Z type deposition   X type deposition
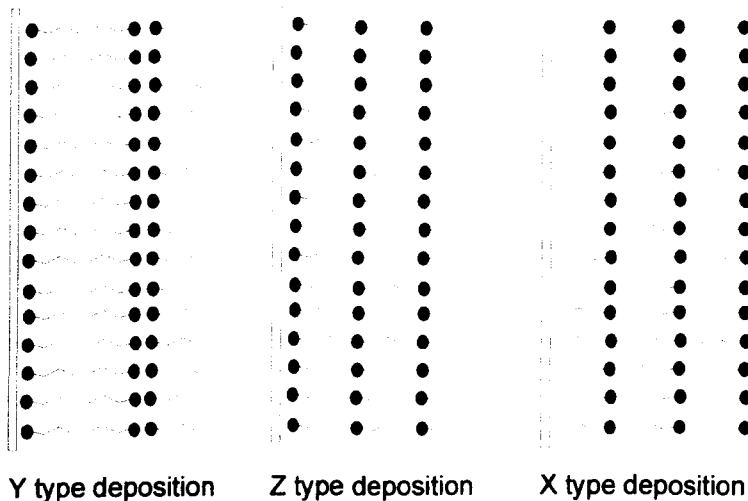
Figure 3.5 Different types of lipid deposition.

For hydrophilic surfaces (e.g. the gold electrodes of a TSM sensor) deposition does not usually occur on the first down-stroke of the substrate through the monolayer and sub-phase. The attraction of the water and the substrate usually causes the meniscus to be pulled across the surface of the substrate thereby preventing lipid from being coated onto the substrate. Lipid molecules will normally be coated onto hydrophilic substances on the first up-stroke of the substrate and then every subsequent pass.

Sub-phase

The majority of LB films are coated onto an aqueous based sub-phase. The composition (especially the metal ion content), pH, and temperature of the sub-phase can have various effects on the quality of the films that are transferred by the LB technique.

The metal ion content of the water sub-phase is important to the type and quality of film. It is the valancy of the ion that is the critical parameter when metals are included into the sub-phase. For example cations with a valency of 1 (e.g. Na^+, and K^+) will increase the solubility of fatty acids in water and will causing micelles to be formed thereby destabilising the monolayer. Cations with a valency of 2 (e.g. Ca^{2+}, and Cd^{2+}) also form the soap of the carboxyl group of fatty acids, but rather than driving the film towards the formation of micelles these soaps are insoluble in water and so form stable monolayers. In addition divalent metal ions will extend the solid region of the isotherm because each metal ion associates with two fatty acid molecules, thereby enabling a more tightly packed monolayer to form.

It will therefore be important to investigate the effect of subphase composition on the lipid films coated using the Langmuir-Blodgett technique. Three different sub-phases (zinc sulphate, calcium sulphate, and water) were investigated as part of these studies.

3.1.1 Method

TSM sensors were cleaned by dipping them in piranha solution (i.e. 1 part of 40 % vol. hydrogen peroxide to 3 parts conc. sulphuric acid) for at least two minutes, followed by a rinse in acetone and then methanol for at least two minutes in each solvent. Between each cleaning processes, and at the end the crystal was rinsed with purified water (Nanopure, resistivity >17 MΩ cm^{-1}). Finally the crystal was air-dried.

Solutions of arachidic acid, stearic acid, or behenic acid in chloroform were prepared at an approximate concentration of 1 mg ml^{-1} and stored in a fridge <8 °C. A sub-phase (comprising either 10^{-3} M zinc sulphate solution, 10^{-3} M calcium sulphate solution or water) was freshly prepared using purified water (resistivity >17 MΩ cm^{-1}). All glassware was thoroughly rinsed with chloroform and purified water prior to use. No plastic containers were used.

The LB trough was cleaned and operated as follows. All parts of the trough were wiped over using surfactant-and-lint free tissues, impregnated with chloroform. Powder free gloves were worn at all times when operating the Langmuir-Blodgett trough. The sub-phase was spread onto the LB trough until the base of the meniscus of the sub-phase reached the top of the compartment sides. The pressure sensor was zeroed and an isotherm of the sub-phase measured (at a barrier speed of 150 mm min^{-1}). If the pressure had not deviated from zero by more than 0.3 N m^{-2} then the surface was assumed to be clean. If the pressure did deviate by more than 0.3 N m^{-2}, then a vacuum pump and fluid trap were used to remove the surface layer; the trough was topped up with fresh sub-phase solution and the process repeated until a clean isotherm was produced.

A 100 μL glass syringe was used to drop 1 mg mL^{-1} lipid solution onto the sub-phase surface, until the pressure started to rise slightly (~10 N m^{-2}). Approximately 50 μL was normally

sufficient. The barrier was opened until the pressure sensor read zero and then an isotherm was constructed (at a barrier speed of 20 mm min^{-1}) by plotting the pressure of the monolayer against the area of the monolayer. The pressure at which the monolayer entered the condensed phase (Figure 3.) was then taken from the isotherm. The control software for the trough was configured to maintain a constant pressure just above that at which the monolayer entered the condensed phase. For the lipid matrix films, the pressure just before the monolayer collapsed was taken from the isotherm. The control software for the trough was configured to maintain a constant pressure at this point.

A cleaned quartz crystal was dipped through the monolayer surface (at speed of 5mm min^{-1} for the fatty acid films and 1 mm min^{-1} for the lipid matrix films). The first dip (up and down) was assumed to deposit one monolayer where as subsequent dips were assumed to deposit two monolayers (these assumptions were consistent with the change in area of the film surface). 13 monolayers of the fatty acid were deposited on to the TSM sensor. After deposition of each monolayer the TSM sensor was allowed to dry in air for approximately 5 min or until all excess water was removed (as determined by visual inspection). The TSM sensor impedance spectra was then recorded using the HP E5100A network analyser.

3.1.1.1 Deposition of fatty acid films using the Langmuir-Blodgett technique

Stearic, arachidic, and behenic acids were deposited onto cleaned, unpolished TSM sensors using the Langmuir-Blodgett technique. The sub-phase used for this deposition was a 10^{-3} M zinc sulphate solution. The shift in resonant frequency of the TSM sensor was determined from the impedance spectra. The theoretical and experimental mass of each Langmuir-Blodgett layer coated was calculated using the Sauerbrey relationship. Results were plotted and fitted using KalidaGraph™.

3.1.1.2 Effect of TSM sensor surface roughness on the deposition of fatty acid films

The effect of the TSM sensor surface roughness on the deposition of three fatty acid films (stearic, arachidic, and behenic acid) was investigated. Two different types of AT-cut quartz resonators were used in the TSM sensor experiment. Unpolished TSM sensors, with a nominal resonant frequency of 9 MHz and an electrode area of 0.19 cm^2 were obtained from EG and G (Wokingham, Berks). Polished TSM sensors with a nominal resonant frequency of 8 MHz and an electrode area of 0.4 cm^2 were obtained from two sources *viz* International Crystal Manufacturing (Oklahoma, USA) and Ieuan Jenkins Ltd (Mid Glamorgan, Wales).

3.1.1.3 Effect of sub-phase composition on the deposition of Langmuir-Blodgett films.

The effect of sub-phase composition on the deposition of fatty acid films by the Langmuir-Blodgett technique was investigated. Cleaned, polished 8 MHz TSM sensors were coated with 1 mg mL^{-1} stearic, arachidic, and behenic acid films. Three different sub-phase compositions were investigated: 10^{-3} M solution of zinc sulphate, 10^{-3} M solution of calcium sulphate, and purified water.

3.1.1.4 Investigation of the fluidity of fatty acid films deposited using the Langmuir-Blodgett technique.

Stearic, arachidic, and behenic acid multilayers were deposited onto polished TSM sensors using the Langmuir-Blodgett technique and a 10^{-3} M calcium sulphate subphase. The fluidity of these fatty acid films was investigated using the impedance spectra of the TSM sensor. The impedance spectra were plotted using KalidaGraph™. Resistance measurements were obtained by fitting the TSM sensor impedance spectra to the Butterworth van Dyke equivalent circuit. Comparison of these two techniques for the interpretation of changes in the material properties of films coated on to a TSM sensor was made.

3.1.1.5   Deposition of lipid matrix films using the Langmuir-Blodgett technique

A 100 mg mL^{-1} solution of the lipid matrix was prepared according to the formula in Table 3.1; this solution was then diluted to 1 mg mL^{-1} for coating purposes. The lipid matrix solutions were stored in a fridge < 8 °C. All glassware was thoroughly rinsed with chloroform and purified water prior to use. No plastic containers were used. Polished TSM sensors were coated with the lipid matrix using a sub-phase of 10^{-3} M solution of calcium sulphate. Experimental and theoretical data was plotted using KalidaGraph™ and compared to arachidic acid films coated using the same conditions.

3.1.2   Results and Discussion

3.1.2.1   Deposition of fatty acid films using the Langmuir-Blodgett technique

In order to assess the method by which the fatty acid films are coated onto the TSM sensor, the lipid transfer and the Langmuir-Blodgett trough isotherms have been analysed. Figure 3.6 is an isotherm produced by the compression of arachidic acid on the Langmuir-Blodgett trough using a zinc sulphate subphase. This isotherm is typical of all the fatty acid films coated using the Langmuir-Blodgett trough (subphase composition did not effect the isotherm). The isotherm shows three distinct phases for the compression of fatty acid on the Langmuir-Blodgett trough, gaseous (>220 cm^2), liquid (approx. 220 to 190 cm^2), and solid (<190cm^2) phases and is consistent with isotherms reported in the literature for this type of film.
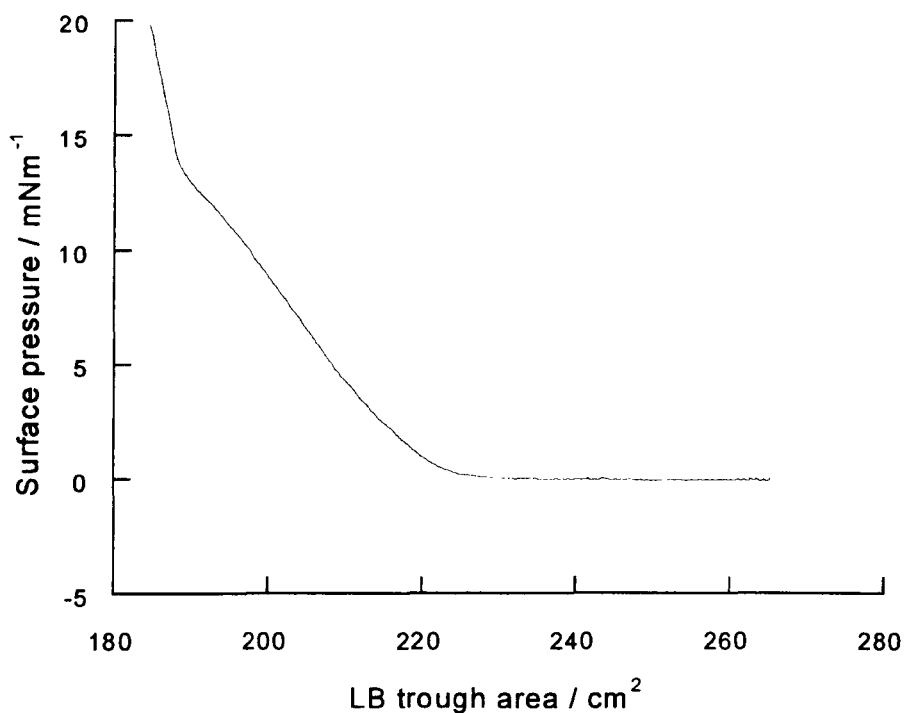
Figure 3.6 Isotherm of an arachidic acid monolayer coated onto a Langmuir-Blodgett trough.

The data plotted in Figure 3.7 demonstrates the relationship between the Langmuir-Blodgett trough area and the position of the TSM sensor as it is dipped through the fatty acid monolayer. Using this it is possible to gain important information about the transfer of the lipid onto the TSM sensor. The data plotted in Figure 3.7 was recorded for the coating of arachidic acid onto a polished TSM sensor using a zinc sulphate subphase. Figure 3.7 is typical of all the fatty acids films and the process was found to be the same when the subphase or sensor was changed. Only the first three dips of the TSM sensor through the monolayer are shown, subsequent dips were identical to dips two and three.
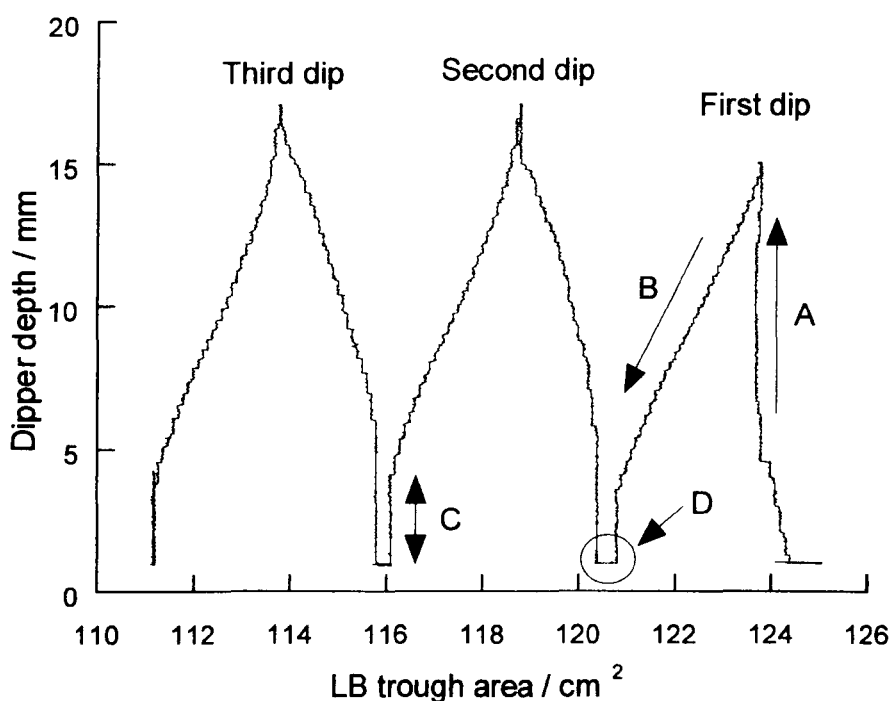
Figure 3.7 Graph showing the transfer of arachidic acid from the Langmuir-Blodgett trough to the TSM sensor. (A) the coating downstroke, (B) the coating upstroke, (C) the time when the sensor is not in contact with the monolayer, and (D) baseline drift.

The peak shapes for most of the dipping processes are symmetrical, with an equal change in the trough area on the downstroke (labelled A) of the dipper, as on the upstroke (labelled B). This suggests that the transfer of lipid to the TSM sensor is both even and reproducible. The only exception to this is the first dip, which shows no change in the trough area on the downstroke of the dipper. The vertical portion of the Graph (labelled C in Figure 3.7) results from the time when the TSM sensor is not in contact with the monolayer and therefore no coating occurs. The area of Figure 3.7 labelled D is the result of small instabilities in the monolayer on the Langmuir-Blodgett trough. In between the Langmuir-Blodgett dips the monolayer film was left for approximately 10 min while the coated TSM sensor was measured. Region D is the

result of the loss of a small amount of lipid from the monolayer into the sub-phase while the measurement process occurs.

The shape of the transfer peaks (Figure 3.7) is consistent with Y-type lipid deposition (Section 3.1). In Y-type deposition, no lipid is deposited onto the substrate on the downstroke of the first dip, and coating begins on the first upstroke. The reason for this is due to electrostatic repulsion between the hydrophilic surface of the sensor and the hydrophobic hydrocarbon chains of the lipid molecules. This means that a monolayer and not a bilayer, is deposited on the first dip. The symmetrical transfer of lipid to the TSM sensor for subsequent dips indicates that for each complete sensor dip a bilayer is transferred to the TSM sensor.

Knowing the type of lipid deposition that was occurring was important as it is required to make the theoretical calculations used later in this Section. The theoretical mass loading for each lipid film was calculated using the Sauerbrey equation to allow comparison with experimental results. The mean area occupied per lipid molecule was calculated* using data obtained from the Langmuir-Blodgett trough (Table 3.2). From the mean area per lipid molecule it was possible to calculate the number of lipid molecules on the TSM sensor surface and therefore the theoretical mass loading.

---

* This calculation was made in the condensed phase. The number of lipid molecules per unit area was calculated using the volume and concentration of lipid and the barrier position of the trough at constant pressure.

Table 3.2 Calculated molecular areas from the Langmuir-Blodgett trough.

Fatty acid molecule	RMM	Molecular area / nm^2	Mean molecular area / nm^2	Standard deviation
Stearic acid	284.5	0.194 0.205 0.204	0.20	0.006
Arachidic acid	312.5	0.186 0.194 0.195	0.19	0.005
Behenic acid	340.6	0.195 0.196 0.196	0.20	0.001
Lipid matrix	300.1[*1]	0.266 0.263 0.266 0.264 0.287	0.27	0.010

The experimental mean molecular areas for stearic, arachidic and behenic acids (Table 3.2), correlate well with values reported in the literature $(0.19nm^2)$[152]. No literature values are available for the lipid matrix film. The results demonstrate that there is a clear difference between the mean molecular area in monolayers formed using a single fatty acid molecule, e.g. arachidic acid, from those constructed from the lipid matrix (t-test, $p<0.05$). This result is not surprising as the lipid matrix contains a number of molecules that we would expect to alter the structure of the monolayer. While stearic acid, arachidic acid, behenic acid, and myristic acid are all saturated fatty acid, with a straight hydrocarbon chain, the lipid matrix contains several unsaturated fatty acids. Palmitoleic acid, oleic acid, and linoleic acid are all unsaturated fatty acids in the '*cis*' configuration. The 'kinks' in the hydrocarbon chains of the unsaturated molecules will therefore mean that theses molecules will take up more space than the straight chain saturated fatty acids. The inclusion of cholesterol in the monolayer would also be

---

[*1] The RMM used is the average RMM for the lipid matrix. This was calculated using the RMM of the individual components and the proportion of them in the matrix.

expected to increase the mean molecular area. Cholesterol has a larger diameter than the saturated fatty acids, as it contains a number of hydrocarbon ring structures.

The difference in the molecular area of the fatty acid and the lipid matrix monolayers might also indicate a difference in the fluidity of the monolayers. Langmuir-Blodgett films of unsaturated fatty acids are usually very densely packed, especially when a multivalent metal ion has been included to reduce the electrostatic repulsion of the head groups. This is demonstrated by the molecular area for the three unsaturated fatty acid films in Table 3.2, which approaches the diameter of the molecule $0.19nm^2$. We would therefore expect little opportunity for molecular movement within the monolayer. The discontinuity added to the system by the unsaturated fatty acids and cholesterol should allow greater fluidity of the membrane. The fluidity of lipid membranes, in particular the lipid matrix, is discussed in greater detail in Chapter 4.

Figure 3.8 shows the mass increase associated with coating up to 13 monolayers of fatty acid onto a cleaned unpolished 9MHz TSM sensor, using a zinc sulphate sub-phase. Each TSM sensor was coated with a different fatty acid film (either stearic acid, arachidic acid, or behenic acid). The experiment was repeated three times and the mean mass change plotted against the number of layers coated.
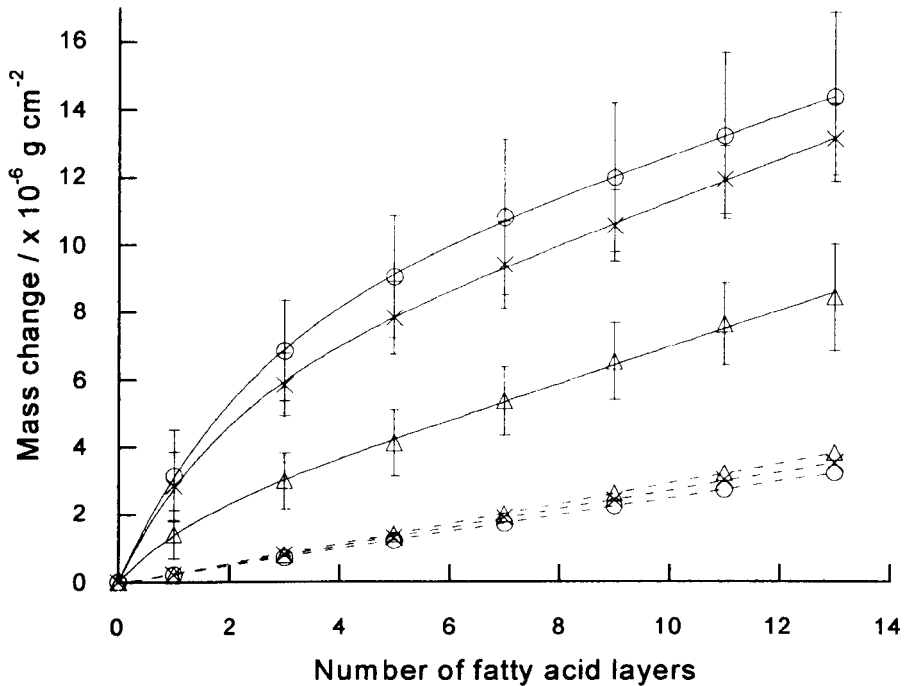
Figure 3.8 Theoretical (broken line) and experimental (continuous line) frequency shifts for three different fatty acids coated using a Langmuir-Blodgett trough using a zinc sulphate sub-phase. Circles represent stearic acid, crosses arachidic acid and triangles behenic acid.

Figure 3.8 shows that the increase in mass calculated using the experimental results is much higher than that calculated theoretically. The experimental results are non-linear, having an initial sharp increase in mass followed by a slower linear increase. The gradients of linear region of the results appear to be greater for the experimental data than for the theoretical data.

It is believed that two separate processes dictate the differences observed between the experimental and theoretical results. The non-linear portion of the experimental results in

Figure 3.8 is most likely to be due to the lipid films not coating on to the TSM sensor as predicted and could be explained by a number of different theory:

1. The entrapment of sub-phase between the lipid films and the TSM sensor a possible reason for the discrepancies between the experimental and theoretical responses. The unpolished TSM sensors used in this experiment have rough surfaces, which, as Schumacher[110] demonstrated (Section 2.1.1.1), can have a large effect on the results obtained. One possible reason for the higher than expected mass shifts is that some of the sub-phase is being 'trapped' in the surface roughness of the crystal. A possible representation of this model is shown (Figure 3.9).

Lipid layers

Trapped water

Quartz crystal
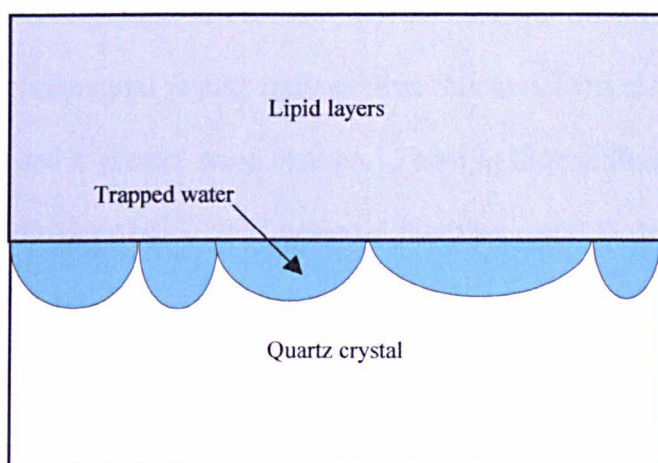
Figure 3.9 A representation of the model proposed to explain the higher than expected frequency shifts.

2. It is possible that the choice of sub-phase in the experiment might affect the lipid films coated onto the TSM sensor surface. It is known that the inclusion of metal ions in the sub-phase can affect the packing of the lipid monolayer on the Langmuir-Blodgett trough, it may be possible that the metal ions are also effecting it on the sensor.

After the initial non-linear relationship the experimental data exhibits a linear increase in mass as more monolayer are added to the TSM sensor surface. Even here, however, the relationship is not as predicted as the experimental data has a larger gradient than the theoretical. These differences in the gradients are probably due to a systematic error in the Sauerbrey calculation used. The most likely reason being the underestimation of the surface area of the TSM sensor. Underestimation of the surface area would mean that more lipid was being coated onto the TSM sensor surface than accounted for in the theoretical calculations.

One other difference between the experimental and theoretical results exists in Figure 3.8. If the relationship between the experimental mass changes and the RMM of the fatty acid is inspected in Figure 3.8 a further discrepancy between the experimental and theoretical results is apparent. The theoretical plots show that we would expect the behenic acid monolayers to have the highest mass change, this is because behenic acid has the highest relative molecular mass, however, the experimental results indicate that this is not the case and that stearic acid and arachidic acid caused a greater mass change. There is little difference between the mass shifts for arachidic and stearic acid. It is believed that this result is due to differences in the TSM sensors used in the investigation. In this experiment the same TSM sensors were used to take the measurements for each lipid film. When the sensors for arachidic acid and behenic acid were swapped and the experiment repeated it was found that the mass change was switched, arachidic acid had the smallest mass change (results not shown). This demonstrates the importance of the individual TSM sensor in the measurements and highlights the need to switch TSM sensors for each replicate in future experiments. The variation between measurements made with different TSM sensor also highlights a potential source of variation in the experiments.

3.1.2.2 Effect of TSM sensor surface roughness on the deposition of fatty acid films

In an attempt to reduce inter-sensor variation and to investigate the effect of sensor surface roughness on the results the TSM sensors used in the investigation were changed. TSM sensors (8 MHz) manufactured using polished quartz, which have a reduced surface roughness were chosen for the comparison. The three fatty acids (stearic, arachidic, and behenic acid) were coated on to the polished TSM sensors using a zinc sulphate subphase (Figure 3.10).
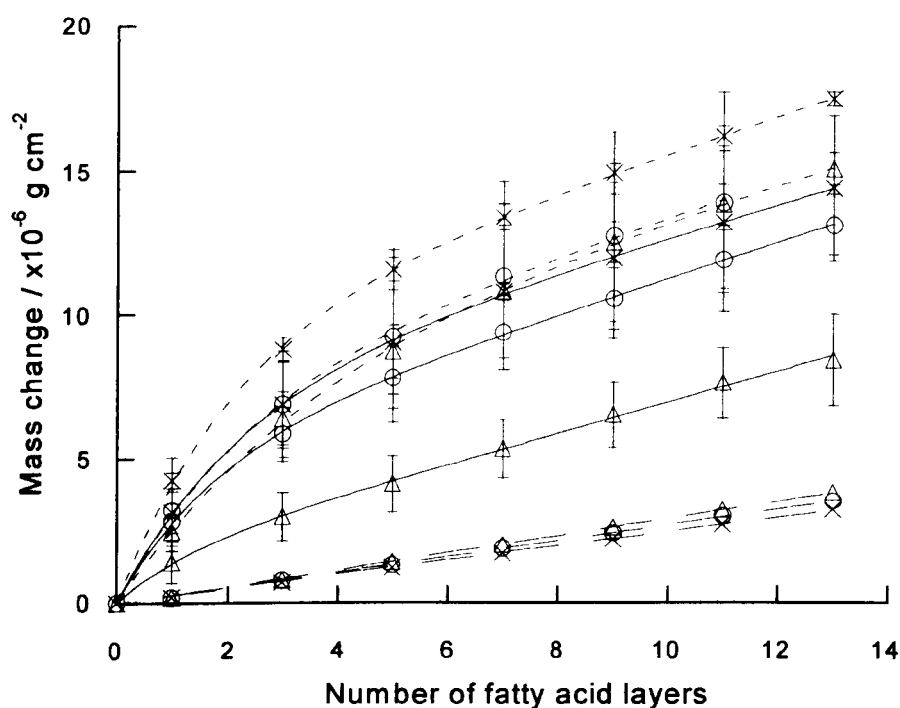
Figure 3.10 A comparison of fatty acids coated on to polished (short broken lines) and unpolished (unbroken lines) TSM sensors, also shows the theoretical value (long broken lines). Crosses represent stearic acid, triangles behenic acid, and circles arachidic acid.

Figure 3.10 show that there is no difference between the mass change measured using polished or unpolished TSM sensors. Only the behenic acid films coated onto unpolished TSM sensors differ significantly from the other films. This is the same measurement that was reported as having a low mass change Figure 3.8, a result that was shown to be due to the particular TSM sensor being used. Since none of the other TSM sensors demonstrate such a small shift it is believed that this result is an anomaly.

Clearly the use of polished TSM sensors has no effect on the Langmuir-Blodgett coating of fatty acid films. This demonstrates that the differences between the experimental and theoretical results are not due to the entrapment of sub-phase in the surface roughness of the TSM sensor.

The difference between the theoretical and experimental results can be explained by a new model in which more fatty acid is coated on to the surface of the crystal due to a larger than expected surface area. If the surface of the TSM sensors is rough (undulating) then the area of that surface will be larger than measured.

Assuming that the surface of the sensor consists of raised hemispheres on a flat base (the height of these hemispheres, determined using AFM, is approximately: unpolished TSM sensor = 1 micrometer, polished TSM sensor = 50 nanometer). Using Equations 3 and 4 we can determine the ratio of the surface area for a rough surface (comprised of raised hemispheres) to a smooth one (perfectly flat):

$$\text{Area of a hemisphere is } A = 2\pi r^2$$

Equation 3.1

$$\text{Area of a circle is } A = \pi r^2$$

From the equations above, it is apparent that the ratio of surface area for a flat surface to one composed of hemispheres will always be 2, irrespective of the radius (i.e. no matter what the size of the surface roughness is the surface area will always be the same). This theory assumes that the surface roughness is shaped like a hemisphere, but a similar relationship is also true for flattened (short and wide) hemispheres and cones, as long as the ratio of the shape height to radius is the same for the rough and polished crystals.

3.1.2.3 Effect of sub-phase composition on the deposition of Langmuir-Blodgett films.

Figure 3.11 shows the frequency shift for arachidic acid deposited onto 8 MHz polished TSM sensors using water, calcium sulphate, and zinc sulphate sub-phases. This experiment was completed to determine the effect that the Langmuir-Blodgett trough subphase had on the coating of the lipid films onto the TSM sensor.
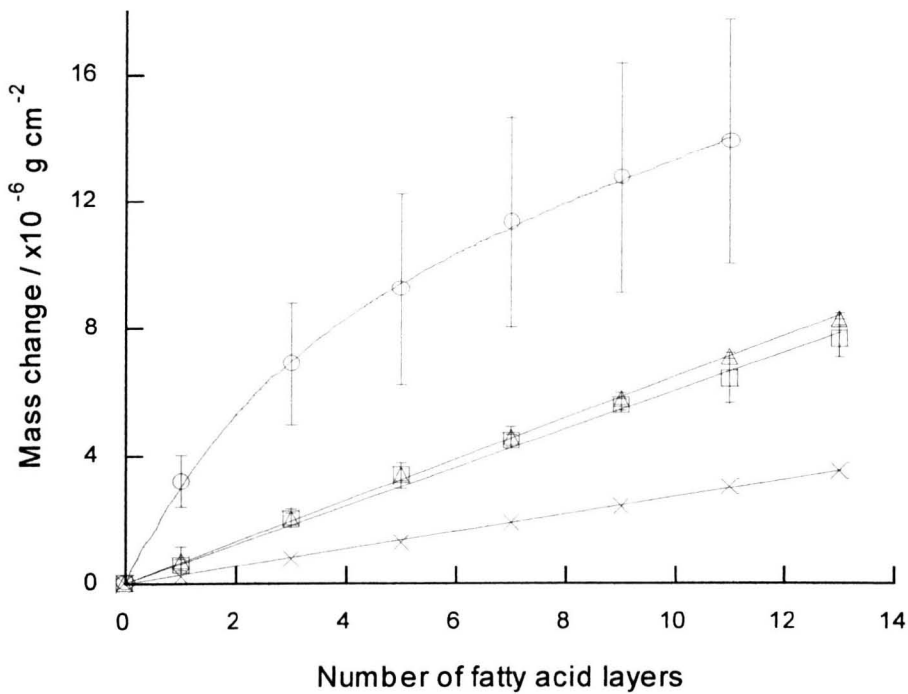
Figure 3.11 Graph showing the effect of sub-phase composition on the mass of the fatty acid mono and multilayers coated. Circles represent the zinc sulphate sub-phase, triangles the water sub-phase, squares the calcium sulphate sub-phase, and crosses the theoretically calculated result.

Figure 3.11 shows that the composition of the sub-phase used in the Langmuir-Blodgett trough clearly has an effect on the coating of the fatty acid monolayer onto the TSM sensor. The fatty acid films coated from water or calcium sulphate sub-phases are of reduced magnitude compared to the films coated using the zinc sulphate sub-phase and show a linear relationship. Inspection of the gradients of the linear parts of the fits show that the gradients for experimental results are approximately the same, and are higher than those of the theoretical data. There are no significant differences between the films coated using the water and

calcium sulphate sub-phases, though both films still produce a larger than predicted mass increase.

The results for the calcium sulphate and water sub-phases clearly demonstrate that the presence of zinc in the layers must have an effect on the composition of the film that differs from the effect of calcium. These differences revolve around the zinc ions and the way that they interact with the fatty acid films and could be due to the uptake of sulphate ions or water, or by affecting the conformation of the lipid layers causing them to coat as micelles rather than monolayers. Further research is required to work out what is happening. The most likely explanation for the results obtained probably lies in a combination of physical changes to the film, which are promoted by the adsorption of zinc onto the solid surface of the sensor.

The only difference in lipid coating observed was that of the monolayer films on the water sub-phases, which were less stable than those coated using a sub-phase containing multi-valent ions (Ca^{2+} or Zn^{2+}). This is because of the interactive forces between the negatively charged polar head groups of the fatty acid molecules. When a sub-phase containing a positively charged metal ion is used, these neutralise the negative charge on the head groups and allow them to associate closer together without becoming unstable. The result of this is that monolayers coated from a water sub-phase often had to be recoated on to the Langmuir-Blodgett trough in between sensor dips.

While the presence of the zinc ions in the sub-phase clearly explains the non-linear nature of the mass relationship it does not explain the differences in gradient that have been demonstrated at higher numbers of monolayers deposited onto the sensor. The most likely explanation for this is the underestimation of the TSM sensor surface area.

3.1.2.4 Investigation of the fluidity of fatty acid films deposited using the Langmuir-Blodgett technique.

The fluidity of the lipid membranes under investigation is an important consideration in TSM measurements. Measurement of the impedance characteristics of the lipid coated TSM sensor will allow interpretation of the material properties of the films.

Figure 3.12 shows the series resonant peak for a TSM sensor coated with different numbers of monolayers of behenic acid. The change in mass reported earlier in this Section is also evident from these spectra as the decrease in frequency of the series resonant peak with the increased number of lipid monolayers on the sensor surface. As expected for thin lipid layers such as the fatty acid films deposited in this Section there is little difference between the shapes of the uncoated TSM sensor impedance spectrum and the coated TSM sensor impedance spectra. This indicates that the lipid films coated are behaving rigidly on the surface of the TSM sensor.
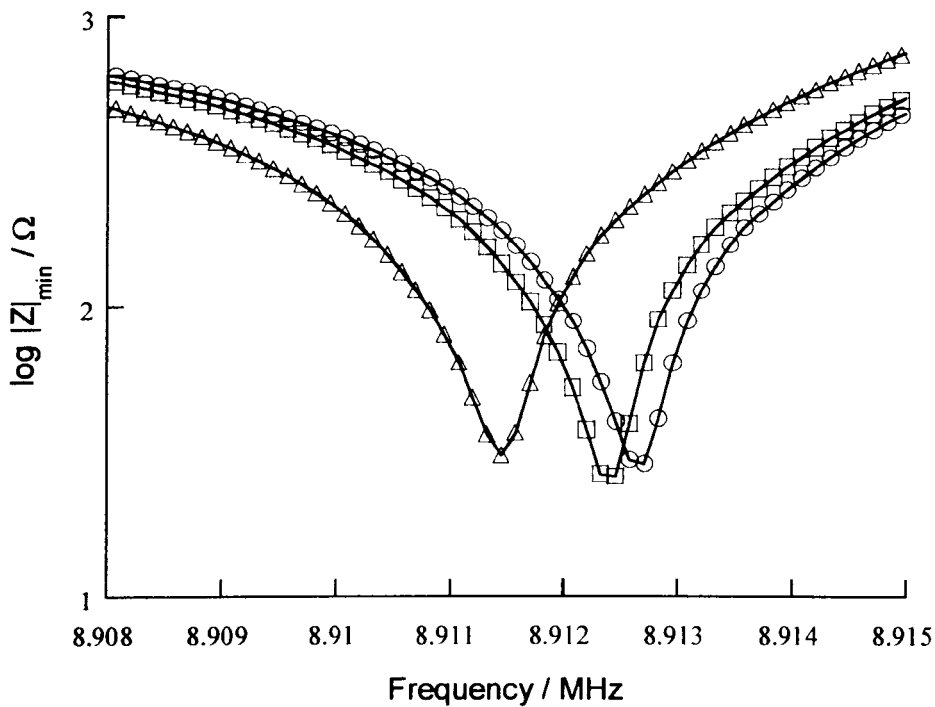
Figure 3.12 Impedance spectrum for mono and multilayers of behenic acid. Circles is the impedance spectra for the blank sensor, squares the impedance spectra with 1 monolayer of behenic acid, and triangles with 13 monolayers of fatty acid.

Another method to assess the change in the impedance spectrum is the measurement of the resistance of the TSM sensor at series resonance (Section 2.1.1.2). The resistance measurements will aid the assessment of any changes in the fluidity of the film, and are obtained from a mathematical fit to the impedance data (such as that presented in Figure 3.12).

Table 3.3 shows that there is no change in the resistance between the blank TSM sensors and those coated with thirteen layers of lipid. The data presented in Table 3.3 was normalised using the blank sensor as the zero measurement. The results indicate that no dampening of the TSM sensor oscillation has been detected and the lipid film is behaving rigidly over the

number of lipid layers measured. While the resistance measurements do not present any additional information on the fluidity the lipid membranes under investigation they do allow the quantification of any shifts that are occurring. Resistance measurements will therefore be the predominant method by which the fluidity of the lipid membranes is assessed in future chapters.

Table 3.3 Resistance measurements for TSM sensors coated with stearic, arachidic, and behenic acid.

Number of layers	Stearic acid replicates			Resistance / Ω Arachidic acid replicates			Behenic acid replicates		
	1	2	3	1	2	3	1	2	3
0	20	16	17	19	18	26	21	24	31
1	23	19	21	16	20	21	19	27	27
3	20	17	17	16	15	22	20	27	29
5	22	23	19	18	17	21	19	29	32
7	35	19	20	18	17	20	23	30	31
9	27	20	18	21	20	24	18	33	30
11	34	22	24	23	25	29	21	33	30
13	31	24	20	27	29	37	20	32	31

Analysis of the data in Table 3.3 demonstrates a high degree of variability in the shift in resistance between the blank TSM sensors and ones coated with 13 layers of fatty acid (mean resistance shift = 4.8 Ω, standard deviation 4.9). This variability should have little effect on the suitability of the sensor system to assess changes in membrane fluidity. Much larger shifts in resistance are expected to be present for the thicker spin coated films, this will make this variability less significant.

3.1.2.5 Deposition of lipid matrix films using the Langmuir-Blodgett technique

Following the successful characterisation of the TSM sensor measurement system using the simple fatty acid molecules a more complex arrangement of lipids (termed the lipid matrix) was coated onto the TSM sensor using the Langmuir-Blodgett technique. Figure 3.13 shows the change in the mass loading of the TSM sensor following coating with arachidic acid and the lipid matrix films.
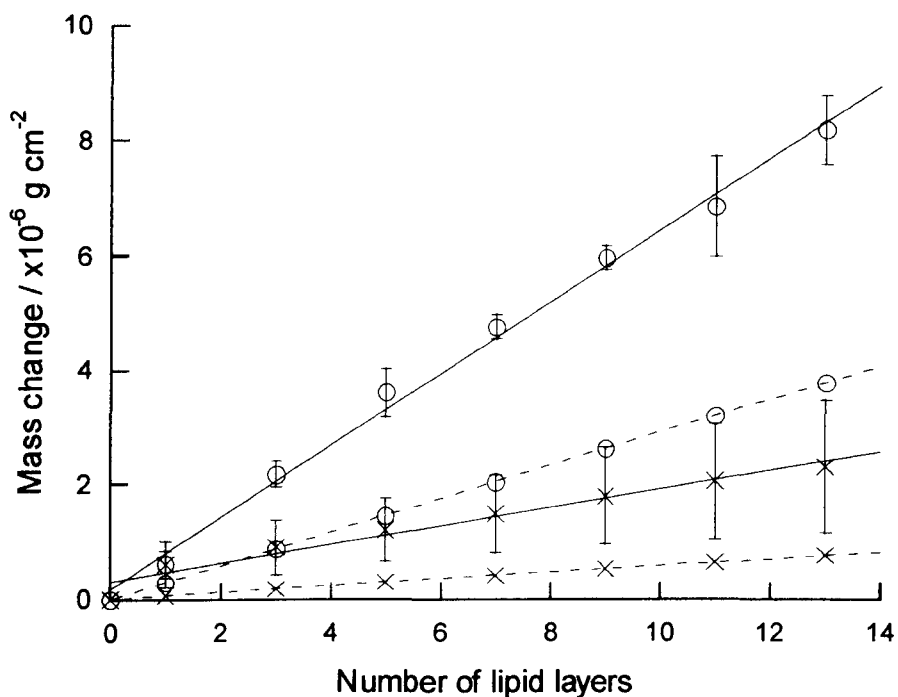
Figure 3.13 Frequency for TSM sensors with the lipid matrix (crosses) and arachidic acid (circles) coated using a calcium sulphate subphase. Broken lines represent the theoretical relationship while the unbroken line is the experimental data.

Figure 3.13 shows that the relationship between the mass loading and number of layers is the same for the lipid matrix as it was for the fatty acid films (arachidic acid is included on the graph as an example). In both cases the relationship is linear and approximately double for the experimental data that of the theoretical data. Therefore, the difference in magnitude between the theoretical and experimental results can be explained by the underestimation of the surface area of the sensor. This provides further support for this explanation of the difference.

Figure 3.14, the impedance spectra for the TSM sensor coated with the lipid matrix shows no difference in the fluidity of the lipid matrix film between one and thirteen monolayers. This result is similar to those that were shown for the fatty acid film coated earlier in the study.
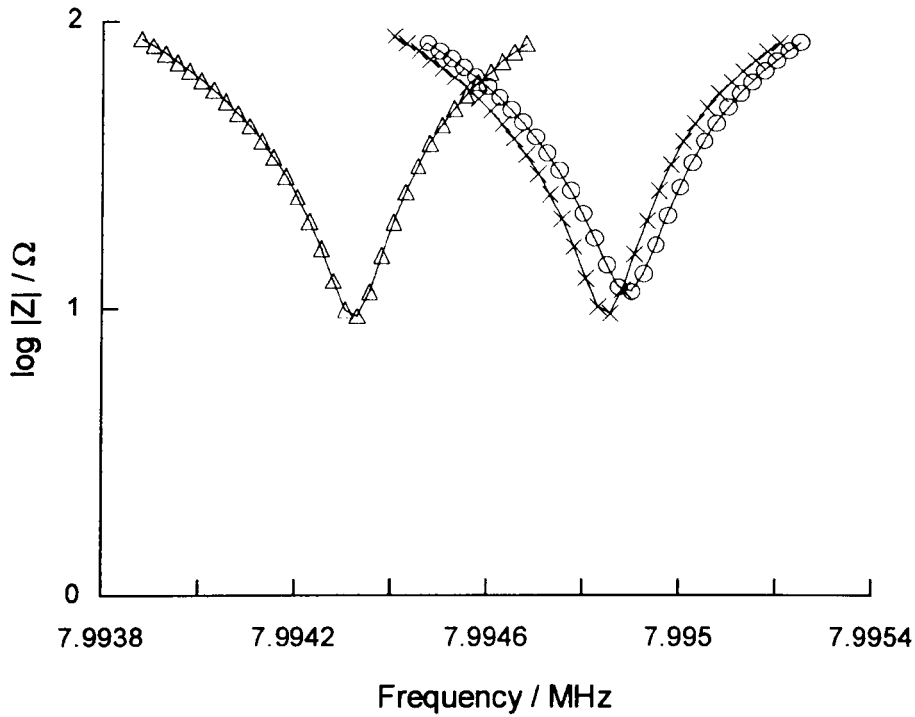
Figure 3.14 Impedance spectra for mono and multilayers of the lipid matrix. Circles is the impedance spectra for the blank sensor, crosses the impedance spectra with 1 monolayer of behenic acid, and triangles with 13 monolayers of fatty acid.

The results of the lipid matrix coating have not highlighted any major differences in the coating or measurement of the lipid films compared with the fatty acid films used to characterise the measurement system. The frequency shifts for both the arachidic acid and lipid matrix films showed the same relationship between the number of layers coated and the frequency shift. The impedance spectra show no detectable change in the fluidity of the lipid films over the range of the coating used in these experiments.

3.1.3 Summary

Four lipid films were deposited onto the TSM sensor using the Langmuir-Blodgett technique. Stearic, arachidic, and behenic acid films were deposited and used to characterise the sensor system. Later a lipid matrix film designed to mimic the stratum corneum was deposited.

- Initial deposition of the 3 fatty acid films using a zinc sulphate subphase revealed clear differences between experimental and theoretical results. Two processes appeared to be effecting the deposition of the lipid layers. One (a non-linear process) affected the coating of the first couple of monolayers of lipid onto the sensor, the other (linear) related to the underestimation of the surface area of the TSM sensors used.

- Investigation using rough and polished TSM sensors revealed that the surface roughness of the TSM sensor did not appear to effect the measurement of Langmuir-Blodgett lipid films.

- The sub-phase from which the Langmuir-Blodgett films were deposited was shown to have a substantial effect on the resulting lipid layers. It was demonstrated that by using a water or 10^{-3} M calcium sulphate sub-phase the non-linear behaviour observed in the initial coating studies could be eliminated. The zinc sulphate sub-phase was effecting the manner in which the lipid was deposited on to the TSM sensor.

- The fluidity of the Langmuir-Blodgett deposited lipid layers was investigated. Resistance measurements revealed that there was no detectable change in film fluidity over the number of layers measured.

- A lipid matrix film, designed to mimic the stratum corneum, was coated onto the TSM sensor using the Langmuir-Blodgett technique. It was found to behave in a similar manner to the simple fatty acid films.

3.2 Spin coating

In this Section a spin coating technique has been used to investigate the lipid matrix films that were coated onto the TSM sensor in Section 3.1. The spin coating technique consists of rotating the crystal wafer of the TSM sensor at high speed while dropping a known volume of lipid onto the electrodes. This technique should allow uniform films of lipid to be reproducibly produced on the TSM sensors surface. The device that is used to produce the spin coated films consists of a rotating stage connected to an electrical motor unit, the quartz wafer is connected to the stage by means of a vacuum drawn by an external vacuum pump, and then rotated at high speed while the lipid is dropped onto the sensor surface.

The reason for the change in coating technique is that while the LB coated TSM sensor system described in Section 3.1 provides a useful method for characterising the response of the sensor to lipid films and the investigation of the lipid membranes[53], there are practical limitations to its application as a biosensor for investigating biological membranes:

1. It is difficult to coat only one electrode of the TSM sensor using the Langmuir-Blodgett technique. In the LB experiments described in Section 3.1 both electrode of the TSM sensor are coated with lipid films. In-order to investigate the partitioning of molecules into the lipid membranes it will be necessary to coat only one electrode so that the film can be exposed to drug solutions. While coating only one electrode of the TSM sensor with lipid is possible using the LB technique by horizontal dipping or covering one side of the sensor this adds unnecessary complexity to the experiments. Spin coating offers an easy way in which to coat one electrode of the sensor.

2. LB films are uniform in construction, consisting of rigid bilayer structures of lipid molecules. This type of film structure does not provide a good mimic of naturally occurring biological membranes, which tend to have a more disorganised structure consisting of tortuous domains of different lipids. Spin coated films will tend to better mimic natural lipid films by the more random manner in which they are deposited.

3. In Section 3.1 it was shown that it was difficult to coat the more complex lipid films onto the gold electrodes of the TSM sensor using the Langmuir-Blodgett technique. The transfer of the lipid film from the LB trough to the surface of the sensor was more erratic and inspection of the transfer graphs indicated that partial stripping might be occurring. The use of spin coating will alleviate this problem as the opportunity for the film to be removed by the subsequent dips has been removed. However, an additional problem may be experienced as the spin coated films have to be hydrated to organise the membrane in to bilayers, so some of the membrane may be lost during this process.

4. The LB technique is a time consuming method of coating if large numbers of bilayers are required. In order to investigate the partitioning of chemical molecules into the lipid membranes it would take days to coat sufficient bilayers onto each sensor to be able to detect the partition phenomena. A spin coating method can be used to coat much larger amounts of lipid onto the sensor in a matter of minutes.

3.2.1 Methods

A 100 mg mL^{-1} solution of the lipid matrix in chloroform was prepared according to the formulae in Table 3.1. All glassware was thoroughly rinsed with purified water prior to use. No plastic containers were used.

TSM sensors were cleaned by removal from the holder submersion in to solutions of piranha, ether, and acetone for at least 10 min in each solvent. The sensor was rinsed with nanopure water after each submersion and then dried in an oven. The sensor was returned to the holder and silver conductive paint used to restore the electrical connections.

A cleaned TSM sensor was removed from the holder and placed onto the custom made spin-coating apparatus. A vacuum was used to attach the TSM sensor to the rotating head of the coater and was then sensor spun at high speed. A 10 μL drop of 100 mg mL^{-1} lipid matrix solution was dropped on to the centre of the crystal electrode using a micropipette, and the sensor was allowed to spin for a further twenty seconds.

The lipid matrix film was hydrated by placing the coated TSM sensor into nanopure water heated to 60 °C (± 0.1 °C). The TSM sensor remained in the water for 20 min and was then removed and allowed to dry in air at room temperature for 10 min.

Impedance measurements were made on the blank, coated (pre-hydration), and coated (post-hydration) sensor using the HP E5100A network analyser. In order for the TSM sensor impedance spectrum to be measured the crystal was returned to the holder after coating, silver conductive paint was used to ensure a good electrical connection.

3.2.2 Results and discussion

Table 3.4 shows the shift in the resonant frequency of TSM sensors following spin coating with lipid matrix films. Measurements of frequency have been made both before and after hydration. The results have been normalised to zero, against the resonant frequency of the blank TSM sensor. Using the Sauerbrey equation it is possible to calculate that the approximate average mass of the lipid matrix film as 40 μg cm^{-2}. Since the spin coated films

are significantly larger than the Langmuir-Blodgett films coated earlier, the acoustic properties of the membrane are much more likely to effect interpretation of the mass using the Sauerbrey equation. Therefore the frequency shift of the TSM sensor and not the mass (calculated by the Sauerbrey equation) will be presented from now on.

Table 3.4 Frequency shift of TSM sensor after coating with lipid matrix film and exposure of the film to water at 60 °C for 20 min.

Frequency shift / Hz			Percentage difference in frequency shift
Blank	Coated	Post-hydration	
0	-5015	-4439	-11
0	-6628	-6310	-5
0	-5818	-6290	+8
0	-5289	-5309	0
0	-5466	-4702	-14
	Average		-4.4

Table 3.4 demonstrates that it is possible to coat lipid matrix films onto TSM sensors using the spin coating technique. From the shift in the resonant frequencies of the TSM sensors we can see that the films formed are significantly larger than those obtained by the Langmuir-Blodgett coating technique, having an average mass of approximately 40 μg cm^{-2} as opposed to approximately 10 μg cm^{-2}. This increased film size means that the investigation of partitioning using the spin-coated biosensor may be possible.

The results also indicate that the spin-coated films are reasonably resilient in liquid conditions. Exposure of the films to water at 60 °C resulted in very little change in the resonant frequency of the TSM sensor indicating little change in the mass of the film. It is not possible to say that no change in the mass of the film has occurred as changes in the fluidity of the film, which might be expected on hydration, could also have an effect on the resonant frequency of the TSM sensor. Changes in the fluidity of the lipid matrix film are considered in Chapter 4.

The changes in TSM sensor resonant frequency that do occur are probably due to a number of different factors that effect the lipid matrix film coat. The most likely factors that might affect

the film are the uptake of water, the reorganisation of the lipid molecules, and the loss of lipid. Inspection of the TSM sensor impedance spectrum in Chapter 4 should give some insight into these different effects on the film, as it will allow investigation of the material properties of the film.

3.2.3 Summary

Lipid matrix films were deposited onto TSM sensors using a spin coating technique. Frequency shifts demonstrated that the films coated were reproducible.

4 INVESTIGATION OF THE FLUIDITY OF LIPID MEMBRANES

The stratum corneum is widely believed to be the main barrier to the penetration of chemical molecules across the skin. Integral to the barrier properties of the stratum corneum is the packing of the intercellular lipids. Many penetration enhancers are thought to reduce the resistance to drug transport through the stratum corneum, by affecting the packing of the intercellular lipids. Some penetration enhancers have been postulated to have their action by increasing the fluidity of the lipid barrier thereby facilitating the passage of drug molecules through the skin (Section 1.1.4). Investigations of the fluidity of the stratum corneum is therefore important for gaining an understanding of the barrier function of the stratum corneum and the mechanism of action of penetration enhancers.

This Chapter investigates the possibilities for using the TSM sensor to study changes in the fluidity of lipid matrix films.

- The fluidity of spin coated lipid matrix films was investigated both before and after hydration at 60 °C. Hydration of the lipid films was performed to allow the arrangement of the lipid matrix into bilayers following deposition. It was anticipated that the arrangement of the matrix and the incorporation of water would effect the fluidity and that these changes could be monitored using the TSM sensor.

- The frequency shift and resistance of TSM sensors coated with lipid matrix films, incorporating 0 to 20 mole percent of Azone®, was investigated in an attempt to detect a concentration dependant change in the fluidity of the lipid matrix (see Section 4.1.2). This experiment was performed to demonstrate whether it was possible to detect changes in film fluidity caused by penetration enhancers.

- The effect of cholesterol inclusion in the lipid matrix was investigated. Cholesterol is an important component in the determining the structure of biological membranes. The effect of its removal on the fluidity of the lipid matrix was investigated.

- The behaviour of the lipid matrix in water was investigated at 25 °C and a range of equilibrium temperatures. It was anticipated that it might be possible to detect changes in the fluidity of the lipid films as they hydrated and when they under went phase transition.

Previously, the TSM sensor has been used as an analytical tool for the detection of the phase transition temperatures of lipid membranes both in air and liquid environments[153, 154]. Some of these measurements relied extensively on the hydration phenomena and the measurement of the increase in the film mass due to hydration at the phase transition temperature.

4.1 Method

Polished TSM sensors were cleaned by submersion into solutions of piranha, ether, and acetone for at least 10 min in each solvent following removal from the holder. The sensor was rinsed with nanopure water after each submersion and then dried in an oven. The sensor was returned to the holder and silver conductive paint used to restore the electrical connections before impedance measurements were made using a HP E5100A network analyser and PI network test fixture.

Spin coating

Lipid matrix films were deposited on cleaned TSM sensors by a spin coating technique. The TSM sensor was removed from the holder and placed onto the custom made spin-coating apparatus. A vacuum was used to attach the TSM sensor to the rotating head of the spin coater

and the sensor then spun at high speed. 10 µL of either 50 or 100 mg mL^{-1} lipid matrix solution was dropped on to the centre of the crystal electrode using a micropipette, and the sensor allowed to spin for a further twenty seconds.

4.1.1 Effect of hydration at elevated temperature on the fluidity of spin coated lipid matrix films. An initial study:

A 100 mg mL^{-1} solution of lipid matrix was prepared in chloroform, based on the formula in Table 3.1. All glassware was thoroughly rinsed with purified water (and dried) prior to use. No plastic containers were used. The lipid matrix solution was deposited onto a cleaned TSM sensor by the spin coating technique. Impedance measurements of the TSM sensor were made both before and after lipid coating. The lipid matrix film was hydrated by placing the coated TSM sensor into water, heated to 60 °C (± 0.1 °C). The TSM sensor remained in the water for 20 min it was then removed and allowed to dry in air for 10 min, or until all excess water had been removed (as determined by visual inspection). The impedance spectrum of the TSM sensor was recorded after hydration.

4.1.2 Effect of Azone® incorporation on the fluidity of lipid matrix films

100 mg mL^{-1} solutions of lipid matrix (Table 3.1) were prepared in chloroform, with the inclusion of 5, 10, 15, and 20 mole percent of Azone®. All glassware was thoroughly rinsed with purified water (and dried) prior to use. No plastic containers were used. The lipid matrix solutions were deposited onto cleaned TSM sensors by the spin coating technique. Impedance measurements of the TSM sensors were made both before and after lipid coating. The lipid matrix films were hydrated by placing the coated TSM sensors into water heated to 60 °C (± 0.1 °C). The TSM sensors remained in the water for 20 min, and were then removed and allowed to dry in air for 10 min, or until all excess water had been removed (as determined by

visual inspection). The impedance spectrum of the TSM sensors were recorded after hydration.

4.1.3 Effect of cholesterol on the fluidity of lipid matrix films

A 100 mg mL^{-1} solution of lipid matrix (Table 3.1) with 0 mole percent cholesterol was prepared in chloroform. All glassware was thoroughly rinsed with purified water (and dried) prior to use. No plastic containers were used. The lipid matrix solution was deposited onto a cleaned TSM sensor by the spin coating technique. Impedance measurements of the TSM sensor were made both before and after lipid coating. The lipid matrix film was hydrated by placing the coated TSM sensor into water heated to 60 °C (± 0.1 °C). The TSM sensor remained in the water for 20 min and were then removed and allowed to dry in air for 10 min, or until all excess water had been removed (as determined by visual inspection). The impedance spectrum of the TSM sensor was recorded after hydration.

4.1.4 Response of lipid matrix films exposed to water at 25 °C

Solutions of lipid matrix (50 and 100 mg mL^{-1}, Table 3.1) with 0, and 20 mole percent of Azone® and 0 mole percent cholesterol were prepared in chloroform. All glassware was thoroughly rinsed with purified water (and dried) prior to use. No plastic containers were used.

Impedance spectra were recorded for the blank and lipid coated TSM sensors, prior to mounting in the flow cell. The TSM sensor was placed into the flow cell and then placed inside a copper cylinder with a cooling coil around the outside. One side of the sensor was exposed to water using the static side of the flow cell (in the case of the coated crystal it was the lipid coated side that was exposed). The temperature of the copper cylinder was controlled

using a Lauda RE 204 water bath and the temperature of the water in the static side of the flow cell recorded using a LogIT temperature probe connected to a PC. The impedance spectrum of the TSM sensor was recorded every 1 min at a constant temperature of 25 °C.

4.1.5 Response of lipid matrix films exposed to water at a range of temperatures

50 and 100 mg mL^{-1} solutions of lipid matrix (Table 3.1) with 0, and 20 mole percent of Azone$^{®}$ and 0 mole percent cholesterol were prepared in chloroform. All glassware was thoroughly rinsed with purified water prior to use. No plastic containers were used.

Impedance spectra were recorded for blank and lipid coated TSM sensors at a range of equilibrium temperatures. The TSM sensor was placed into the flow cell and then placed in the copper cylinder. One side of the sensor was exposed to water using the static side of the flow cell (in the case of the coated crystal it was the lipid coated side that was exposed). The temperature of the copper chamber was controlled using a Lauda RE 204 water bath and the temperature of the water in the static side of the flow cell recorded using a LogIT thermocouple connected to a PC. The impedance spectrum of the TSM sensor were recorded every 1 min at a range of equilibrium temperatures between 20 °C and 60 °C.

4.2 Results and discussion

4.2.1 Fluidity of spin coated lipid matrix films

Table 4.1 shows R_2, the change in the resistance at series resonance of lipid coated TSM sensors on hydration (Section 2.1.1.2), in water at 60 °C. The results have been normalised to

the cleaned (blank) sensor and show that there is a small increase in resistance (6 Ω) on coating the TSM sensor with the lipid matrix. This increase in resistance is due to acoustic losses in the lipid film coated onto the TSM sensor i.e. the lipid film exhibits a degree of fluidity.

Table 4.1 R_2 of TSM sensor at series resonance after coating with lipid matrix film and exposure of the film to water at 60 °C for 20 min.

	R_2 / Ohms	
Blank	**Coated**	**Post-hydration**
0	7	15
0	6	36
0	10	36
0	0	42
0	5	92
Mean	6 ($\pm$ 4)	44 ($\pm$ 29)

Table 4.1 also shows that changes in the fluidity of the lipid film occur on hydration. A shift in the mean resistance from 6 Ω before hydration, to 44 Ω post-hydration demonstrates a change in the material properties of the matrix. These changes result from the rearrangement and hydration of the lipid film on exposure to water at 60°C. The change in frequency of the TSM sensor coated with the lipid matrix film is shown in Table 3.4, and indicates that there was no difference between the frequency before and after hydration. This lack of frequency shift indicated that there was no detectable change in film mass. Therefore if water is being incorporated into the lipid film then the amount must be small. This is expected as the lipid film is measured dry both before and after hydration any change in frequency is therefore more likely to be due to the rearrangement of the lipid molecules in the film.

The series resistance measurements made on the lipid matrix coated TSM sensors demonstrates that it is possible to detect changes in the fluidity of lipid membranes using this technique. This opens up the possibility of investigating the mode of action of penetration enhancer and the role of individual lipid components in the membrane.

4.2.2 Effect of Azone® incorporation on the fluidity of lipid matrix films

It is possible to demonstrate using simple lipid films such as arachidic acid that the penetration enhancer Azone® effects the density of a lipid film. The mean molecular area of a lipid components in a Langmuir-Blodgett film is shown in Table 4.2. The results demonstrate that the mean area of a lipid molecules increases on the addition of Azone®. This corresponds well with the findings of other Langmuir-Blodgett studies of Azone®[52].

Table 4.2 The difference in the molecular area of the lipid films containing Azone® (n=3).

Composition of Langmuir-Blodgett film	Mean molecular area / nm^2	Standard deviation
Arachidic acid	0.21	0.00
Arachidic acid and 20 mole % Azone®	0.26	0.02

It is hypothesised that a TSM sensor measurements system will be able to detect the presence of Azone® in the lipid matrix film by the change in the film fluidity that it will cause.

Table 4.3 shows the effect that varying the mole percentage of Azone® included in the lipid matrix has on the resonant frequency of the matrix-coated TSM sensor. There is no statistical difference (one-way ANOVA, $p < 0.05$), either before or after hydration, between the frequency shifts for the TSM sensors coated with pure lipid matrix and with the lipid matrix including Azone®.

Table 4.3 Mean shift in resonant frequency of TSM sensors coated in lipid matrix film with various mole percentages of Azone® added (n=5).

Azone® concentration / mole percent	Mean shift in resonant frequency / Hz (Standard deviation)		
	Blank	Coated	Post-hydration
0	0	-5643 (623)	-5410 (872)
5	0	-5383 (1044)	-5593 (1378)
10	0	-5415 (591)	-5483 (1048)
15	0	-5325 (285)	-5404 (349)
20	0	-6029 (961)	-5850 (918)

It is possible to conclude from the above that no significant differences exist in the weight of film on the sensor, before and after hydration. It is unlikely therefore, that there is any loss of

lipid during the hydration process, or that there is any increase in water retained by the film as the Azone® concentration is increased. This is important as it demonstrates that any differences in the resistance shift (R_2) of the TSM sensor, are not due to the amount of lipid coated onto the TSM sensor. Differences in the resonant frequency of the film coated TSM sensors, before and after hydration are all within ±5 % of each other. These small variations are therefore probably due to a number of different factors including: the amount of lipid on the film, the degree of hydration of the film, and the arrangement of the lipid on the sensor.

Even though the inclusion of Azone® into the lipid matrix films seem to have no discernable effect on the shift in resonant frequency of the TSM sensor, this does not mean that the Azone® does not have an effect on the fluidity of the film.

Table 4.4 and Figure 4.1 show the shift in the resistance of the TSM sensor for lipid matrix films containing between 0 and 20 mole percent Azone®. Both the Figure and Table are included to allow numerical analysis and examination of the trend in the data. Analysis of the results using a one-way ANOVA test indicates that before hydration there is no statistical difference between the lipid matrix films ($p < 0.05$). Further analysis of the results shows that it is the lipid matrix film with 20 mole % Azone® included is statistically different at a slightly higher probability $p < 0.06$ from those with 0 to 15 mole % Azone®, moreover no discernable trend was observed for the lipid matrix coated TSM sensors with 0 to 15 mole % Azone® included (Figure 4.1 A).

Statistical analysis using a one-way ANOVA test, of the results for the lipid matrix coated TSM sensors, post-hydration, reveals significant differences between data sets ($p < 0.05$). A clear trend can be seen in which the TSM sensor resistance increases with an increasing mole % of Azone®(Figure 4.1 B and Table 4.4).

From the observed differences in TSM sensor R_2 it is possible to infer that the addition of Azone® to the lipid matrix has also caused a change in the fluidity of the lipid film, both before and after hydration. For concentrations of Azone® ranging from 0 to 15 mole percent no difference is seen in the fluidity of the lipid membrane prior to hydration, however, at a concentration of the 20 mole percent the significantly higher resistance ($p<0.06$) indicates that the matrix possesses a greater fluidity. This indicates that Azone® may have a non-linear concentration dependant effect on the fluidity of membranes with a threshold amount of Azone® required before a change in membrane fluidity can be seen, other studies have found that the relationship can be linear[52, 55] or concentration dependant[155]. If the results for the hydrated lipid matrix films are now considered, then an increase in the lipid matrix fluidity in all the lipid membranes is observed when compared to the Azone® free lipid matrix. This change in fluidity appears to approximately linear (Figure 4.1B and Table 4.4), though the 20 mole percent film appears to have a larger increase in the minimum impedance (and therefore fluidity) than any of the other stepwise increases.
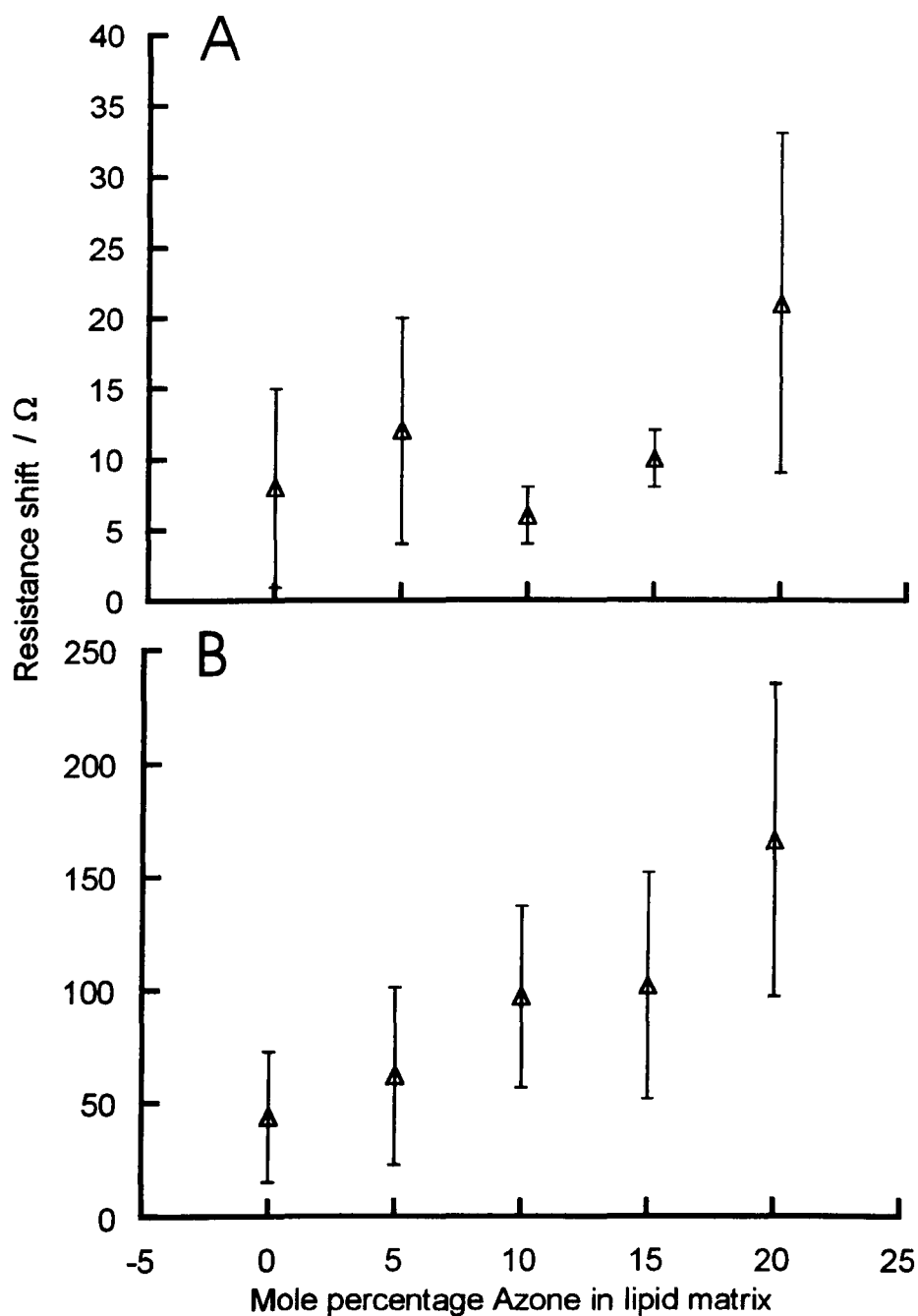
Figure 4.1 The relationship between minimum resistance magnitude and mole percentage Azone® present in the lipid matrix; (A) before hydration and (B) post-hydration.

Table 4.4 The mean shift in resistance of TSM sensors following coating with lipid matrix film containing various mole percentages of Azone®.

Azone® concentration / mole percent	Mean resistance shift / Ω (standard deviation)		
	Blank	Coated	Post-hydration
0	0	8 (7)	44 (29)
5	0	12 (8)	62 (39)
10	0	6 (2)	97 (40)
15	0	10 (2)	102 (50)
20	0	21 (12)	166 (69)

4.2.3 Effect of cholesterol on the fluidity of lipid matrix films

In order to investigate the properties of the lipid matrix, and the role of individual component within it cholesterol was removed from the membrane and the effect that this had examined. Table 4.5 shows the frequency shifts for cholesterol free lipid matrix films coated onto a TSM sensor. The results show that the cholesterol free films have approximately the same mass as the films that have been coated earlier in the studies.

Table 4.5 Shift in resonant frequency for blank and lipid coated (before and after hydration) TSM sensors. The lipid matrix used includes no cholesterol.

Replicate	Shift in resonant frequency of TSM sensor / Hz		
	Blank	Coated	Post-hydration
1	0	-5467	-5560
2	0	-5499	-4896
3	0	-5151	-4611
4	0	-5200	-5034
5	0	-4922	-5142
6	0	-5129	-5069
7	0	-5488	-5536
8	0	-5087	-5040
Mean (standard deviation)	0 (0)	-5243 (216)	-5111 (314)

The frequency shifts in Table 4.5 show no significant difference (Mann-Whitney test, $p > 0.05$) between the lipid films before and after hydration indicating that the mass of the film is not changing over the course of the experiment. The higher number of replicates completed in this experiment than in previous was due to a greater degree of variation in the resistance shifts, shown in Table 4.6.

Table 4.6 Shift in resonant frequency for blank and lipid coated (before and after hydration) TSM sensors. The lipid matrix used includes no cholesterol.

Replicate	Shift in minimum resistance of TSM sensor / Ω		
	Blank	Coated	Post-hydration
1	0	19	185
2	0	23	38
3	0	13	175
4	0	24	44
5	0	9	178
6	0	7	66
7	0	21	255
8	0	10	86
Mean (standard deviation)	0 (0)	16 (7)	128 (80)

The observed mean TSM sensor resistance (R_2 = 16 ± 7 Ω, Table 4.6) indicates that the cholesterol free lipid matrix has some degree of fluidity when compared with the cholesterol containing matrix (R_2 = 8 ± 7 Ω, Table 4.4). This is followed by a further increase in fluidity when the film is hydrated, R_2 = 128 ± 80 Ω (Table 4.6) compared to R_2 = 44 ± 29 Ω (Table 4.4) for the cholesterol rich lipid matrix. This result is similar to that observed for the lipid matrix films that were investigated earlier. However, the results for the cholesterol free films have a larger variation than for the other films. This may indicate the importance of cholesterol in the structure and stability of the lipid matrix film under investigation.

4.2.4 Response of lipid matrix films exposed to water at 25 °C

In order to further investigate the action of Azone® on the lipid matrix films coated onto the TSM sensor a series of experiments investigating the behaviour of the lipid film in a liquid environment were performed. Blank and coated (lipid matrix films and lipid matrix films including 20 mole % Azone®) TSM sensors were exposed to water at 25°C. It was anticipated that these experiments would reveal differences in the hydration behaviour of the lipid films.

This work was also important in establishing the behaviour of the film for partitioning experiments where the films will be used in liquid media.

Figure 4.2 shows the effect of placing lipid coated TSM sensors in water at a constant temperature of 25 °C (measurements were taken at 1 min intervals). Clear differences can be seen between the lipid coated TSM sensors and the control measurements made using blank TSM sensors. The lipid films (lipid matrix and lipid matrix with 20 % Azone[®]) both show the same relationship between frequency and the time spent in the water (Figure 4.2 A); i.e. an initial decrease in the sensor frequency is followed by a sharp increase that continues until the resonant peak is lost above the measurement threshold of the instrument. The whole process took approximately 90 to 300 min, with the Azone[®] loaded lipid matrix films tending to complete the process quicker than those that did not (though a certain amount of overlap between the two sets exists).

Figure 4.2 **(A)** The frequency shift and **(B)** resistance of TSM sensors coated with lipid films (100 mg mL^{-1}) left in water at 25 °C. Filled symbols represent the blank TSM sensors, unfilled symbols with the solid line the TSM sensors coated with the 20 % Azone® lipid matrix film, and unfilled symbols with a broken line the TSM sensors coated with the lipid matrix film. The symbols do not represent the actual number of data points but are included solely to differentiate between lines.

If the trend in the frequency of the lipid coated sensors is considered then it is possible to understand the changes that are occurring to the film on exposure to water at 25°C. The Sauerbrey equation indicates that a decrease in the frequency of the sensor means that an increase in film mass is occurring and visa-versa. The implication is that two processes have occurred, the first is that the film gains mass initially and then the second is that the film loses mass. Measurement of film mass before and after exposure to water in the static side of the flow cell demonstrates no significant loss of lipid (the mean percentage film loss is -1 % ± 22 %, n = 5). These changes could be due to a number of different processes including: rearrangement of the lipid on the sensor surface and the uptake of water by the film. In addition, it is possible that changes in the fluidity of the lipid film could have had an effect on the frequency measurement. This is because of the absorption of energy, associated with any increase in the fluidity of the film, could effect not only the resistance shift but also the frequency shift. This effect will probably be much more significant for the lipid matrix films measured in a liquid environment than those measured earlier, in a dry state, this is because of the much larger shifts in resistance expected in a liquid.

The change in the R_2 of the TSM sensor (Figure 4.2 B) should give us more information on the processes occurring. In Figure 4.2 B, the difference between the lipid coated and control TSM sensor is clear, with the control measurement having a constant resistance while the resistance of the TSM sensors coated with lipid films increases with hydration time until the resonance peak of the sensor is lost.

The shift in resistance for the lipid films signifies that the fluidity of the lipid membrane is changing over the course of the experiment. This change is probably due to the gradual incorporation of water into the lipid membrane and rearrangement of the lipid films. Since a large change in the resistance is involved it is more likely that the majority of the response is

due the uptake of water. Similarly to the change in frequency (Figure 4.2 A), the rate by which the resistance changes is greater for the lipid films containing Azone[®] than for those, which do not, thereby indicating that the process of structural rearrangement followed by film hydration is facilitated by the inclusion of Azone[®]. X-ray scattering experiments have also provided evidence that high water concentration in human stratum corneum reduces the ordering of the lipids[27].

While two processes occurred in the measurements of TSM sensor frequency, the changes in the resistance show only one. This increase in the fluidity of the film is not linear however and increases in rate with time. It is therefore possible that the second process, indicated by the frequency shift, is a result of the increase in the fluidity. The increasing rate of the process is the reason why this change in fluidity only becomes significant in the later stages of the experiment. The first process is probably due to rearrangement and/or hydration of the films although no additional supporting evidence is provided for this.

The large shifts in frequency and resistance that have been evident in the experiments using the 100 mg mL^{-1} lipid solutions meant that in some cases the experiments could not be completed, owing to excessive dampening of the resonance peak, therefore it was decided to repeat the experiments using a lower concentration of lipid (50 mg mL^{-1}), in an attempt to eliminate this problem. Figure 4.3 A shows the frequency shift for blank and coated TSM sensors, which have been coated with 50 mg mL^{-1} lipid matrix films. These sensors bear some resemblance to the 100 mg mL^{-1} films (Figure 4.2 A). The 50 mg mL^{-1} lipid films show an initial decreases in the frequency followed by an increase that eventually level out with the frequency remaining largely constant after this. The 100 mg mL^{-1} films showed the same initial trend but then the frequency shift did not level out and continued to increase until the measurement was lost. The

50 mg mL^{-1} film containing Azone® finishes with a higher frequency shift than those films that did not, this difference was not very large though.
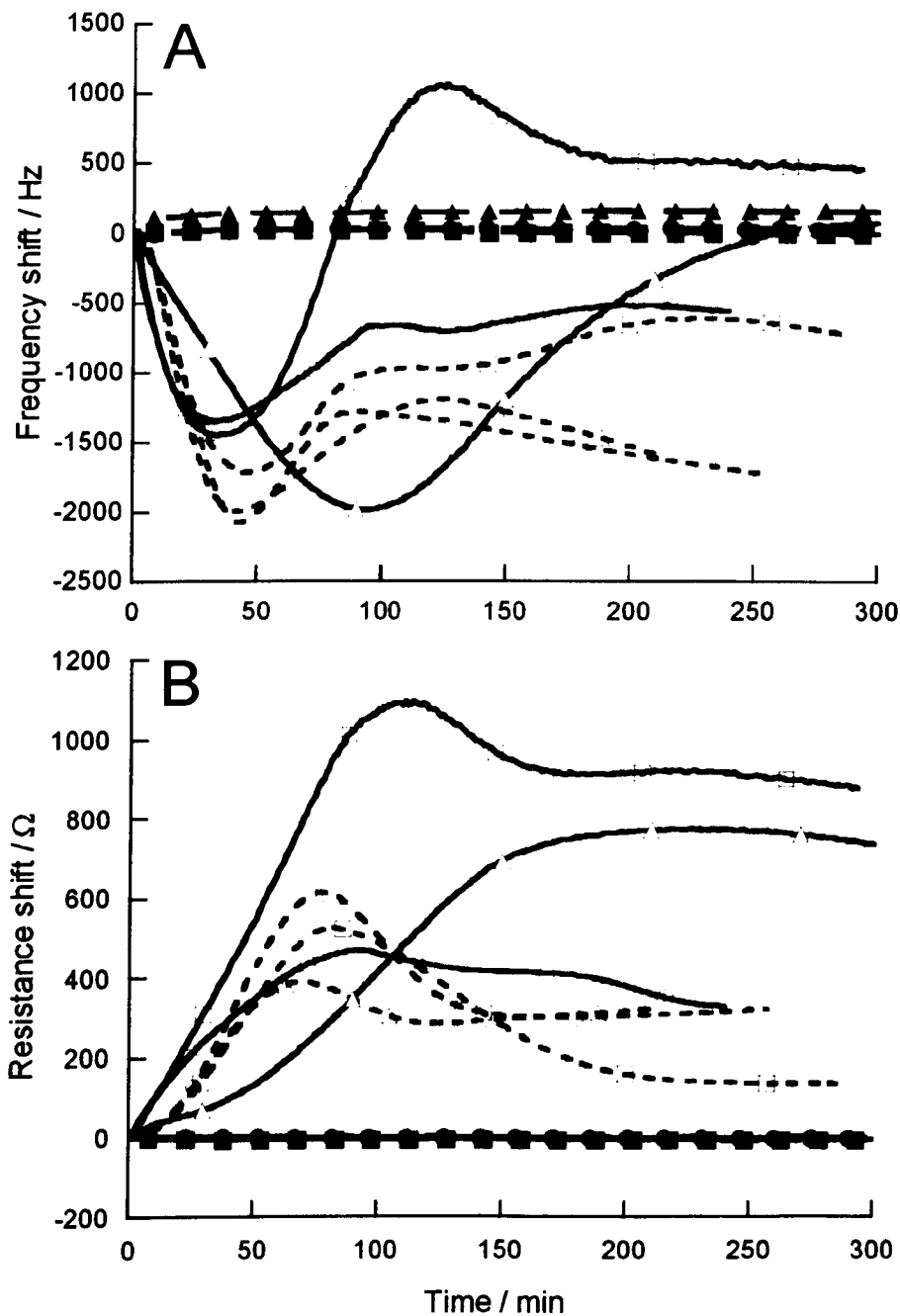
Figure 4.3 **(A)** The frequency and **(B)** resistance shift of TSM sensors coated with lipid films (50 mg mL^{-1}) left in water at 25 °C. Filled symbols represent the blank TSM sensors, unfilled symbols with the solid line the TSM sensors coated with the 20 % Azone® lipid matrix film, and unfilled symbols with a broken line the TSM sensors coated with the lipid matrix film. The symbols do not represent the actual number of data points but are included solely to differentiate between lines.

The resistance trends observed (Figure 4.3 B) for the 50 mg mL^{-1} are the same as those for the 100 mg mL^{-1} films. However, the 50 mg mL^{-1} films exhibit smaller resistance shifts, allowing the complete trend to be observed without the measurement range of the instrument being exceeded. Figure 4.3 B shows that the change in the fluidity of the lipid film does eventually slow and level out, the films have probably reached the maximum hydration and therefore no further change occurs.

The frequency shift of cholesterol free lipid matrix coated TSM sensor films is shown in Figure 4.4 A. The response shows a sharp initial decrease in the frequency of the sensor followed by a slower increase that eventually levels out towards the end of the experiment.
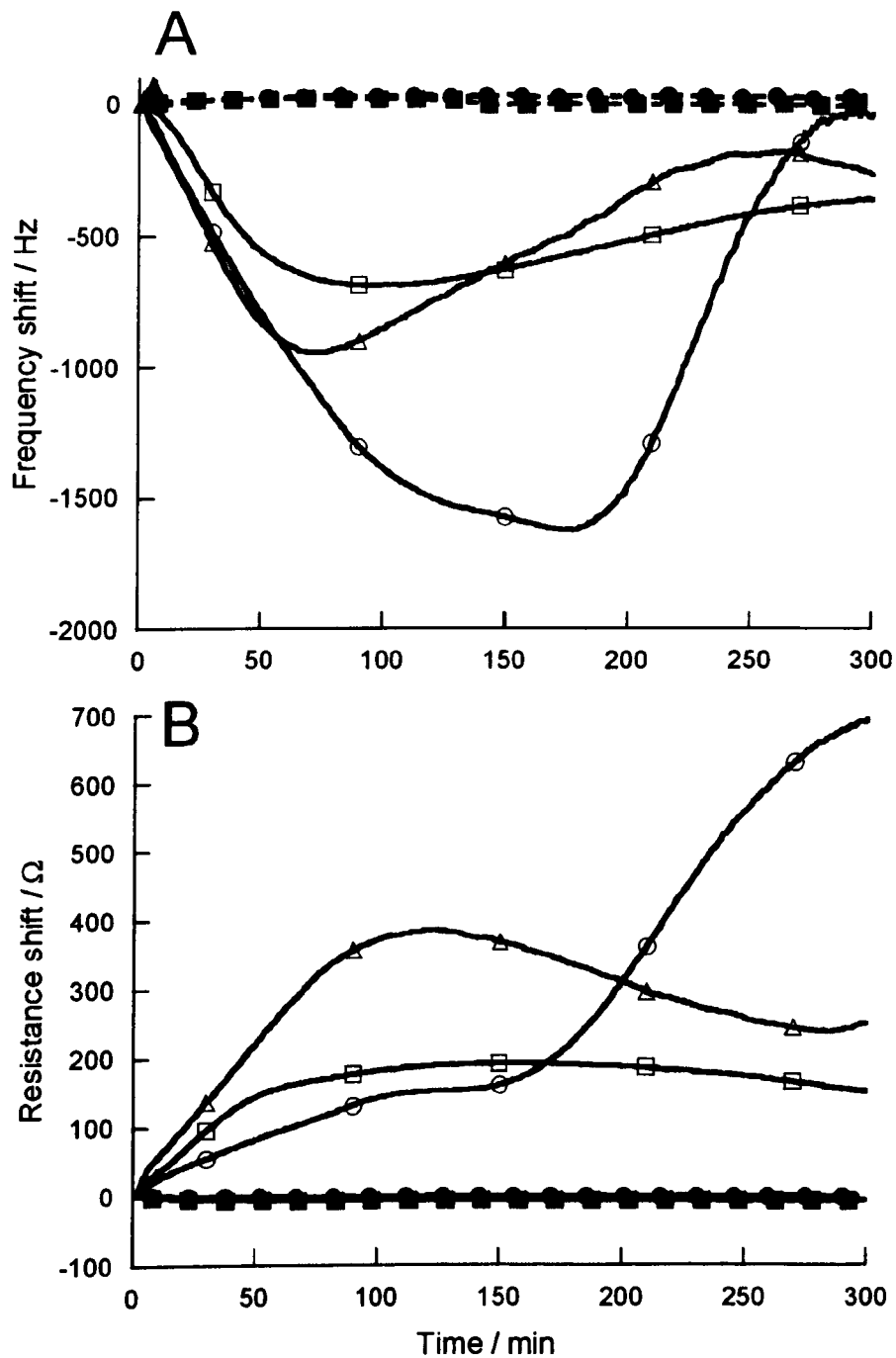
Figure 4.4 **(A)** The frequency and **(B)** resistance shift of TSM sensors coated with lipid films (100 mg mL^{-1}) left in water at 25 °C. Filled symbols represent the blank TSM sensors, unfilled symbols the TSM sensors coated with the lipid matrix film with no cholesterol included. The symbols do not represent the actual number of data points but are included solely to differentiate between lines.

The frequency response (Figure 4.4 A) of the TSM sensor for the cholesterol free lipid matrix films show similarities with the cholesterol containing lipid matrix films. Compared to the 100 mg mL^{-1} lipid matrix films (containing cholesterol) the response is reduced but does possesses approximately the same trends with the broadness of the trough being of a similar size (Figure 4.2 A). When the depth of the trough is compared to the 50 mg mL^{-1} lipid matrix films (containing choleserol) the magnitude of the trough is also (slightly) reduced, though the trough widths for the cholesterol free films are broader.

Figure 4.4 B shows the change in resistance associated with the frequency shift shown in Figure 4.4 A. The resistance of the TSM sensor coated with cholesterol free lipid matrix film indicates a change in the fluidity of the film. As with the previous results the resistance measurements show a degree of variability that masks the exact relationship. The general trend seems to be for an initial slow increase in the resistance indicating an increase in the fluidity of the lipid matrix films, which levels off with time.

Similar trends are seen for the resistance shifts as were present for the frequency measurements. The sensor response follows the same general trends that were seen for the 50 mg mL^{-1} and 100 mg mL^{-1} films but the response tends to be smaller and the variability between the replicates greater. The results seem to indicate the importance of cholesterol in the organisation of the lipid matrix membrane. The higher degree of variability experienced with the cholesterol free membrane indicating the importance of cholesterol in the stability of the membrane on the sensor. The smaller resistance response of the cholesterol free film indicates that the hydration of the film is also affected, with possibly less water being incorporated onto the membrane than in the films that include cholesterol.

The final set of results taken in this Section shows the response of the TSM sensors coated with 50 mg mL^{-1} cholesterol free lipid matrix film when they are placed in water at 25 °C. The

frequency (Figure 4.5 A) response shows an initial dip or level part of the plots, followed by an increase in the frequency shift, and then a steady decrease over the course of the rest of the experiment.

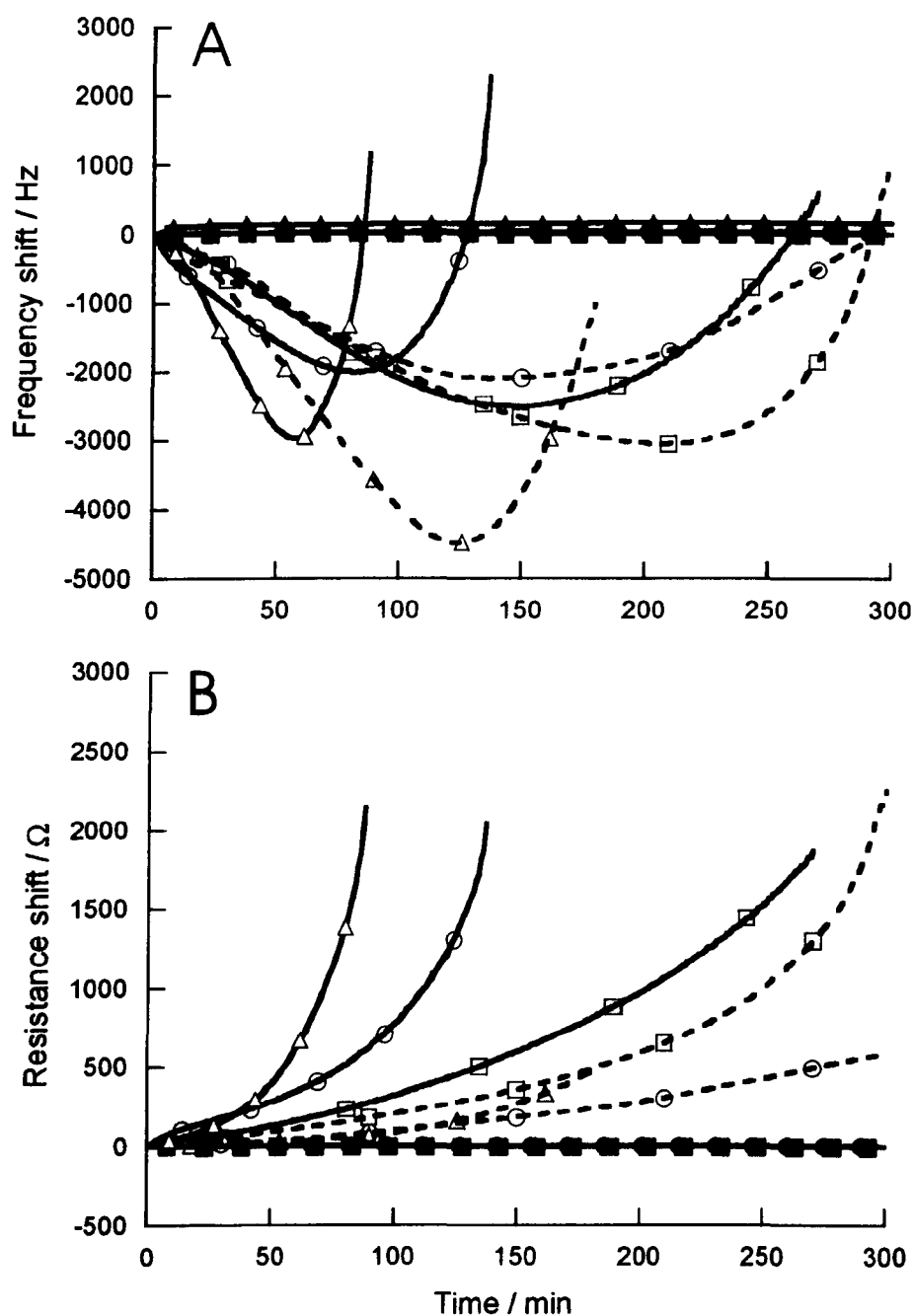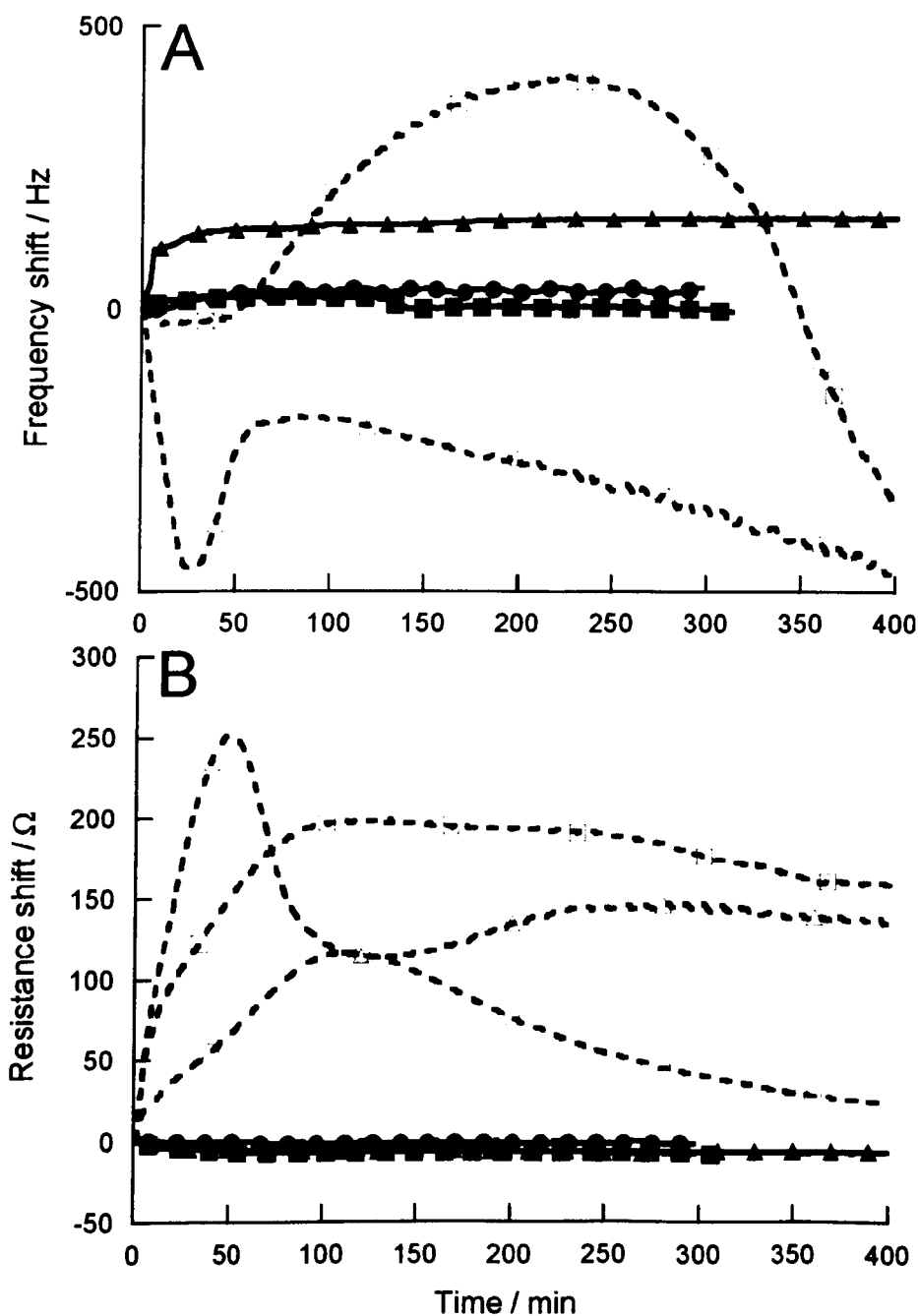**Figure 4.5** (A) The frequency and (B) resistance shift of TSM sensors coated with lipid films (50 mg mL^{-1}) left in water at 25 °C. Filled symbols represent the blank TSM sensors, unfilled symbols the TSM sensors coated with the lipid matrix film with no cholesterol included. The symbols do not represent the actual number of data points but are included solely to differentiate between lines.

The resistance shift (Figure 4.5 B) shows an initial sharp increase in the response, which levelled out and remained constant until the end of the experiment. Unlike the frequency shifts this response does have some resemblance to the trends observed for the lipid matrix films. Once again the cholesterol free films show a smaller response and a higher degree of variability than the films that included cholesterol.

Throughout the investigation of the cholesterol free films have shown a high degree of variability that has made it difficult to determine what trends exist. This tends to suggest that cholesterol has an important role in the response of the lipid matrix membranes. Cholesterol has been shown to have an important role in the stabilisation of biological phospholipid membranes, here it seems that the lack of cholesterol has led to a lack of stability in the fatty acid membranes that we have been using. In addition the frequency and resistance responses of the cholesterol free films are much smaller than the films that included cholesterol. This indicates that the structural changes in the membrane induced by the lack of cholesterol means that less water is included into the membrane on hydration.

4.2.5 Response of lipid matrix films exposed to water at a range of temperatures

Figure 4.6 A shows the change in the frequency of TSM sensors coated with lipid films (lipid matrix and lipid matrix containing 20 % Azone®) at a range of equilibrium temperatures between approximately 25 °C and 60 °C. Data was recorded at 1 min. intervals but only data recorded at the equilibrated temperature is shown.

The small number of replicates in this experiment is a result of experimental difficulties in obtaining the data. The previous experiment showed that the lipid films were left in water the

frequency and resistance of the TSM sensor increase rapidly until the measurement limit of the instrumentation was reached. The measurements presented here did not reach this limit before the end of the experiment; the incomplete data sets that did reach the measurement limit before the end of the experiment are not shown. Figure 4.6 A shows the frequency of the coated TSM sensors increased as the temperature increased, however the rate of increase was not constant and appears to decrease as the temperature increases. For the lipid matrix films including 20 % Azone® the increase levels out at about 30 °C.

Figure 4.6 **(A)** The frequency and **(B)** resistance shift of lipid coated TSM sensors (100 mg mL^{-1}) in water at a range of equilibrium temperatures. Filled symbols represent the blank TSM sensors, unfilled symbols with the solid line the TSM sensors coated with the 20 % Azone® lipid matrix film, and unfilled symbols with a broken line the TSM sensors coated with the lipid matrix film.

The frequency shifts in Figure 4.6 A indicate that the film mass decreased over the course of the experiment. For the lipid matrix films containing Azone® this decrease levelled off at about 35 °C but for the lipid matrix films it continued over the course of the experiment. The initial increase in frequency is probably due to a change in the fluidity of the film as was the case in Figure 4.2 A and B. In fact we would expect the initial stages of this experiment to follow the trend seen for the film at 25 °C. The initial dip in frequency that is seen in Figure 4.6 A is not plotted as it occurred while the temperature for the first data point was equilibrating. The rate of frequency and resistance change is reduced when compared to the films at 25 °C.

The temperature dependency of the resistance measurements for the lipid coated TSM sensors are shown in Figure 4.6 B. At the start of the experiment the resistance of the films increases with temperature, then at a temperature of between 25 °C and 35 °C depending on the film, this trend is reversed and the resistance starts to decrease. The TSM sensors coated with films containing Azone® then level off and the sensor coated with the lipid matrix film begins to increase again. Due to the limited nature of the data it is difficult to tell whether this difference is an artefact or not.

The shift in the resistance of the lipid coated TSM sensors coated with the lipid film shows that the change in frequency (i.e. mass) is probably related to a change in fluidity. The resistance measurements show that the fluidity of the Azone® containing film stops increasing at about 25 °C and then decreases slightly before remaining approximately constant. The lipid matrix film that does not contain Azone® has a slightly different relationship with the increase in fluidity reversing at a temperature range of approximately 35 °C to 45 °C and then increasing again (possibly an anomaly caused by the lack of replicates). The reduction in the fluidity to the

subsequent plateau corresponds reasonably well with one reported phase transition of the lipid matrix film (25°C to 45°C[2]). It is therefore possible that the changes in the TSM sensor resistance may be the result of the phase transition of the membranes. In addition Azone[®] has been shown to reduce and broaden the phase transition temperatures in lipid films[61, 55]. If it is the phase transition that is being detected then it is reasonable to suggest that this affects the temperature at which the resistance starts to drop. This may partly explain the differences between the films containing Azone[®] and those that do not.

Figure 4.7 A shows the frequency shifts over a range of temperatures for 50 mg mL^{-1} lipid films. In contrast to the previous experiment (at 100 mg mL^{-1}) the lipid films were allowed to equilibrate at 25 °C before the temperature run was started, previously this was not possible as the shifts were outside the measurement range of the equipment. In Figure 4.7 A no difference is seen between the lipid matrix film and the blank TSM sensor indicating that the film is not changing over the course of the experiment. The film containing Azone[®] does show some change in frequency over the range measured; this takes the form of a linear change.

Figure 4.7 **(A)** The frequency and **(B)** resistance shift of lipid coated TSM sensors (50 mg mL^{-1}) in water at a range of equilibrium temperatures. Filled symbols represent the blank TSM sensors, unfilled symbols with the solid line the TSM sensors coated with the 20 % Azone® lipid matrix film, and unfilled symbols with a broken line the TSM sensors coated with the lipid matrix film.

Figure 4.7 B shows the shift in resistance for the films. Once again the shifts differ from those taken using the higher lipid concentration. In both cases the shifts that are recorded are substantially reduced when compared to the previous experiment. While the results recorded at 25 °C are approximately half the magnitude at 50 mg mL^{-1} that they were at 100 mg mL^{-1} (considering the minimum frequency shift recorded), these results are approximately an order of magnitude smaller. No clear trend is apparent in the resistance results either; the lipid matrix films tend slightly towards an increase in the film resistance while the film including Azone$^{®}$ show a slight decrease.

The small shifts for both the resistance and frequency indicates that little is happening to the films over the temperature ranges used here. Comparison of the resistance shifts recorded here to those recorded previously in a liquid environment demonstrates how small these shifts are. It therefore seems that there is a threshold amount of lipid that must be coated onto the sensor before the change in fluidity associated with a change in temperature can be detected. These films have of course reached equilibrium with respect to the incorporation of water into the film and therefore smaller resistance shifts might be predicted.

Figure 4.8 A show the frequency shift of the TSM sensor coated with cholesterol free lipid matrix films at a range of temperatures between 25 °C and 60 °C. Similarly to the experiments done with the 50 mg mL^{-1} films, these films were allowed to equilibrate at 25 °C before the temperature was increased. The results therefore represent the response of the lipid coated TSM sensor to the change in temperature. This TSM sensor response showed an initial decrease in the frequency until about 35 °C followed by either a levelling or a slight increase in the response.
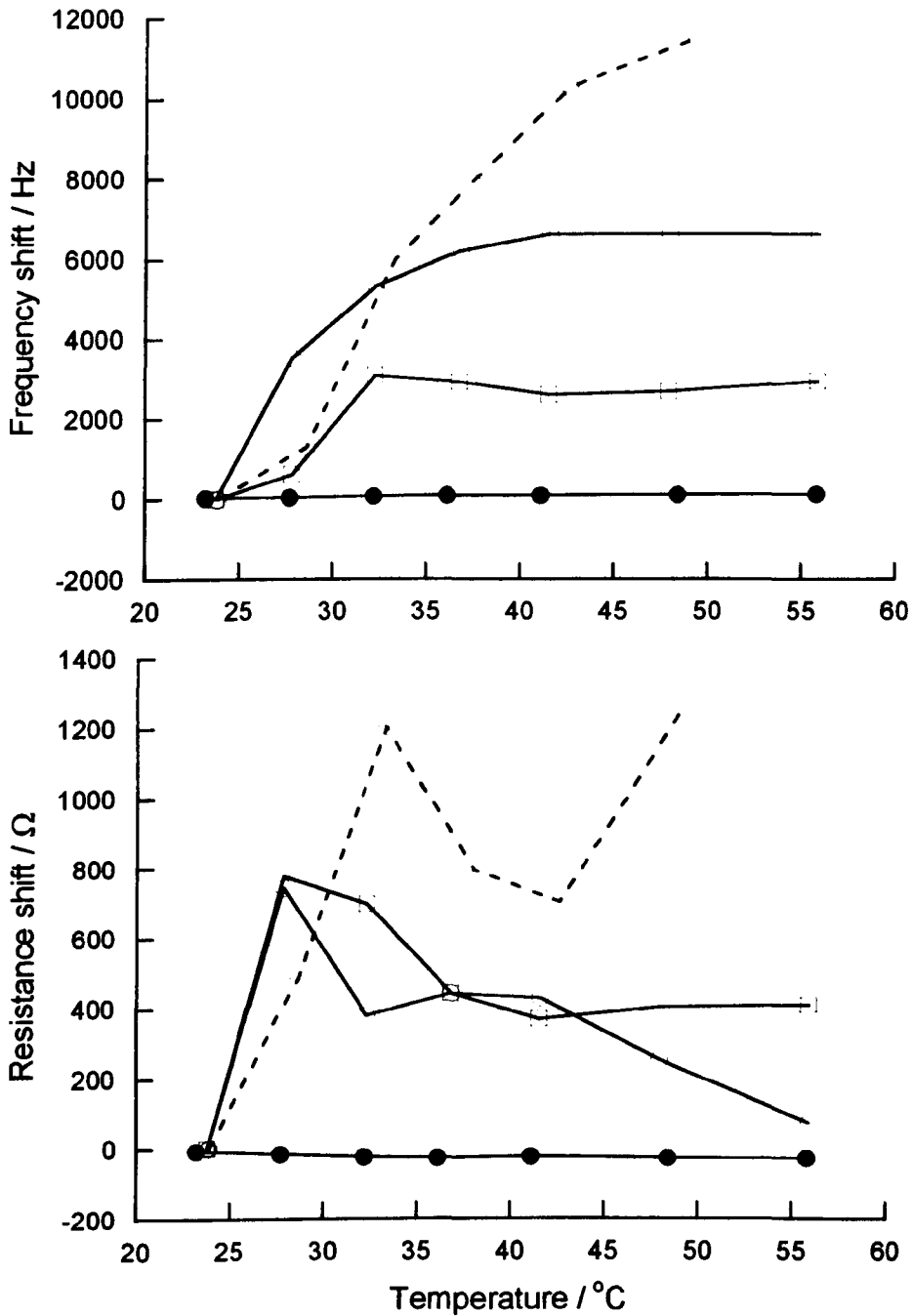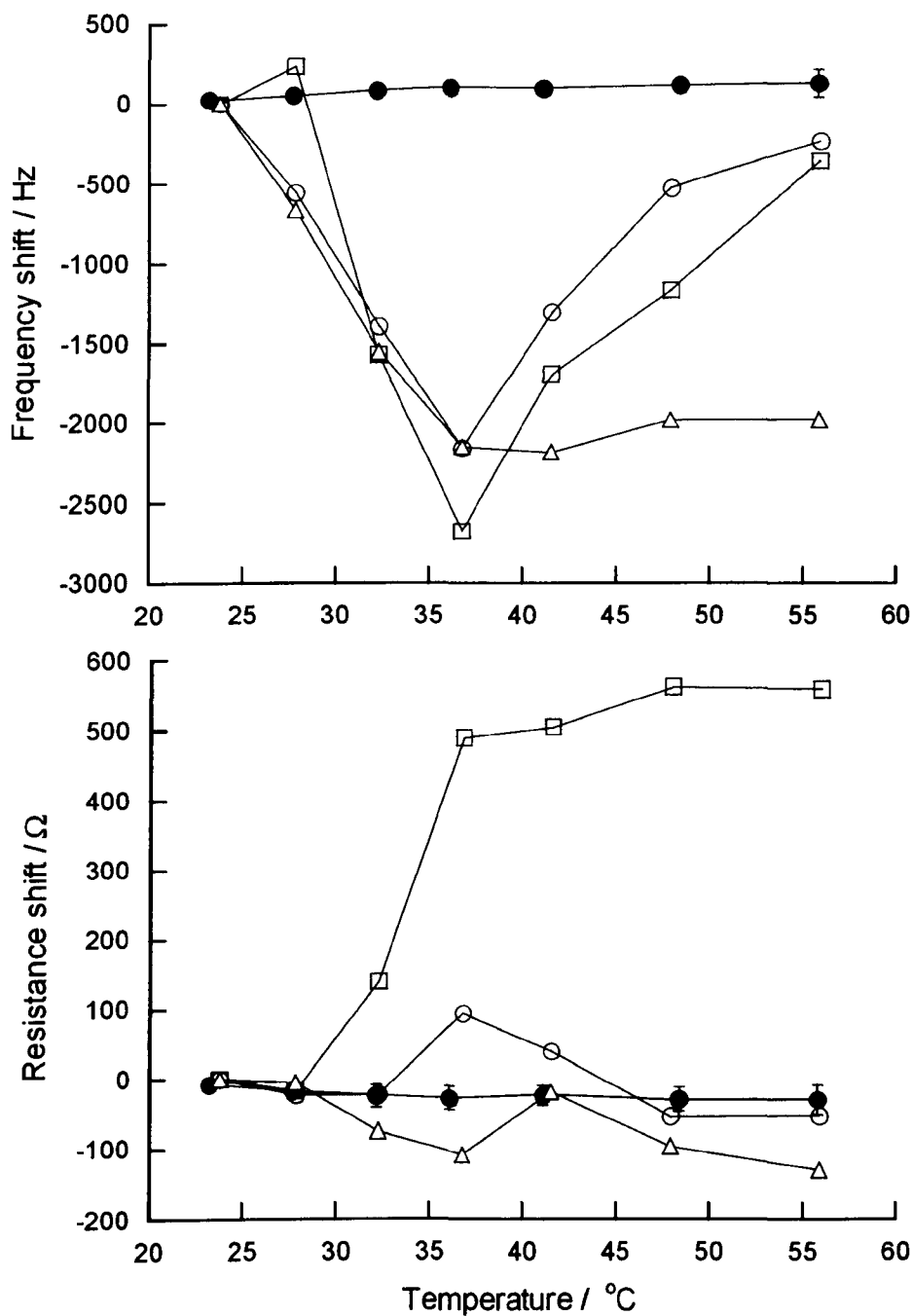
Figure 4.8 **(A)** The frequency and **(B)** resistance shift of lipid coated TSM sensors (100 mg mL^{-1}) in water at a range of equilibrium temperatures. Filled symbols represent the blank TSM sensors, unfilled symbols the TSM sensors coated with the lipid matrix film with no cholesterol included.

If the shifts in frequency of the cholesterol free lipid coated TSM sensors are compared to the shifts described earlier for the lipid matrix films, it can be seen that the two responses differ extensively. Compared to the 100 mg mL^{-1} lipid matrix films, the frequency response is much smaller and of the opposite direction. This is not unexpected, as the previous results did not allow the equilibration of the lipid film in the buffer prior to the experiment. Even compared to the response of the 50 mg mL^{-1} lipid matrix films, the frequency response recorded is still greatly reduced.

Figure 4.8 B shows the shift in the resistance of TSM sensors coated with the cholesterol free lipid matrix film compared to the blank TSM sensors. The results show a degree of variability in the response that makes it difficult to determine if any trends exist. In general it appears that there is no shift in the resistance of the TSM sensors over the temperature range measured. This indicates that the fluidity of the cholesterol free lipid matrix films is not changing.

Similarly to the frequency response, the resistance measurements for the cholesterol free films bear little resemblance to the results recorded previously for either the 100 mg mL^{-1} or 50 mg mL^{-1} cholesterol containing films. From the results, it is possible to see that cholesterol must play an important role in the response of the lipid matrix membranes. The variability of the cholesterol free lipid membranes indicates that cholesterol plays an intrinsic role in the structure and stability of the lipid membrane.

Although the response of the 100 mg mL^{-1} cholesterol free lipid matrix films was not as large as the ones that contained cholesterol, 50 mg mL^{-1} films were also coated as a comparison. Figure 4.9 A and B shows the response of TSM sensors coated with 50 mg mL^{-1} cholesterol free lipid matrix films. The frequency shift (Figure 4.9 A) decreased initially and then leveled out, remaining approximately constant for the remainder of the experiment.
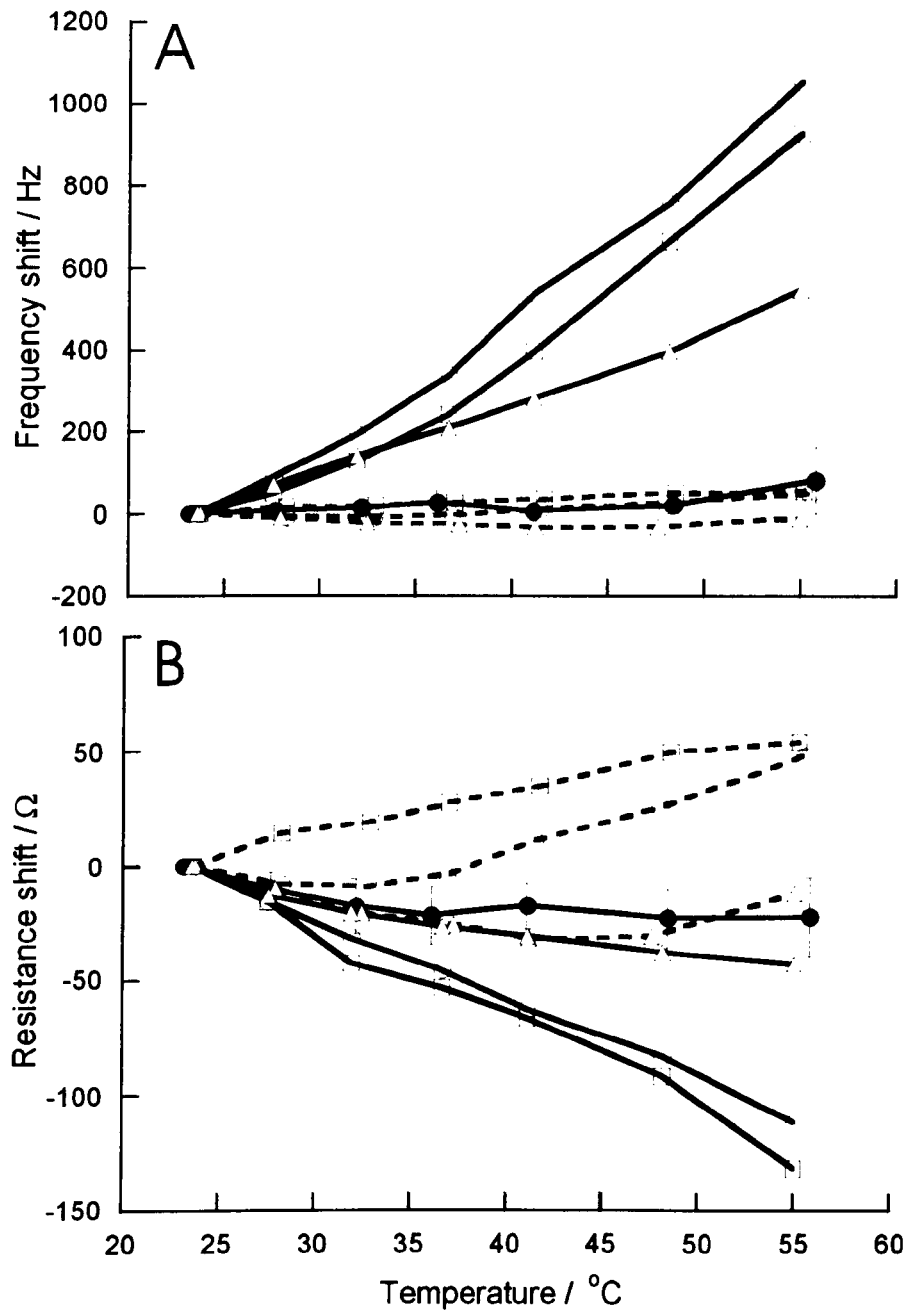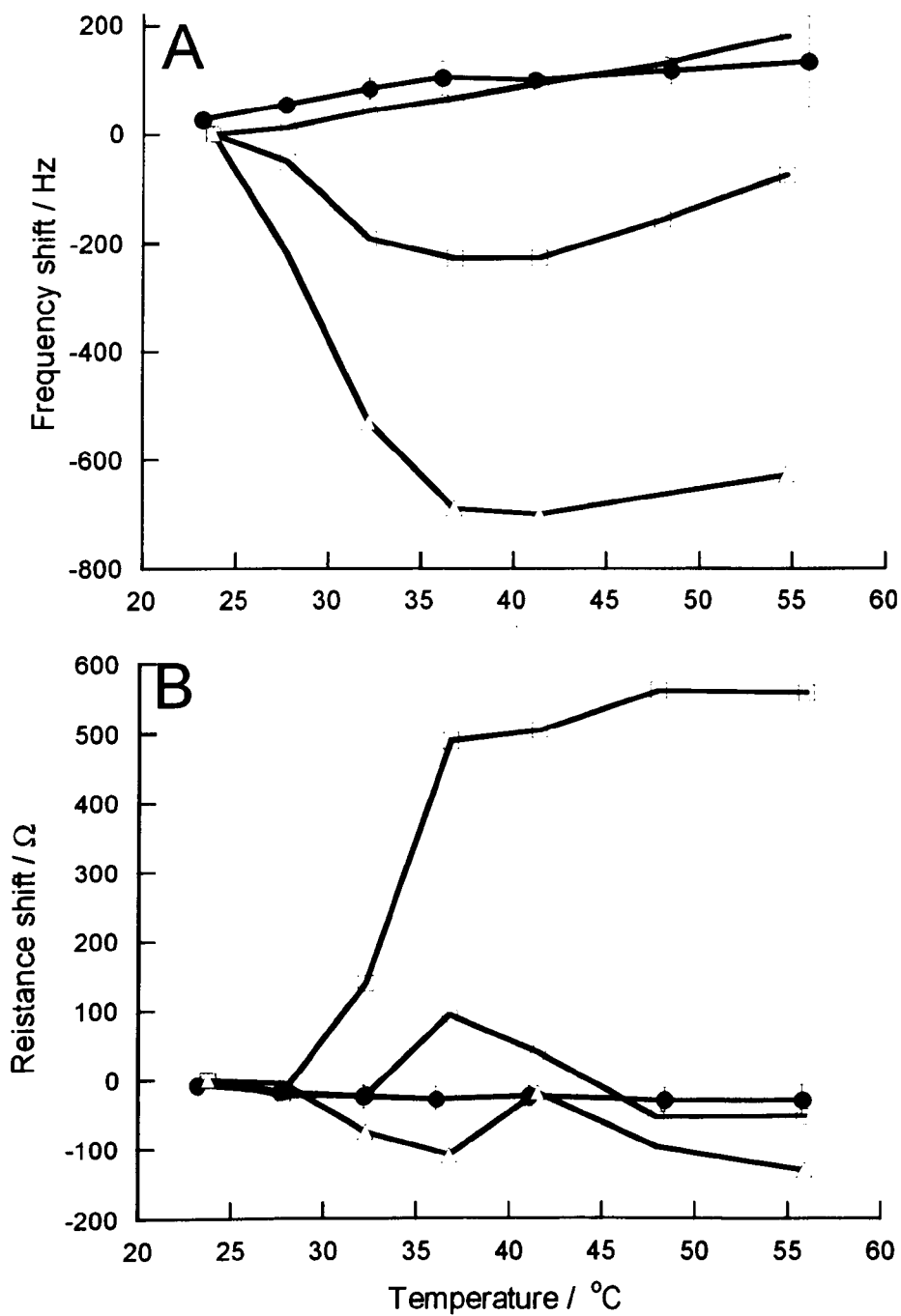
Figure 4.9 **(A)** The frequency and **(B)** resistance shift of lipid coated TSM sensors (50 mg mL^{-1}) in water at a range of equilibrium temperatures. Filled symbols represent the blank TSM sensors, unfilled symbols the TSM sensors coated with the lipid matrix film with no cholesterol included.

The resistance shift (Figure 4.9 B) does the opposite of the frequency shift showing an initial increase in the resistance followed before it levels out. In both cases the results recorded are highly variable however, thereby introducing some doubt on the validity of the trends.

The variability in the 50 mg mL^{-1} response for both frequency and resistance make it difficult to determine what trends exist for the results. The small nature of the shifts seem to indicate that there is little change in the cholesterol free lipid films over the temperature range that has been measured. This is a similar result to that recorded for the 50 mg mL^{-1} lipid matrix films. The high degree variability is the same as has been seen for other cholesterol free films.

4.3 Summary

The fluidity of the lipids of the stratum corneum can have a large effect on the flux of a drug across the epidermis. This Chapter investigated the fluidity of a lipid matrix using the novel technique of thickness shear mode sensors.

- Investigation of lipid matrix coated TSM sensors demonstrated that it was possible to measure a change in the fluidity of the film. The resistance of the TSM sensor at the resonant frequency was used to demonstrate that the spin coated lipid films coated onto the surface were fluid and that a further increase in fluidity occurred on hydration.

- The effect of the penetration enhancer Azone® on the spin coated lipid matrix films was investigated. Inclusion of between 0 and 20 mole percent Azone® produced no difference in the mass of the lipid matrix films (as monitored by frequency) but produced a linear increase in the resistance of the TSM sensor indicating a progressive increase in the fluidity of the film.

- Removal of cholesterol from the lipid matrix films was found to make little difference to the mass and fluidity of the films formed. However, the variability of the results measured was increased perhaps indicating the role of cholesterol in film stability.

- TSM sensor with lipid matrix films deposited (including those containing Azone® and lacking cholesterol) were place into the liquid cell and exposed to water at 25 °C. The films containing Azone® exhibited a more rapid change in mass and fluidity than the standard lipid matrix films, probably due to an increased rate of hydration. Cholesterol free films showed a high degree of variability when exposed to these conditions.

- Differences were observed between lipid films coated from 50 mg mL^{-1} and 100 mg mL^{-1} solutions. Trends in resistance and frequency shifts as functions of temperature, cholesterol inclusion and hydration time were highly sensitive to the mass of matrix on the sensor, thereby suggesting that these investigations would benefit from finding an optimum film mass.

- The frequency and resistance of TSM sensors coated with lipid films was investigated over a range of temperatures. Films that included Azone® exhibited a greater change in film mass and fluidity over the range of temperatures investigated. Trends for the 100 mg mL^{-1} lipid matrix films may indicate the detection of phase transitions.

5 BREWSTER ANGLE MICROGRAPHS

The Brewster angle microscope (BAM) is an imaging technique capable distinguishing between substrates with different refractive indices. This feature makes the technique very useful for the imaging lipid films in which different phases of lipid are present.

5.1 Theory

In most cases, when a beam of p-polarised light is incident to a dielectric optical substrate, part of the light is reflected from the substrate surface and part is refracted within the substrate. However, at a specific angle of the light to the substrate, known as the Brewster angle, all the light is refracted into the substrate. Thin films can be imaged on the surface of the substrate using this process.

The BAM consists of a laser from which the source of polarised light is obtained, and a camera/detector, to record the light reflected from the dielectric optical substrate (Figure 5.1). The laser light is directed incident to the substrate at an angle close to the Brewster angle (the light is not p-polarised at this point but contains a lot of s-polarised light, which is strongly reflected). The beam is centred in the camera and the light is p-polarised using a filter. The camera and laser are then adjusted to produce a reflectivity minimum. For solid substrates, such as the gold electrodes of the TSM sensor, the BAM is utilised like an ellipsometer with a fixed compensator. The polarisation of the light beam is adjusted to achieve the minimum reflectance from the substrate. A film coated onto the substrate can then be imaged by slight adjustment to the polarisation of the light and the detector. A film is then coated on to the substrate. Because the film has a different Brewster angle to the substrate it will reflect some of the incident light. The camera records the light reflected by the film and an image is

produced. The image will show the distribution of the film on the substrate and also any difference in the film structure e.g. differences in composition and/or phase behaviour. Using the BAM it is possible to image lipid films on the liquid surface of the LB trough and also on the gold surfaces on the TSM sensor.
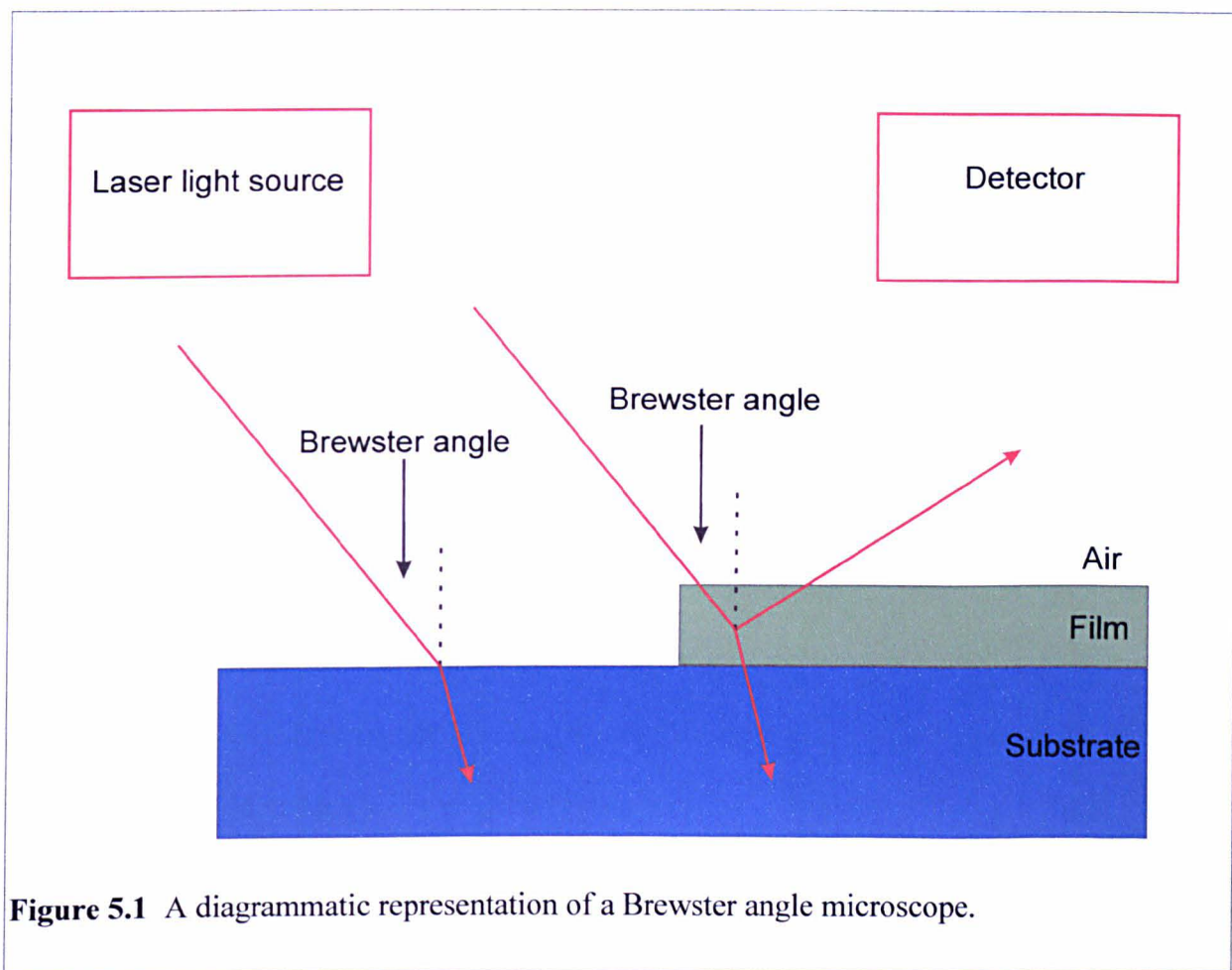
Figure 5.1 A diagrammatic representation of a Brewster angle microscope.

5.2 Method

Images of blank, coated (pre-hydration), and coated (post-hydration) TSM sensors were made using the Brewster angle microscope (BAM). Cleaned TSM sensors were removed from the holder, placed on to the stage of the Brewster angle microscope and images of the electrode

taken in three different areas. The imaging process was repeated after the TSM sensor was coated with a lipid matrix film and after the sensor had been hydrated.

BAM images were taken as follows:

1. The laser strength was set at 1 % and the laser switched on with the shutter in place.

2. The goniometers were set to 53 °. The angle of the goniometers is more critical for measurements on a liquid than solid.

3. Position the compensator into the laser beam, set the polarisation to 45°, and the analyser to 90 °.

4. The sample was positioned on the microscope stage, the shutter removed, and the sample positioned in the laser beam. The camera sensitivity is set automatically by pressing "auto set".

5. The angle A was rotated to minimise the signal, this was then repeated with P. The camera sensitivity was auto set. This process was repeated until the signal minimum was achieved.

6. When a very dark background has been achieved it is possible to image the lipid film on the gold surface and obtain micrographs.

It is worth noting that the BAM uses a class 3b laser and that relevant safety precautions need to be taken during its operation.

5.3 Results and Discussion

Images of the TSM sensor taken using the Brewster angle microscope confirm that a change in the lipid matrix organisation occurred on hydration (Figure 5.2).
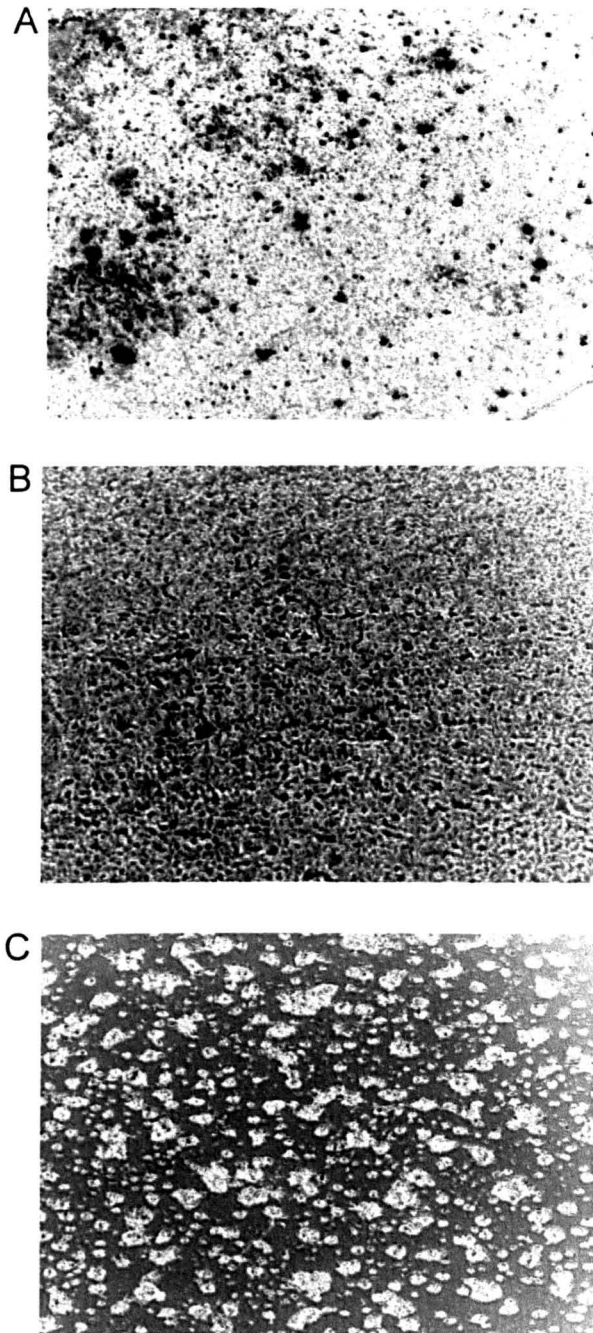
Figure 5.2 Brewster angle microscope images of: (A) blank TSM sensor, (B) a lipid coated TSM sensor before hydration (C) a lipid coated TSM sensor after hydration.

Clear differences in the Brewster angle micrographs can be seen between the blank, coated, and hydrated images of the TSM sensor shown in Figure 5.2. The image of the blank TSM

sensor indicates a grainy surface to the TSM sensor; this is consistent with the atomic force microscopy results[156] which showed that the surface of the polished TSM sensors that we are using posses small undulations with an average diameter of 10.1nm (±3.5). The surface of the TSM sensor coated with the lipid matrix film has a much smoother appearance than the blank sensor. The small undulations present on the blank sensor have disappeared. This change in appearance indicate two things:

1. The surface irregularities of the TSM sensor are being filled with the lipid matrix giving the sensor a smoother appearance. This is in contrast to the Langmuir-Blodgett films where the thin fatty acid films coated followed the surface irregularities of the sensor (Chapter 3).

2. That the lipid components of the matrix are evenly distributed on the surface of the sensor. If there were any separation of the individual lipid component then the domains would be visible on the micrographs.

After hydration of the lipid matrix film the image of the TSM sensor surface shows the existence of two distinct areas with different refractive properties. This indicates that some separation of the lipid components into individual domains has occurred. It is only possible to speculate which of the lipid components, if indeed it is lipid, was the cause of these domains. It is unlikely that the domains are water despite the hydration of the lipid film since the film has been dried before it is imaged; it is more likely that it is either the cholesterol or unsaturated fatty acids. The frequency shifts measured (Table 3.4) for the lipid matrix film agreed with this. Unsaturated fatty acids e.g. oleic acid have been demonstrated to form 'pools' in the stratum corneum lipids when they are used as penetration enhancers and could possibly be doing the same in the lipid matrix membrane[43]. Cholesterol has a chemical

structure that is significantly different from the fatty acid molecules and is therefore the most likely component to separate into individual domains.

5.4 Summary

Lipid matrix films were imaged using the BAM before and after hydration. The micrographs showed clear differences between the deposited films. Post-hydration the lipid films imaged showed a degree of separation with regions of differing refractive indices appearing.

6 INVESTIGATION OF DRUG PARTITIONING INTO LIPID MEMBRANES

This Chapter investigates the potential of TSM sensors to measure the partitioning of drug molecules into a lipid membrane that mimics the stratum corneum. The partitioning of a model drug substance (ibuprofen) into the lipid matrix film will be investigated using the TSM sensor system that has been characterised in previous chapters. The performance of the measurement system will be investigated using the liquid cell in both flow and static conditions, with the effect of the buffer, the flow rate, and mixing also investigated.

- In the flow cell the effect of different pHs and ionic strengths of buffer were investigated. Under flow conditions the high shear forces exerted on the lipid matrix by the passage of the media could have a large effect on the measurement. The tenacity of the lipid matrix on the TSM sensor surface was therefore investigated using several different types of media and flow conditions. Once the conditions had been optimised the partitioning of ibuprofen into the lipid matrix films were investigated.

- Another way of reducing the shear placed on the lipid matrix films is to use the static side of the flow cell. The static side has the advantage that the liquid does not exert a shear force on the lipid layer as it is placed in the chamber and therefore less lipid should be lost, and less stresses placed on the TSM sensor. The static cell also needs to be disturbed less during the experiment as no syringes need to be attached to inject the buffer, this reduces the chances of introducing air bubbles. The most obvious disadvantage of using the static side of the liquid cell will be ensuring that the liquids added to the chamber mix well and instantaneously. In order to assess the mixing of liquids placed in the static chamber of the liquid cell, then the mixing of a saline solution and water was investigated. Since the saline solution has a different density

and viscosity from water it should be possible to detect the addition of the solution by a change in the frequency and resistance. This should allow an assessment of the effectiveness of the mechanical stirrer method. The partitioning of ibuprofen into the lipid matrix will then be investigated.

6.1 Theory

TSM sensor measurements have been used previously to investigate biological processes involving lipid membranes. These studies can be broadly split into two groups; those performed in the gas phase and those in the liquid phase. Measurements made in the gaseous phase have the advantage that they are relatively simple and allow the use of a Sauerbrey-like relationship between frequency shift and mass change. Liquid measurements, while mimicking the *in vivo* situation better, require a more complicated approach to the interpretation of the results as mass and material changes of the film need to be separated.

The selective adsorption of chemical molecules from the gas phase to self-assembled monolayers has been investigated using TSM sensors[148, 149]. Quartz crystal microbalances were investigated for use with monolayers for molecular recognition, that would allow the adsorption behaviour and kinetics of some simple organic compounds and alkanethiols with various functional groups to be observed and quantified. While studies in the gas phase will reduce errors in interpretation of frequency shifts using Sauerbrey type equations, many of the molecules are not in a natural state, thereby limiting the application to biological systems. Molecular recognition in the gas phase using TSM sensors does have application for monitoring industrial process e.g. detection of acetone levels. Molecular recognition of molecules in the liquid phase has also been investigated including the selective detection of isoniazid in body fluids[157]

A wide range of experiments using TSM sensor have been performed on biological membranes, including protein binding, and partitioning. A few of these studies are reviewed here:

The effect of metal ions on phospholipid membranes has been investigated[158, 159] in solution. The interaction of metal ions with monolayers of lipids are well known, the positive effects that such interactions can have are often utilised in the construction of Langmuir-Blodgett films. Calcium ions are also known to have important roles in a number of biomembrane processes e.g. cell fusion and active transport. Ebara *et al.*[158] demonstrated that changes induced in phospholipid membrane by the presence or absence of calcium ions in solution, were measurable using an electrochemical TSM sensor and were able to determine dissociation constants for the process using the frequency shift of the sensor. The results that Ebara *et al.* obtained using the TSM sensor, correlated well with electrochemical measurement, but showed significant difference from NMR measurements.

The interaction and binding of protein molecules to phospholipid films[160, 161] at the air/water interface has been investigated using TSM sensor frequency shift. The non-specific interaction of mellitin and β-globulin to a phospholipid film was measured in liquid and dry states and at various surface pressures of film, the more specific interactions of concancavalin A to glycolipid membranes was also investigated. For the non-specific binding processes the authors were able to draw conclusions about how the proteins were associating with the lipid film from the changes in film mass that they observed. For concancavalin A, kinetic studies were possible demonstrating a fast binding and slow dissociation process.

TSM sensors have also been used to investigate the kinetics of liposome fusion to the surface of TSM sensors. These studies as well as investigating the change in frequency as the liposomes fused also monitored the dissipation of the acoustic wave in the film enabling

additional information about the fusion process to be elucidated[162]. This technique has also been used to investigate other biological interfacial processes[163.]

Partitioning processes of molecules from solution into lipid and polymer membranes has also been investigated[164, 165, 146, 166, 167, 145, 168]. These studies have investigated the partitioning of a range of molecules including hydrophobic alcohols, cholesterol, surfactants, cyclodextrins, and odourants and perfumes. Correlations have been drawn between the results obtained from the TSM sensor experiments and independent measurements such as the partition coefficient, have enabled the investigation of several processes including eye irritancy, and odour sensing. These previous studies have demonstrated that it is possible to determine solute partitioning into lipid membranes using the TSM sensor. However, there are some limitations to these studies. Most of the studies mentioned assume that the films/membranes under study do not alter in their physical properties during the study. This assumption is important as changes in the physical properties of the film cause a change in the frequency of oscillation of the TSM sensor which indistinguishable from that caused by a change in the film mass. More recent partitioning studies, performed in the liquid phase, have investigated the effect of viscoelastic changes in polymer films used to measure the partition coefficients of organic compounds[86].

Changes to the physical properties of a film under study can make interpretation of results difficult in TSM sensor experiments, but this problem is surmountable. In this project the use of impedance analysis of the TSM sensor will enable any changes in the physical properties of the film to be determined. This has dual benefit. Firstly, the contribution to the frequency shift, of any changes in the physical properties of the film can be assessed. Secondly, the impedance measurements will enable the action of the molecules under study on the membrane to be investigated. These principles have been demonstrated in the investigations of lipid fluidity in Chapter 4.

6.2 Method

100 mg mL^{-1} and 50 mg mL^{-1} solutions of the lipid matrix in chloroform were prepared according to the formulae in Table 3.1. All glassware was thoroughly rinsed with purified water prior to use. No plastic containers were used.

All liquids used in the experiments were sonicated to remove dissolved gasses that might effect the measurements. Phosphate buffers were prepared by dissolving 13.5 g of potassium dihydrogen orthophosphate dissolving in nanopure water adjusting to pH (either 5.0 or 7.4) using potassium hydroxide and then making up to 1000 mL using nanopure water. Sodium chloride was added to the solution before adjustment of the pH, when appropriate to the experiment.

TSM sensors were cleaned by removal from the holder, submersion into solutions of piranha, diethyl ether, and acetone for at least 10 min in each solvent. The sensor was rinsed with nanopure water after each submersion and then dried in an oven. The sensor was returned to the holder and silver conductive paint used to restore the electrical connections before impedance measurements were made.

The cleaned TSM sensor was removed from the holder and placed onto the custom made spin-coating apparatus. A vacuum was used to attach the TSM sensor to the rotating head of the coater and was then sensor spun at high speed. A 10 µL drop of 100 mg mL^{-1} lipid matrix solution was dropped on to the centre of the crystal electrode using a micropipette, the sensor was allowed to spin for a further twenty seconds. Impedance measurements of the TSM sensor were made before and after coating with the lipid film using a HP E5100A network analyser and PI network test fixture. Where the TSM sensor had been removed from the holder silver

conductive paint used to restore the electrical connections before impedance measurements were made.

6.2.1 Measurements made using the liquid cell flow chamber

The TSM sensor coated with a 100 mg mL^{-1} lipid matrix film was placed in the liquid cell with the lipid membrane facing the flow side of the cell. Buffer and drug solutions were injected into the liquid cell using a surgical syringe driver connected to the flow cell by PTFE tubing, at a flow rate of either 0.5 or 1.0 mL min^{-1}. Changes to the buffer solution were achieved by switching syringes in the driver. In order to limit the impact of swapping syringes the PTFE tubing was firmly attached to the work surface. Various media were used in the investigation, including nanopure water, saline solution, phosphate buffers (pH 5.0 and 7.4), and saline/phosphate buffers. Saturated ibuprofen solutions were made by dissolving ibuprofen in nanopure water.

The frequency and resistance of the TSM sensor was measured at time intervals of between 20 to 60 seconds using the HP E5100A network analyser and PI network test fixture.

6.2.2 Measurements made using the liquid cell static chamber

The TSM sensor coated with a 50 mg mL^{-1} lipid matrix film was placed in the liquid cell with the lipid membrane facing the static side of the cell. 0.4 mL of buffer was placed into the static chamber using a pipette and left until measurements settled. 0.4 mL of drug solution or buffer was then placed into the static chamber. A mechanical stirrer continuously mixed the solutions in the static cell while buffer and drug solutions were present. The impedance of the TSM sensor was continuously recorded while the experiments was running at intervals of 60 secs using the HP E5100A network analyser and PI network test fixture.

Mixing of the solutions in the liquid cell was assessed by measuring the change in frequency and resistance of the TSM sensor when 0.4 mL of 1 %w/v saline was added to 0.4 mL nanopure water that was already in the static part of the cell.

Ibuprofen partitioning was assessed by adding 0.4 mL of saturated ibuprofen solution to 0.4 mL water in the static side of the liquid cell, while the frequency and resistance of the TSM sensor was measured.

6.3 Results and discussion

6.3.1 Measurements made using the liquid cell flow chamber

The first set of experiments presented is for the use of the flow side of the liquid cell. The main advantages that the flow side of the liquid cell has over the static side are the ease with which the liquid media can be changed without the need for mixing, and the fact that the experiment is completely sealed from the environment.

Table 6.1 shows the percentage film loss on exposure of the lipid matrix coated TSM sensors to various buffer solutions. The results, Table 6.1, clearly show that both of these factors do have an effect on the stability of the lipid film on the TSM sensor.

Table 6.1 Stability of the lipid matrix when exposed to various solutions flowed over the surface of the TSM sensor.

Treatment	Percentage film loss	Mean	Standard deviation
Water	41		
Water	20		
Water	40	34	22
Water	6		
Water	63		
8 % saline / phosphate buffer (pH 7.4)	85		
8 % saline / phosphate buffer (pH 7.4)	89		
8 % saline / phosphate buffer (pH 7.4)	67	69	18
8 % saline / phosphate buffer (pH 7.4)	50		
8 % saline / phosphate buffer (pH 7.4)	56		
8% saline / phosphate buffer (pH 5.0)	3		
8% saline / phosphate buffer (pH 5.0)	-2		
8% saline / phosphate buffer (pH 5.0)	8	4	5
8% saline / phosphate buffer (pH 5.0)	2		
8% saline / phosphate buffer (pH 5.0)	9		
Phosphate buffer pH (5.0)	39		
Phosphate buffer pH (5.0)	15		
Phosphate buffer pH (5.0)	19	40	24
Phosphate buffer pH (5.0)	60		
Phosphate buffer pH (5.0)	70		
1 % saline solution	20		
1 % saline solution	52		
1 % saline solution	50	51	20
1 % saline solution	59		
1 % saline solution	73		
1 % saline / phosphate buffer (pH 5.0)	40		
1 % saline / phosphate buffer (pH 5.0)	56		
1 % saline / phosphate buffer (pH 5.0)	32	41	21
1 % saline / phosphate buffer (pH 5.0)	11		
1 % saline / phosphate buffer (pH 5.0)	66		

The buffer that removed the least lipid from the surface of the TSM sensor was the phosphate buffer (pH 5.0) with 8 % sodium chloride included. This result was much better than the lipid films exposed to either a low salinity solution or a higher pH solution. Interestingly films were also reasonably stable when exposed to nanopure water. The significance of this result is that the pH 5.0 phosphate buffer with 8 % sodium chloride should be the buffer of choice for future experiments, however, this solution caused the oscillation of the TSM sensor to be dampened to such an extent that measurement was no longer possible. This was also the case for the

phosphate buffer at pH 7.4 including 8 % saline and the 1 % saline phosphate buffer at pH 5.0. The implication of this is that it was decided to use water in the partitioning experiments using the flow side of the liquid cell.

The flow of liquid over the surface of the TSM sensor will exert a shear force on the lipid film coated there. The effect that the rate of flow, and therefore the shear force, had on the adherence of the lipid to the sensor electrodes was investigated.

Table 6.2 Effect of flow rate on the retention of the lipid matrix to the TSM sensor, after 2 min exposure to phosphate buffer (pH 7.4).

Flow rate / mL min^{-1}	Percentage loss of lipid	Mean	Standard deviation
0.5	40		
0.5	40		
0.5	50	51	11
0.5	65		
0.5	60		
1.0	56		
1.0	80		
1.0	58	55	17
1.0	48		
1.0	32		

Table 6.2 demonstrates that the flow rate has no effect on the adherence of the lipid to the TSM sensor over the range of rates investigated.

Figure 6.1 and Figure 6.2 show typical partitioning experiments performed in the flow side of the liquid cell using a flow rate of 1 mm min^{-1}. The Figures demonstrate a large degree of variability present in both the frequency and resistance measurements on injection of both water and an ibuprofen solution. The injection of drug into the flow chamber does tend to produce a larger shift in frequency than the water injection but this shift is in the opposite direction in the two experiments. It is also apparent that the water injections also caused equally large shifts on certain occasions (Figure 6.2).
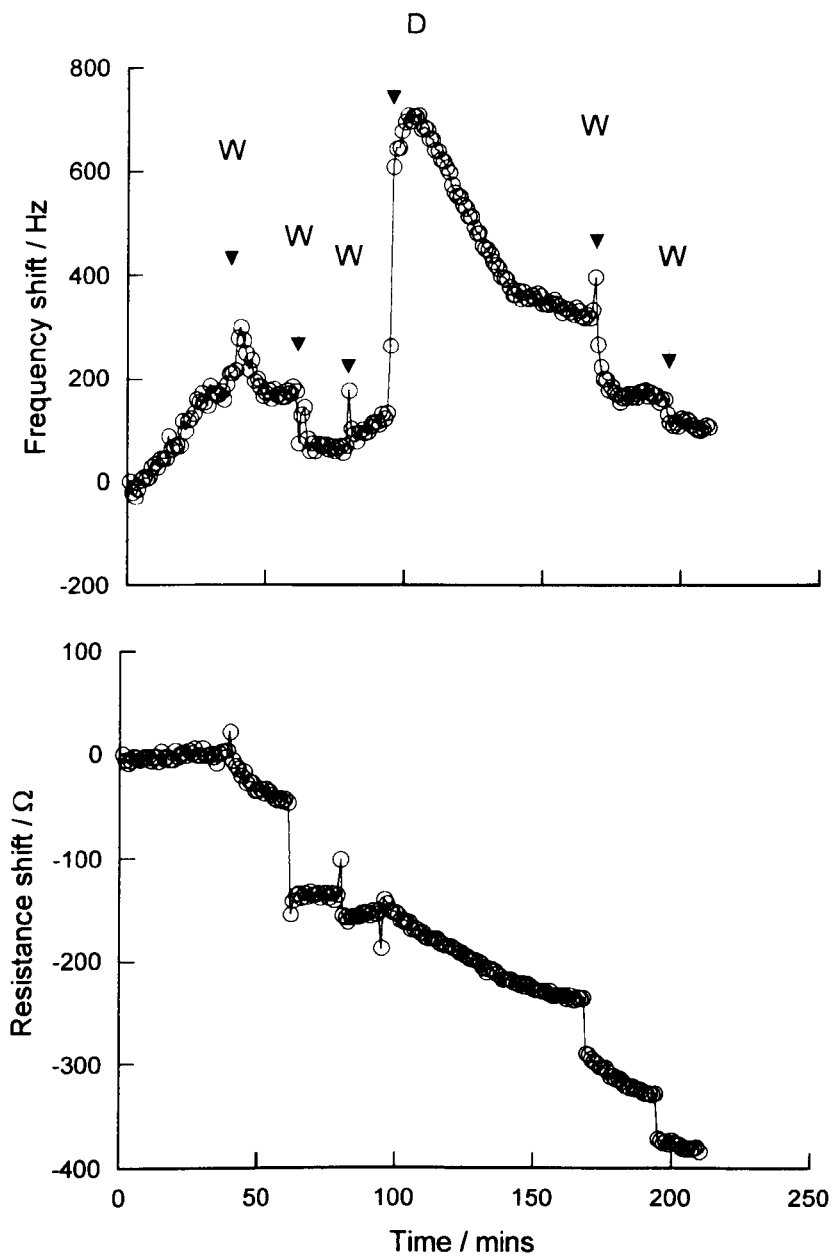
Figure 6.1 Partitioning experiment using the flow chamber of the liquid cell. W indicates and injection of water while D indicates an injection of drug solution.
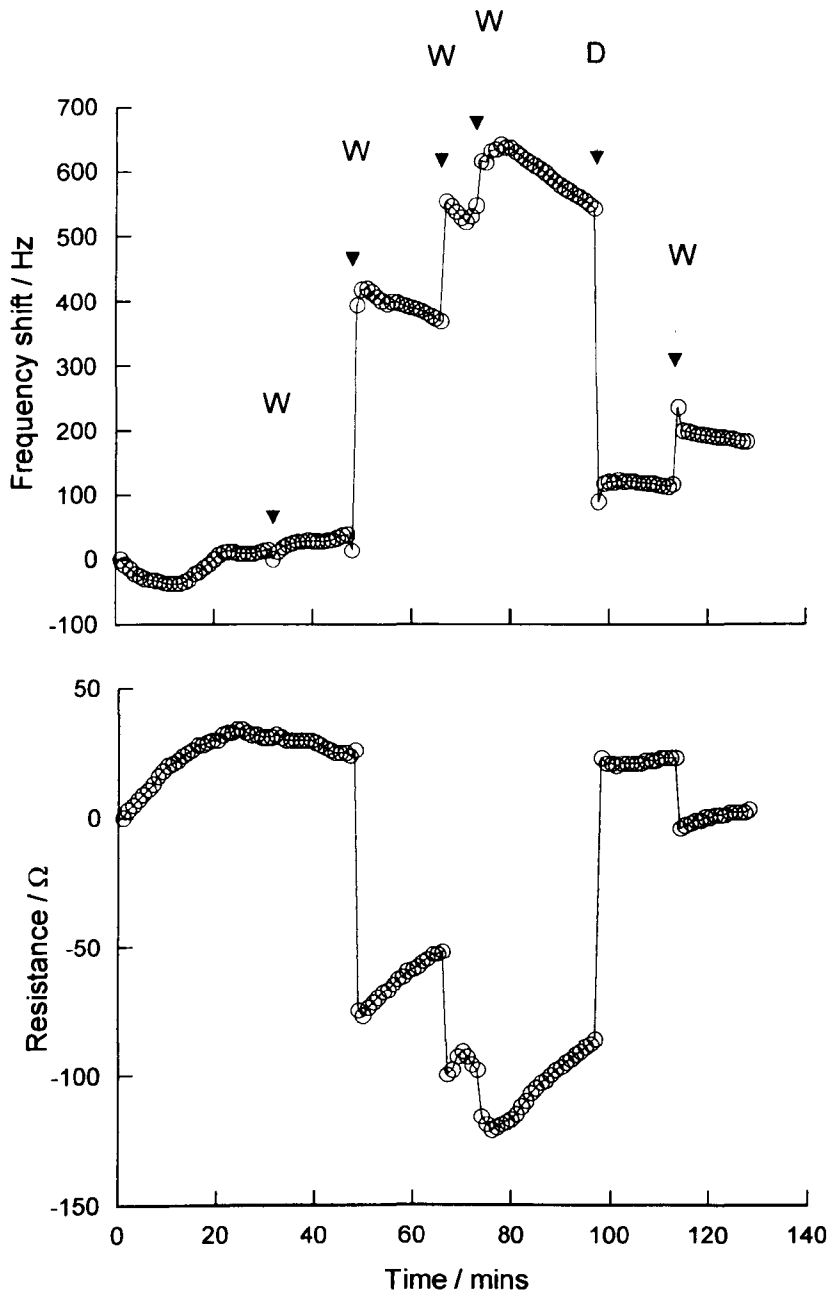
Figure 6.2 Partitioning experiment using the flow chamber of the liquid cell. W indicates and injection of water while D indicates an injection of drug solution.

The variability shown in the frequency and resistance measurements shown in Figure 6.1 and Figure 6.2 indicates that this method is not suitable for the measurement of drug partitioning. The large shifts recorded on the injection of water into the flow side of the cell would make it difficult to detect if any partitioning was occurring. In addition, the ibuprofen injections themselves show shifts in both frequency and resistance in both directions. It is thought that several reasons are responsible for the variability of the measurements taken in the flow side of the liquid cell:

1. Loss of a variable amount of lipid on injection of the buffer.

2. Effect of flow of liquid causing stress to the sensor.

3. Air bubbles in the flow cell, trapped when the syringes are changed.

4. Stresses placed on the sensor in the cell by movements of the tubes, though attempts were made to limit this impact.

In an attempt to remove some of the causes of the variability in the measurements, the static side of the liquid cell was investigated as a method for measuring drug partitioning.

6.3.2 Measurements made using the liquid cell static chamber

The mean percentage change in frequency of lipid matrix film when exposed to water and mixed in the static chamber of the liquid cell was -1 % ($\pm$ 22 %, n = 5). This is an improvement on the frequency shifts measured in the flow chamber of the liquid cell and demonstrates that the lipid matrix is more stable on the TSM sensor.

Figure 6.3 shows the change in frequency and resistance of lipid coated TSM sensors on addition of saline solution to the static side of the flow cell. A sharp shift in frequency and

resistance can be seen on the addition of the solution for the majority of the replicates. The shifts recorded are fairly small when compared to the changes that have been observed for other liquid measurements.
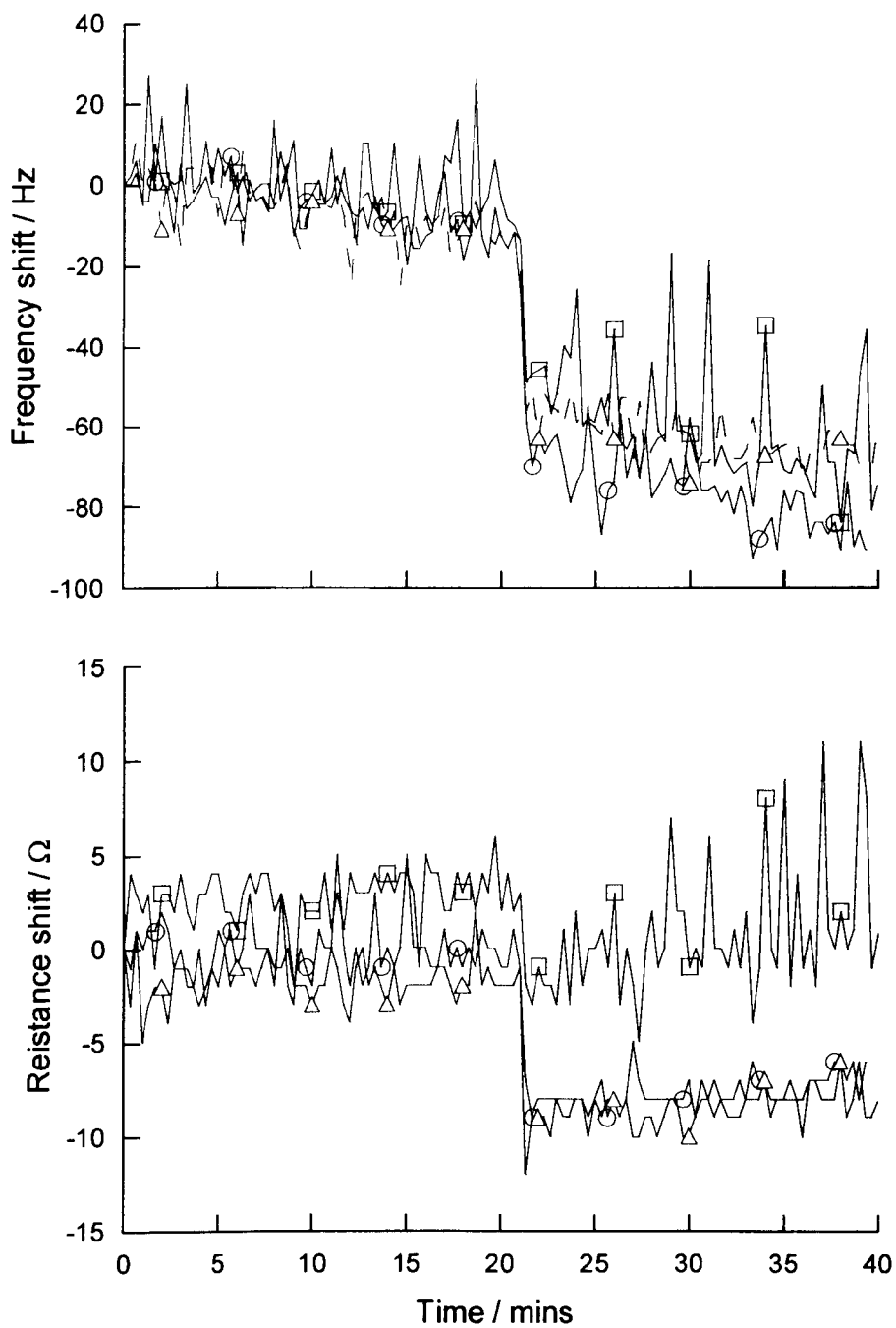
Figure 6.3 Three replicates (circles, squares, and triangles) showing the addition of a saline solution to water in the static chamber of the liquid cell. The injection occurs at 21 min. Measurements are made at 1 min intervals.

Figure 6.3 demonstrates that the mixing of the two liquids in the static chamber of the liquid cell is almost instantaneous. The drop in the frequency and resistance that occurs on the addition of the saline solution to the water is sharp with little or no equilibration required while the liquids mix. This means that the static side of the liquid cell can be used to investigate the partitioning of ibuprofen into the lipid matrix film without having to take into account mixing in the cell.

Figure 6.4 shows representative results for the partitioning of ibuprofen into the lipid matrix membrane. While the results still show more variation than desired, two of the ibuprofen partitioning experiments do appear to have measured an increase in the film mass that could be interpreted as ibuprofen partitioning into the membrane.
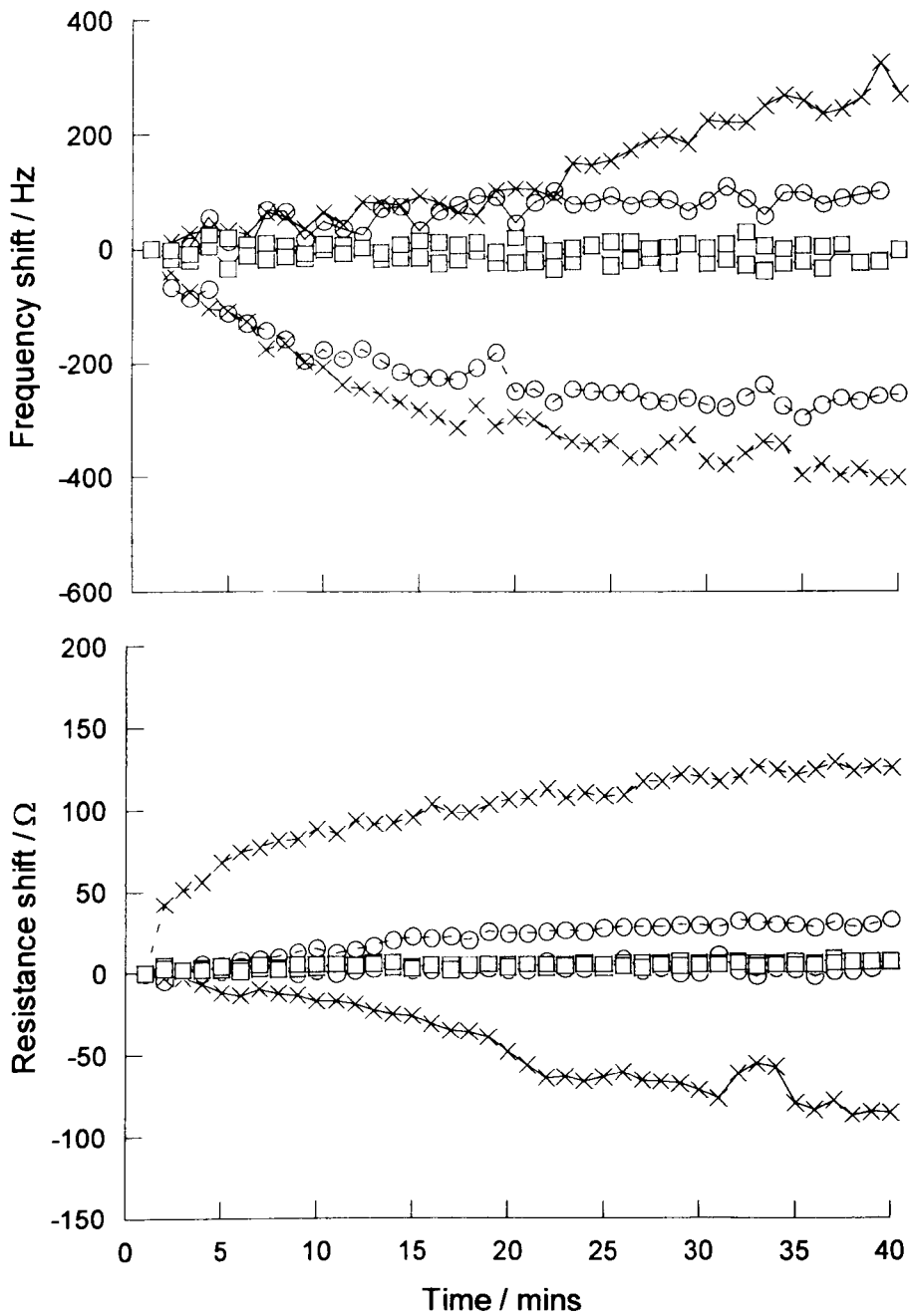
Figure 6.4 Ibuprofen partitioning (dashed lines) and control measurements (solid lines) for three replicate experiments (crosses, circles, and squares).

Figure 6.4 indicates that the technique has some promise for the measurement of drug partition coefficients and could be used as a pharmaceutical development tool. The change in the frequency of the TSM sensor on application of the ibuprofen solution indicates that the lipid film is increasing in mass in two cases out of three. The inconsistency of the data demonstrates the need for further development of the technique, primarily the lipid film coated on to the sensor and the manner in which it interacts with the media. While this is not conclusive evidence that partitioning is occurring this is the most likely explanation. The changes in the resistance of the lipid matrix coated TSM sensors does indicates that little change in the fluidity of the lipid films is occurring, though the results are fairly variable and could do with further investigation.

6.4 Summary

Two different experimental set-ups were investigated for the partitioning experiments, i.e. a cell in which the liquid was flowed across the TSM sensor surface, and a cell in which the liquid was 'static' on the sensor surface.

- The stability of the lipid layer on the surface of the TSM sensor under flow conditions was investigated. The lipid layer was found to be too unstable for this type of measurement to be made.

- When the static side of the flow cell was used, the lipid layer deposited onto the TSM sensor was found to be stable enough for partitioning experiment to be performed. Exposure of the TSM biosensor to an ibuprofen solution produced shift in frequency and resistance consistent with partitioning of the drug into the lipid layer.

7 GENERAL DISCUSSION

7.1 Initial characterisation of lipid films

TSM sensors studies of Langmuir-Blodgett films revealed substantial differences between the theoretical and experimental mass of the membranes. Investigation of three fatty acids (stearic acid, arachidic acid, and behenic acid), coated using a zinc sulphate subphase, demonstrated that the lipid films had a greater than expected mass. Plots of membrane mass versus the number of layer coated demonstrated that the response was non-linear.

Further investigation of the Langmuir-Blodgett films using two different subphases (i.e. calcium sulphate and water) demonstrated that the difference between experimental and theoretical results was, in part, due to the subphase. The calcium sulphate and water subphases produce lipid films with a mass closer to theoretical, and more importantly with a linear relationship between mass and number of layers. These results demonstrated that even coating of the sensor was occurring.

The similarity in the mass response, between the lipid films coated using water and calcium sulphate subphases, showed that the high experimental masses were unlikely to be due the inclusion of the metal ions into the lipid film. The fact that the lipid films were dried prior to measurement, the large differences between theoretical and experimental results, and Langmuir-Blodgett theory (which suggests that water would not be included in the film), allowed the inclusion of water in the lipid films to be discounted as a reason for the discrepancy. However, the use of the pure water did highlight the advantage of including calcium sulphate in the subphase. The monolayers formed on a water subphase were found to

be less stable (the lipid films slowly collapsed after coating) than those on one that included calcium ions.

The type of TSM sensor used in the investigation was changed to one possessing a smaller surface roughness, because entrapment of subphase in the surface roughness of the sensor was one possible reason for the high mass loading encountered. This switch was found to make little difference to the mass measured for each layer of fatty acid and the entrapment of subphase was discounted as a reason for the discrepancy.

The reason for the discrepancy between the experimental and theoretical mass of the lipid films was an under-prediction of the micro-surface area of the TSM sensor. The Sauerbrey equation, that was used to calculate the fatty acid film mass, includes the surface area of the TSM sensor. The figure used for this surface area was underestimated, as the undulations on the surface of the TSM sensor were not taken into account. This may account for the difference between the experimental and theoretical masses for both the polished and rough TSM sensors.

It was demonstrated that the lipid matrix could be coated onto the TSM sensor using the Langmuir-Blodgett technique. The lipid matrix films were found to follow the same relationship as the fatty acid films, though the packing of the lipid was slightly less dense due to the larger nature of some of the molecules.

The fluidity of the Langmuir-Blodgett films coated onto the TSM sensor was also investigated. Two different methods of assessing this fluidity were used in the interpretation of the TSM sensor impedance spectrum:

- The shapes of the TSM sensor impedance spectrum were compared. Broadening and reduction in depth of the TSM sensor impedance peak, at series resonance, was used to indicate if an increase in the film fluidity had occurred.

- The electrical resistance for the loaded film was derived from the Butterworth van Dyke equivalence circuit. The resistance value corresponds to the dampening of the acoustic wave in the coated film, and therefore will increase as the fluidity of the film increases.

The fluidity of the lipid films investigated did not change appreciably as more monolayers were coated onto the TSM sensor. This result was not however unexpected due to the small thickness and regular packing of the films that the Langmuir-Blodgett technique produces. Both features of the Langmuir-Blodgett films would impart 'solid' like character to the films, thereby minimising any viscous loss in the film.

The deposition of lipid matrix films by a spin coating technique was investigated. Unlike Langmuir-Blodgett film, which are highly organised, spin coated lipid layers are less structured and therefore a better mimic for biological membranes. It was also anticipated that the spin coating technique would produce thicker films and therefore allow better detection of drug partitioning in later experiments. The lipid matrix films produced by the spin coating technique were on average 4 times greater in mass than the Langmuir-Blodgett films.

7.2 Studies on the fluidity of lipid films

The thinness of the lipid films deposited by the Langmuir-Blodgett technique onto TSM sensors restricted the measurement of film fluidity. The development of the spin coating technique allowed the deposition of much thicker lipid films and therefore permitted the study of these films fluidity. Fitting of the TSM sensor impedance spectrum to a modified Butterworth Van Dyke circuit permitted the elucidation of the resistance (R_2), which is related to acoustic losses in the film (Section 2.1.1.2). Monitoring changes in resistance (R_2) was the means by which the fluidity of lipid films was investigated. R_2 was determined for lipid matrix films deposited by spin coating onto TSM sensors. Results showed a small increase in

resistance on coating of the TSM sensors with lipid films, and a much larger increase on hydration of the film. This result demonstrated that it was possible to measure changes in the fluidity of the lipid films using the TSM sensor measurement system. The small initial increase in resistance demonstrated that the lipid matrix films had a degree of fluidity when coated onto the sensor, this fluidity increased when the films were hydrated (and then dried). In addition, brewster angle micrographs (Section 5.3) demonstrated a change in the organisation of the lipid matrix on the TSM sensor surface when the film was hydrated.

The penetration enhancer Azone® has been shown to increase the fluidity of the stratum corneum lipids thereby increasing the flux of drug through the skin. Azone® was incorporated into the lipid matrix (0 to 20 mole percent) in order to assess the suitability of the TSM sensor measurement system for detecting changes in the membrane caused by penetration enhancement. No difference in the frequency was detected between the TSM sensors coated with films containing Azone® and those, which did not include it. This indicates that there is no difference in the mass of the films. Resistance measurements indicated that there was no difference in fluidity of the lipid matrix film (with or with out Azone®) prior to hydration. However, post-hydration an Azone® concentration dependant linear increase in film fluidity existed. This demonstrates the potential for the TSM sensor as a scientific tool for investigating the mode of action of penetration enhancers. The TSM sensor offers several benefits over conventional techniques used to measure the fluidity on lipid membranes including:

- The lipids do not have to be modified in order to measure the fluidity i.e. deuterated labels are not required.

- The fluidity of the whole membrane is measured and not individual components.

- It is a direct measure of fluidity and does not need to be inferred from a change in phase transition or membrane density.

- TSM measurements are related to an established mechanical property i.e. the shear modulus of the film.

The effect of cholesterol on the fluidity of the lipid matrix membrane was also investigated. Lipid matrix films were deposited onto the TSM sensor with the cholesterol removed. The absence of cholesterol had no discernable effect on the mass of the lipid matrix films coated onto the sensor, though the fluidity (R_2) was increased. When the hydration of these cholesterol free films was investigated the reproducibility of the results were affected. The cholesterol free lipid matrix films had a much larger variation in frequency and resistance, possibly highlighting the importance of cholesterol in the stability of the lipid layer.

The behaviour of three lipid films (lipid matrix, lipid matrix including 20 mole percent Azone®, and lipid matrix including 0 mole percent cholesterol) was investigated in liquid media. The lipid films were exposed to water at 25 °C and at a range of equilibrium temperatures between 25 and 60 °C. The purpose of this experiment was twofold:

1. To ascertain whether changes in the fluidity of the films could be measured as the lipid hydrated.

2. To determine the behaviour of the lipid films in a liquid environment as a prelude to the partitioning experiments.

The lipid films exposed to water at 25 °C exhibited large shifts in both frequency and resistance. These changes were dependant on both the composition and the concentration of the lipid deposited. TSM sensors coated with 100 mg mL^{-1} lipid matrix films exhibited large

shift in both frequency and resistance, which typically exceeded the measurement range of the instrument over the course of the experiments. Sensors with 50 mg mL^{-1} lipid films deposited on them exhibited smaller shifts in frequency and resistance. These changes in the film stopped between 150 and 200 min, providing a stable region in the frequency and resistance on which partitioning experiments could be performed. This result has important implications for later studies as it demonstrates that the amount of lipid deposited onto the TSM sensors may be critical to the data obtained and its interpretation.

The presence of Azone® in the lipid matrix film had an effect on the hydration behaviour of the films deposited. The 100 mg mL^{-1} films containing Azone® had a faster rate of both frequency and resistance change than the lipid matrix films that did not. The rate of change in frequency and resistance for the 50 mg mL^{-1} films did not appear to differ though the films containing Azone® had higher final values for frequency shift and R_2 than those that did not. One of the mechanisms of action of Azone® has been suggested to be by affecting the hydrogen bonding within the lipid layer[61], this may be the reason for the differences. Measurements made on the cholesterol free lipid films revealed a high degree of variability in the results, making interpretation of the changes difficult.

Measurement of lipid matrix coated TSM sensor frequency and R_2 were made at a range of equilibrium temperatures on the lipid matrix films. Interestingly the films containing 0 and 20 mole percent Azone® may have exhibited changes in resistance and frequency that related to the phase transition of the lipid films. Further investigation of this phenomenon is required for this to be confirmed.

7.3 Studies on partitioning

Preliminary experiments into the measurement of drug partitioning into the lipid coated TSM biosensors revealed promising results that indicated that such experiments should be possible. Initial investigations revealed that the lipid matrix film was not stable on the surface of the TSM sensor under flow conditions. This instability was probably due to the shear forces created in the lipid film as the liquid flowed across them. Partition experiments were therefore performed under static conditions where the liquid was placed on the surface of the TSM biosensor and slowly stirred. Measurements of frequency and resistance shifts showed a change in the film properties indicating that ibuprofen (the model drug) was entering the lipid membrane in some of the measurements made. While it is obvious that this is not a robust measurement technique for monitoring drug partitioning it does show that the potential exists to develop it into one.

8 FURTHER WORK

8.1 Further development of the TSM biosensor.

Further advances could be made in the development of the TSM sensor measurement system. Key areas that require further attention include:

- Development of the flow cell. Careful design of a new flow cell system would allow greater stability in the liquid based measurements. Key elements in the flow cell design are reduction in the stress created on the film by water flow, and control of the stress placed on the TSM sensor by the flow cell.

- Development of the lipid layers coated onto the TSM sensor would improve the accuracy and stability of the biosensor device. In particular the use of linker molecules to either, electrostatically or covalently bind the lipid to the TSM sensor could be advantageous. This would also aid the partitioning experiments reducing the potential for lipid loss from the sensor under flow conditions.

- The modification of the lipid matrix film to more closely mimic the stratum corneum lipids might make a difference to the application of the technique once it has been developed into a more robust method. In particular the inclusion of a ceramide fraction could be considered.

8.2 Investigation of lipid fluidity.

In order to fully understand the changes in the frequency and resistance and how they relate to the fluidity of lipid membranes it will be necessary to introduce an independent measure of

fluidity. The use of a technique such as FT-IR or Raman spectroscopy would provide invaluable information on the changes that are occurring in the membrane allowing a greater understanding of the capability of the TSM measurement system.

It would be interesting to investigate penetration enhancers with different modes of action to see if the differences can be determined using the TSM sensor technique. For example oleic acid has been reported as forming domains in lipid membranes, it may be possible to measure a difference in the response of lipid membranes including this enhancer when compared to Azone[®].

8.3 Investigation of drug partitioning.

A very limited number of studies have been done to investigate the partitioning of drug molecules into the lipid matrix. After the TSM biosensor system has been fully developed it is important that a wide range of different drug are investigated. The partition coefficients of drugs with a range of physical characteristics (size, lipophilicity, solubility etc) should be compared to literature values and comparison drawn. The effect of using buffers should also be investigated.

In order for the TSM sensor technique to be a useful tool in preformulation of transdermal drug products it must be capable of high through-put screening. The TSM sensor measurement technique will therefore need to be adapted so that multiple measurements can be made on one lipid membrane or multiple membranes measured on one TSM sensor. Multichannel TSM[168] devices have been developed and should provide a solution to this practical problem.

APPENDIX 1

Theoretical calculation for frequency and resistance shifts in a liquid.

This appendix shows the basis by which theoretical calculations for the shift in frequency and R_2 were made:

Table A1 The change in density and viscosity of water with temperature.

Temperature / °C	Density / g mL^{-1}	Viscosity / cp
20	0.99823	1.002
25	0.99707	0.8904
30	0.99567	0.7975
35	0.99406	0.7194
40	0.99224	0.6529
45	0.99025	0.5960
50	0.98807	0.5468
55	0.98573	0.5040
60	0.98324	0.4665

The shift in frequency (Kanazawa and Gordon relationship, Equation 2.2):

$$\Delta f = -f_0^{\frac{1}{2}} \left(\eta_L \rho_L \middle/ \pi \mu_Q \rho_Q \right)^{\frac{1}{2}}$$

where Δf is the shift in resonant frequency compared to a blank sensor (Hz), f_0 is the resonant frequency of the blank sensor (Hz), η_L is the viscosity of the liquid (poise), ρ_L is the density of the liquid (g mL^{-1}), μ_Q is the shear modulus of quartz (dyne cm^{-2}), and ρ_Q is the density of quartz (g cm^{-3}).

The resistance (Equation 2.15):

$$R_2 = \frac{N\pi}{4K_{em}^2 C_0} \left(\frac{\rho_L \eta_L}{2\omega_s \mu_Q \rho_Q} \right)^{\frac{1}{2}}$$

where R is the resistance (Ω), N is the harmonic number (1), ρ_L is the density of the liquid (g mL^{-1}), η_L is the viscosity of the liquid (poise), K_{em} is the electromagnetic coupling coefficient (dimensionless), ω_s is the angular frequency of series resonance (Hz), μ_Q is the shear modulus of quartz (dyne cm^{-2}), and ρ_Q is the density of quartz (g cm^{-3}).

APPENDIX 2

Structures of Typical Stratum Corneum Lipid Classes

This appendix shows the structures of the common lipids found in the stratum corneum:
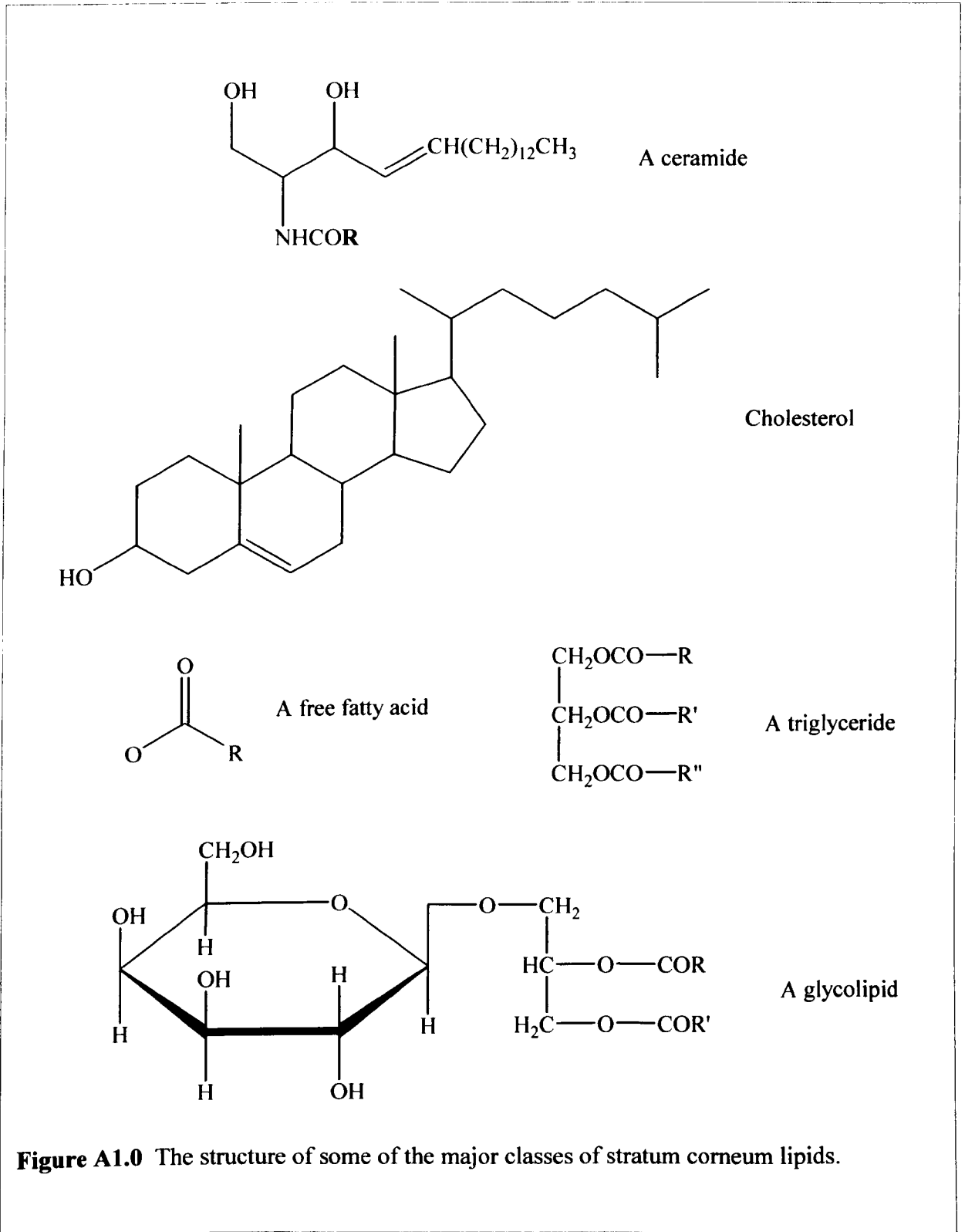
Figure A1.0 The structure of some of the major classes of stratum corneum lipids.

PUBLICATIONS

This appendix contains selected abstracts and papers published by the author:

1. UKAPS Conference (June 1999, Manchester):
"Characterisation of fatty acid multilayers using a TSM biosensor"

2. International Journal of Pharmaceutics (Reason *et al.*, 2000. Int. J. Pharm. 195, 25-28):
"Characterisation of fatty acid multilayers using a TSM biosensor"

3. British Pharmaceutical Conference (September 1999, Cardiff):
"The TSM biosensor: A novel technique for characterising lipid membranes"
The abstract to an oral presentation presented in Cardiff.

4. AAPS Conference (November 1999, New Orleans):
"The effect of quartz resonator topography on the response of a TSM biosensor"

5. British Pharmaceutical Conference (September 2000, Birmingham):
"A thickness shear mode biosensor investigation of the mucoadhesive properties of low crystallinity cellulose films."

6. British Pharmaceutical Conference (September 2001, Glasgow):

7. International Journal of Pharmaceutics (Reason *et al.*, 2001. Int. J. Pharm. 222, 121-128):
"A TSM sensor investigation of low crystallinity cellulose films"

UKAPS Conference (28th-30th June 1999, Manchester)

CHARACTERISATION OF FATTY ACID MULTILAYERS USING A TSM BIOSENSOR

<u>Matthew Reason</u>[a], Geoff Smith[a], Roger Latham[c],
Paul Teesdale-Spittle[b], Justine Ramsden[a], Brian Henry[d]
[a]School of Pharmacy and Pharmaceutical Sciences, [b]Department of Chemistry, [c]Faculty of Applied Sciences, De Montfort University, Leicester, LE1 9BH, UK.
[d]Pfizer Central Research, Sandwich, Kent, CT13 9NJ, UK

Thickness shear mode (TSM) biosensors have many potential applications within pharmaceutical sciences as a means of measuring mass changes (in the nanogram range), film thickness, viscosity and shear moduli. The possible application of the TSM sensor that we are investigating is a biosensor for measuring drug partition coefficients in lipid membranes. In order to realise this potential application, some fundamental understanding is required of the behaviour of lipid films on the sensor.

The present study characterises the behaviour of fatty acid multilayers as a suitable model, chemical system. Frequency shifts and impedance spectra were measured for multilayers of three fatty acid films (stearic acid, arachidic acid and behenic acid) coated on to the sensor using a Langmuir-Blodgett trough.

The results indicate that the frequency shift is non-linear at lower numbers of fatty acid layers and an inverse relationship is observed between fatty acid chain length and frequency shift. Both of these findings are attributed to topographical effects associated with the roughness of the sensor surfaces.

At high numbers of layers, changes in the impedance spectra indicate viscoelastic behaviour in thicker membranes. As increased numbers of layers are added to the surface it is believed, both inter and intramolecular motion may increase, resulting in the film behaving progressively more viscoelastically. These viscoelastic changes occur until the bulk viscoelastic properties of the fatty acid film is reached, at which point further spectral changes are simply a result of increasing film thickness. A linear frequency shift is observed at higher numbers of layers which is almost Sauerbrey like in response.

This work demonstrates the importance of fully characterising the physical behaviour of the lipid multilayers prior to using these systems for the measurement of drug partition coefficients.

REFERENCES

[1] Okahata, Y., Ye, X., Shimizu, A. and Ebato, H. (1989). "Interactions of bioactive compounds with lipid membranes deposited on a quartz crystal microbalance." *Thin Solid Films* **180**: 51-59.

[2] Moghimi, H. R., Williams, A. C. and Barry, B. W. (1996). "A lamellar matrix model for stratum corneum intercellular lipids. I. Characterisation and comparison with stratum corneum intercellular structure." *International journal of pharmaceutics* **131**: 103-115.

[3] Sauerbrey, G. W. (1959). "Use of oscillator quartz crystals for weighing thin layers and micro-weighing." *Zeitschrift fur Physik* **155**: 206-212.

[4] Hadgraft, J. (2001). "Skin, the final frontier." *International Journal of Pharmaceutics* **224** (1-2): 1-18.

[5] Lucklum, R., Behling, C. and Hauptmann, P. (1999). "Role of mass accumulation and viscoelastic film properties for the response of acoustic-wave based chemical sensors." *Analytical Chemistry* **71** (13): 2488-2496.

[6] Berti, J. J. and Lipsky, J. J. (1995). "Transcutaneous drug-delivery - a practical review." *Mayo Clinic Proceedings* **70** (6): 581-586.

[7] Brancaleon, L., Bamberg, M. P., Sakamaki, T. and Kollias, N. (2001). "Attenuated total reflection-fourier transform infrared spectroscopy as a possible method to investigate biophysical parameters of stratum corneum in vivo." *Journal of Investigative Dermatology* **116** (3): 380-386.

[8] Barry, B. W. (1988). "Topical Preparattions". in *"Pharmaceutics. The science of dosage form design"*. M. E. Aulton. Edinburgh, Churchill Livingstone: 381-411.

[9] Barry, B. W. (1983). *"Dermatological formulations"*. New York, Marcel Dekker.

[10] Bunge, A. L., Guy, R. H. and Hadgraft, J. (1999). "The determination of a diffusional pathlength through the stratum corneum." *International Journal of Pharmaceutics* **188** (1): 121-124.

[11] Suhonen, T. M., Bouwstra, J. A. and Urtti, A. (1999). "Chemical enhancement of percutaneous absorption in relation to stratum corneum structural alterations." *Journal of Controlled Release* **59** (2): 149-161.

[12] Weaver, J. C., Vaughan, T. E. and Chizmadzhev, Y. (1999). "Theory of electrical creation of aqueous pathways across skin transport barriers." *Advanced drug delivery reviews* **35**: 21-39.

[13] Elias, P. M. (1988). "Structure and function of the stratum corneum permeability barrier." *Drug Development Research* **13**: 97-105.

[14] Norlen, L. (2001). "Skin barrier formation: The membrane folding model." *Journal of Investigative Dermatology* **117** (4): 823-829.

[15] Abraham, W. and Downing, D. T. (1992). "Lamellar structures formed by stratum corneum lipids in vitro: A deuterium nuclear magnetic resonance (NMR) study." *Pharmaceutical Research* **9** (11): 1415-1421.

[16] Barry, B. W. (1987). "Mode of action of penetration enhancers in human skin." *Journal of Controlled Release* **6**: 85-97.

[17] Hadgraft, J. and Guy, R. H., Eds. (1989). *"Transdermal drug delivery: development issues and research issues"*. in "Drugs and the pharmaceutical sciences". New York, Dekker.

[18] Lampe, M. A., Burlingame, A. L., Whitney, J., Williams, M. L., Brown, B. E., Roitman, E. and Elias, P. M. (1983). "Human Stratum-Corneum Lipids - Characterization and Regional Variations." *Journal of Lipid Research* **24** (2): 120-130.

[19] Elias, P. M. and Friend, D. S. (1975). "The permeability barrier in mammalian epidermis." *Journal of Cell Biology* **65**: 180-191.

[20] Elias, P. M., Goerke, J. and Friend, D. S. (1977). "Mammalian epidermal barrier layer lipids: composition and influenece on structure." *The journal of investigative dermatology* **69**: 535-546.

[21] Elias, P. M., Braown, B. E., Fritsch, P., Goerke, J., Gray, G. M. and White, R. J. (1979). "Localization and composition of lipids in neonatal mouse stratum granulosum and stratum corneum." *The journal of investigative dermatology* **73**: 339-348.

[22] Swartzendruber, D. C., Wertz, P. W., Kitko, D. J., Madison, K. C. and Downing, D. T. (1989). "Molecular models of the intercellular lipid lamellae in mammalian stratum corneum." *The Journal of Investigate Dermatology* **92** (2): 251-257.

[23] Wertz, P. W., Abraham, W., Landmann, L. and Downind, D. T. (1986). "Preparation of liposomes from stratum corneum lipids." *Journal of investigative dermatology* **87** (5): 582-584.

[24] Abraham, W., Wertz, P. W. and Downing, D. T. (1988). "Effect of epidermal acylglucosylceramides and acylceramides on the morphology of liposomes prepared from stratum corneum lipids." *Biochimica et biophysica acta* **939** (2): 403-408.

[25] Abraham, W. and Downing, D. T. (1989). "Preparation of model membranes for skin permeability studies using stratum corneum lipids." *Journal of investigative dermatology* **93** (6): 809-813.

[26] Bouwstra, J. A., Thewalt, J., Gooris, G. S. and Kitson, N. (1997). "A model membrane approach to the epidermal permeability barrier: An X-ray diffraction study." *Biochemistry* **36**: 7717-7725.

[27] Bouwstra, J. A., Gooris, G. S., Vanderspek, J. A. and Bras, W. (1991). "Structural Investigations of Human Stratum-Corneum By Small- Angle X-Ray-Scattering." *Journal of Investigative Dermatology* **97** (6): 1005-1012.

[28] Bouwstra, J. A., Gooris, G. S., Salomons-de Vries, M. A., van der Spek, J. A. and Bras, W. (1992). "Structure of human stratum corneumm as a function of temperature and hydration: A wide-angle X-ray diffraction study." *International Journal of Pharmaceutics* **84**: 205-216.

[29] Bouwstra, J. A., Gooris, G. S., Vanderspek, J. A., Lavrijsen, S. and Bras, W. (1994). "The Lipid and Protein-Structure of Mouse Stratum-Corneum - a Wide and Small-Angle Diffraction Study." *Biochimica Et Biophysica Acta-Lipids and Lipid Metabolism* **1212** (2): 183-192.

[30] Bouwstra, J. A., Gooris, G. S., Bras, W. and Downing, D. T. (1995). "Lipid Organization in Pig Stratum-Corneum." *Journal of Lipid Research* **36** (4): 685-695.

[31] White, S. H., Mirejovsky, D. and King, G. I. (1988). "Structure of Lamellar Lipid Domains and Corneocyte Envelopes of Murine Stratum-Corneum - an X-Ray-Diffraction Study." *Biochemistry* **27** (10): 3725-3732.

[32] Garson, J. C., Doucet, J., Leveque, J. L. and Tsoucaris, G. (1991). "Oriented Structure in Human Stratum-Corneum Revealed By X-Ray- Diffraction." *Journal of Investigative Dermatology* **96** (1): 43-49.

[33] Wilkes, G. L., Nguyen, A. L. and Wildhauer, R. (1973). *Biochemica et Biophysica Acta* **304**: 267-275.

[34] Cornwell, P. A., Barry, B. W., Stoddart, C. P. and Bouwstra, J. A. (1994). "Wide-Angle X-Ray-Diffraction of Human Stratum-Corneum - Effects of Hydration and Terpene Enhancer Treatment." *Journal of Pharmacy and Pharmacology* **46** (12): 938-950.

[35] Gay, C. L., Guy, R. H., Golden, G. M., Mak, V. H. W. and Francoeur, M. L. (1994). "Characterization of Low-Temperature (Ie, Less-Than-65-Degrees- C) Lipid Transitions in Human Stratum-Corneum." *Journal of Investigative Dermatology* **103** (2): 233-239.

[36] Bouwstra, J. A., Gorris, G. S., Cheng, K., Weerheim, A., Bras, W. and Ponec, M. (1996). "Phase behavior of isolated skin lipids." *Journal of Lipid Research* **37** (5): 999-1011.

[37] Forslind, B. (1994). "A Domain Mosaic Model of the Skin Barrier." *Acta Dermato-Venereologica* **74** (1): 1-6.

[38] Barry, B. W. (2001). "Novel mechanisms and devices to enable successful transdermal drug delivery." *European Journal of Pharmaceutical Sciences* **14** (2): 101-114.

[39] Barry, B. W. (1988). "Action of Skin Penetration Enhancers - the Lipid Protein Partitioning Theory." *International Journal of Cosmetic Science* **10** (6): 281-293.

[40] Barry, B. W. (1991). "Lipid-Protein-Partitioning Theory of Skin Penetration Enhancement." *Journal of Controlled Release* **15** (3): 237-248.

[41] Goodman, M. and Barry, B. W. (1988). "Action of Penetration Enhancers On Human-Skin As Assessed By the Permeation of Model-Drugs 5-Fluorouracil and Estradiol .1. Infinite Dose Technique." *Journal of Investigative Dermatology* **91** (4): 323-327.

[42] Williams, A. C. and Barry, B. W. (1991). "Terpenes and the Lipid Protein Partitioning Theory of Skin Penetration Enhancement." *Pharmaceutical Research* **8** (1): 17-24.

[43] Francoeur, M. L., Golden, G. M. and Potts, R. O. (1990). "Oleic acid: its effects on stratum corneum in relation to (trans) dermal drug delivery." *Pharmaceutical Research* **7** (6): 621- 627.

[44] Hadgraft, J., Peck, J., Williams, D. G., Pugh, W. J. and Allan, G. (1996). "Mechanisms of action of skin penetration enhancers/retarders: Azone and anologues." *International journal of pharmaceutics* **141**: 17-25.

[45] Moghimi, H. R., Williams, A. C. and Barry, B. W. (1997). "A lamellar matrix model for stratum corneum intercellular lipids .5. Effects of terpene penetration enhancers on the structure and thermal behaviour of the matrix." *International Journal of Pharmaceutics* **146** (1): 41-54.

[46] Aungst, B. J., Blake, J. A. and Hussain, M. A. (1990). "Contributions of Drug Solubilization, Partitioning, Barrier Disruption, and Solvent Permeation to the Enhancement of Skin Permeation of Various Compounds With Fatty-Acids and Amines." *Pharmaceutical Research* **7** (7): 712-718.

[47] López, A., Pellett, M. A., Llinares, F., Díez-Sales, O., Herráez, M. and Hadgraft, J. (1997). "The enhancer effect of several phenyl alcohols on percutaneous penetration of 5-Fluorouracil." *Pharmaceutical research* **14** (5): 681-685.

[48] Bhatia, K. S. and Singh, J. (1999). "Effect of linolenic acid ethanol or limonene ethanol and iontophoresis on the in vitro percutaneous absorption of LHRH and ultrastructure of human epidermis." *International Journal of Pharmaceutics* **180** (2): 235-250.

[49] Levang, A. K., Zhao, K. and Singh, J. (1999). "Effect of ethanol/propylene glycol on the in vitro percutaneous absorption of aspirin, biophysical changes and macroscopic barrier properties of the skin." *International journal of Pharmaceutics* **181**: 255-263.

[50] Moghimi, H. R., Williams, A. C. and Barry, B. W. (1998). "Enhancement by terpenes of 5-fluorouracil permeation through the stratum corneum: Model solvent approach." *Journal of Pharmacy and Pharmacology* **50** (9): 955-964.

[51] Degim, I. T., Usla, A., Atay, T., Akay, C. and Cevheroglu, S. (1999). "The effects of Azone and capsaicin on the permeation of naproxen through human skin." *International Journal of Pharmaceutics* **179**: 21-25.

[52] Schückler, F. and Lee, G. (1991). "The influence of azone on monomolecular films of some stratum corneum lipids." *Inetrnational Journal of Pharmaceutics* **70**: 173-186.

[53] Lopez-Castellano, A., Cortell-Ivars, C., Lopez-Carballo, G. and Herraez-Dominguez, M. (2000). "The influence of Span (R) 20 on stratum corneum lipids in Langmuir monolayers: comparison with Atone (R)." *International Journal of Pharmaceutics* **203** (1-2): 245-253.

[54] Engblom, J. and Engström, S. (1993). "Azone and the formation of reversed mono- and bicontinuous lipid-water phases." *International journal of Pharmaceutics* **98**: 173-179.

[55] Schückler, F. and Lee, G. (1992). "Relating the concentration-dependent action of Azone and dodecyl-L-pyroglutamate on the structure of excised human stratum corneum to changes in drug diffusivity, partition coefficient and flux." *International Journal of Pharmaceutics* **80**: 81-89.

[56] Harrison, J. E., Watkinson, A. C., Green, D. M., Hadgraft, J. and Brain, K. (1996). "The Relative Effect of Azone® and Transcutol® on Permeant Diffusivity and Solubility in Human Stratum Corneum." *Pharmaceutical Research* **13** (4): 542-546.

[57] Pilgram, G. S. K., Engelsma-van Pelt, A. M., Koerten, H. K. and Bouwstra, J. A. (2000). "The effect of two atones on the lateral lipid organization of human stratum corneum and its permeability." *Pharmaceutical Research* **17** (7): 796-802.

[58] Mizushima, J., Kawasaki, Y., Tabohashi, T., Kitano, T., Sakamoto, K., Kawashima, M., Cooke, R. and Maibach, H. I. (2000). "Effect of surfactants on human stratum corneum: electron paramagnetic resonance study." *International Journal of Pharmaceutics* **197** (1-2): 193-202.

[59] van den Bergh, B. A. I., Wertz, P. W., Junginger, H. E. and Bouwstra, J. A. (2001). "Elasticity of vesicles assessed by electron spin resonance, electron microscopy and extrusion measurements." *International Journal of Pharmaceutics* **217** (1-2): 13-24.

[60] Coderch, L., Fonollosa, J., Estelrich, J., De La Maza, A. and Parra, J. L. (2000). "Influence of cholesterol on liposome fluidity by EPR - Relationship with percutaneous absorption." *Journal of Controlled Release* **68** (1): 85-95.

[61] Beastall, J. C., Hadgraft, J. and Washington, C. (1988). "Mechanism of action of azone as a percutaneous penetration enhancer: lipid bilayer fluidity and transition temperature effects." *Internation journal of pharmaceutics* **43**: 207-213.

[62] Suhonen, T. M., Pirskanen, L., Raisanen, M., Kosonen, K., Rytting, J. H., Paronen, P. and Urtti, A. (1997). "Transepidermal delivery of beta-blocking agents: Evaluation of enhancer effects using stratum corneum lipid liposomes." *Journal of Controlled Release* **43** (2-3): 251-259.

[63] Harrison, J. E., Groundwater, P. W., Brain, K. R. and Hadgraft, J. (1996). "Azone induced fluidity in human stratum corneum. A fourier transform infared spectroscopy investigation using the perdeuterated analogue." *Journal of controlled release* **41**: 283-290.

[64] Yokomizo, Y. (1996). "Effect of phosphatidylcholine on the percutaneous penetration of drugs through the dorsal skin of guinea pigs in vitro; And analysis of the molecular mechanism, using attenuated total reflectance Fourier transform infrared (ATR-FTIR) spectroscopy." *Journal of Controlled Release* **42** (3): 249-262.

[65] Bommannan, D., Potts, R. O. and Guy, R. H. (1990). "Examination of Stratum-Corneum Barrier Function Invivo By Infrared-Spectroscopy." *Journal of Investigative Dermatology* **95** (4): 403-408.

[66] Cheng, S. and Chen, Y. (1988). "Study on erythrocyte fluidity by laser raman spectroscopy." *Cell Biol. Int. Rep.* **12**: 205-211.

[67] Williams, A. C., Edwards, H. G. M. and Barry, B. W. (1992). "Fourier transform Raman spectroscopy. A novel application for examining human stratum corneum." *International Journal of Pharmaceutics* **81** (1): R11-R14.

[68] Wehnelt, K., Schlecht, P. and Mayer, A. (1993). "*Dielectric Properties of the Protein Water System*". Water Biomolecule Interactions, SIF, Bologna.

[69] Williams, A. C., Barry, B. W., Edwards, H. G. M. and Farwell, D. W. (1993). "A critical comparison of some Raman spectroscopic techniquis for studies of human stratum corneum." *Pharaceutical research* **10** (11): 1642-1647.

[70] Kitson, N., Thewalt, J., Lafleur, M. and Bloom, M. (1994). "A model membrane approach to the epidermal permeability barrier." *Biochemistry* 33: 6707-6715.

[71] Bezema, F. R., Marttin, E., Roemelé, Brussee, J., Boddé, H. E. and de Groot, H. J. M. (1996). "^{2}H NMR Evidence for dynamic disorder in human skin induced by the penetration enhancer Azone." *Spectrochimica Acta Part A* 52: 785-791.

[72] Yokomizo, Y. (1997). "Effect of phosphatidylglycerol on the in vitro percutaneous drug penetration through the dorsal skin of guinea pigs, and analysis of the molecular mechanism, using (ATR-FTIR) spectroscopy." *International Journal of Pharmaceutics* 147 (2): 219-231.

[73] Gao, S. and Singh, J. (1997). "Mechanism of transdermal transport of 5-fluorouracil by terpenes: Carvone, 1,8-cineole and thymol." *International Journal of Pharmaceutics* 154 (1): 67-77.

[74] Caban, J. B., Moerland, T. S., Gibbs, S. J., McFadden, L. and Locke, B. R. (1999). "Transdermal water mobility in the presence of electrical fields using MR microscopy." *Magnetic Resonance Imaging* 17 (8): 1183-1191.

[75] Guy, R. H. and Hadgraft, J. (1989). "Mathematical model of percutaneous absorption". in *"Percutaneous absorption"*. R. L. Bronaugh and H. I. Maibach. New York, Marcel dekker: 13-26.

[76] Kirjavainen, M., Monkkonen, J., Saukkosaari, M., Valjakka-Koskela, R., Kiesvaara, J. and Urtti, A. (1999). "Phospholipids affect stratum corneum lipid bilayer fluidity and drug partitioning into the bilayers." *Journal of Controlled Release* 58 (2): 207-214.

[77] Aungst, B. J., Rogers, N. J. and Shefter, E. (1986). "Enhancement of naloxone penetration through human skin in vitro using fatty acids, fatty alcohols, surfactants, sulfoxides and amides." *International Journal of Pharmaceutics* 33: 225-234.

[78] Kaiser, T., Gudat, P., Stock, W., Pappert, G., Grol, M., Neumeier, D. and Luppa, P. B. (2000). "Biotinylated steroid derivatives as ligands for biospecific interaction analysis with monoclonal antibodies using immunosensor devices." *Analytical Biochemistry* 282 (2): 173-185.

[79] Su, H., Williams, P. and Thompson, M. (1995). "Platinum anticancer drug binding to DNA detected by thickness-shear-mode acoustic wave sensor." *Analytical Chemistry* 67 (5): 1010-1013.

[80] Kieser, B., Fietzek, C., Schmidt, R., Belge, G., Weimar, U., Schurig, V. and Gauglitz, G. (2002). "Use of a modified cyclodextrin host for the enantioselective detection of a halogenated diether as chiral guest via optical and electrical transducers." *Analytical Chemistry* 74 (13): 3005-3012.

[81] Okahata, Y., Kawase, M., Niikura, K., Ohtake, F., Furusawa, H. and Ebara, Y. (1998). "Kinetic measurements of DNA hybridization on an oligonucleotide-immobilized 27-MHz quartz crystal microbalance." *Analytical Chemistry* 70 (7): 1288-1296.

[82] Furtado, L. M., Su, H., Thompson, M., Mack, D. P. and Hayward, G. L. (1999). "Interactions of HIV-1 TAR RNA with tat-derived peptides discriminated by on-line acoustic wave detector." *Analytical Chemistry* 71 (6): 1167-1175.

[83] Hook, F., Kasemo, B., Nylander, T., Fant, C., Sott, K. and Elwing, H. (2001). "Variations in coupled water, viscoelastic properties, and film thickness of a Mefp-1 protein film during adsorption and cross- linking: A quartz crystal microbalance with dissipation monitoring, ellipsometry, and surface plasmon resonance study." *Analytical Chemistry* 73 (24): 5796-5804.

[84] Janshoff, A., Wegener, J., Sieber, M. and Galla, H.-J. (1996). "Double-mode impedance analysis of epithelial cell monolayers cultured on shear wave resonators." *European Biophysics Journal* 25: 93-103.

[85] Buckin, V. and Kudryashov, E. (2001). "U,trasonic shear wave rheology of weak particle gels." *Advances in colloid and interface science* 89-90: 401-422.

[86] Patel, R., Zhou, R. N., Zinszer, K., Josse, F. and Cernosek, R. (2000). "Real-time detection of organic compounds in liquid environments using polymer-coated thickness shear mode quartz resonators." *Analytical Chemistry* 72 (20): 4888-4898.

[87] Stellnberger, K.-H., Wolpers, M., Fili, T., Reinartz, C., Paul, T. and Stratmann, M. (1997). "Electrochemical quartz microbalance in modern corrosion research." *Faraday discussions* 107: 307-322.

[88] Thompson, M. and Hayward, G. L. (1997). "*Mass response of the thickness-shear mode acoustic wave sensor in liquids as a central misleading dogma*". Proceedings of the IEEE Conference on Frequency Control.

[89] Stockbridge, C. D. (1966). "Resonance frequency versus mass added to quartz crystals." *Vacuum Microbalance Techniques* 5: 193-205.

[90] Behrndt, K. H. (1971). "Long-term operation of crystal oscillators in thin-film dposition." *The journal of vacuum science and technology* 8 (5): 622-626.

[91] Miller, J. G. and Bolef, D. I. (1968). "Sensitivity enhancement by the use of acoustic resonators in cw ultrasonic spectroscopy." *Journal of Applied Physics* 39 (10): 4589-4593.

[92] Miller, J. G. and Bolef, D. I. (1968). "Acoustic wave analysis of the operation of quartz-crystal film-thickness monitors." *Journal of Applied Physics* **39**: 5815-5816.

[93] Lu, C. (1984). "Intyroduction and historical overview of applications of piezoelectric quartz crystal microbalance". in *"Applications of piezoelectric quartz crystal microbalances"*. C. Lu and A. W. Czanderna. Oxford, Elsevier. **7**: 1-17.

[94] Lu, C. and Lewis, O. (1972). "Investigations of film-thickness determination by oscillating quartz resonators with large mass load." *Journal of Applied Physics* **43** (11): 4385-4390.

[95] Kanazawa, K. K. and Gordon, J. G. (1985). "Frequency of a quartz crystal microbalance in contact with liquid." *Analytical Chemistry* **57**: 1770-1771.

[96] Glassford, A. (1978). "Response of a quartz crystal microbalance to a liquid deposit." *Journal of Vacuum Science and Technology* **15**: 1836-1843.

[97] Konash, P. and Bastiaans, G. (1980). "Piezoelectric crystals as detectors in liquid chromatography." *Analytical Chemistry* **52**: 1929-1931.

[98] Nomura, T. and Minemura, A. (1980). *Nippon Kagaku Kaishi* **1980**: 1621.

[99] Guilbault, G. G. (1984). "Applications of quartz crystal microbalances in analytical chemistry". in *"Applications of piezoelectric quartz crystal microbalances"*. C. Lu and A. W. Czanderna. Oxford, Elsevier. **7**: 251-279.

[100] Nomura, T. (1981). "Single-drop method for determination of cyanide in solution with a piezoelectric quartz crystal." *Analytica Chimica Acta* **124**: 81-84.

[101] Nomura, T. and Okuhara, M. (1982). "Frequency shifts of piezoelectric quartz crystals immersed in organic liquids." *Analytica Chimica Acta* **142**: 281-284.

[102] Yao, S.-Z. and Zhou, T.-A. (1988). "Dependence of the oscillation frequency of a piezoelectric crystal on the physical parameters of liquids." *Analytica Chim. Acta* **212**: 61-72.

[103] Kanazawa, K., Keiji. and Gordon, J., G. (1985). "The oscillation frequency of a quartz resonator on contact with a liquid." *Analytica Chimica Acta* **175**: 99-105.

[104] Bruckenstein, S. and Shay, M. (1985). "Experimental aspects of the use of the quartz crystal microbalance in solution." *Electrochimica Acta* **30**: 1295-1300.

[105] Lee, P. C. Y. and Huang, R. (2002). "Effects of a liquid layer on thickness-shear vibrations of rectangular AT-cut quartz plates." *Ieee Transactions On Ultrasonics Ferroelectrics and Frequency Control* **49** (5): 604-611.

[106] Thompson, M., Kipling, A., Duncan-Hewitt, W., Rajakovic, L. and Cavic-Vlasak, B. (1991). "Thickness-shear-mode acoustic wave sensors in the liquid phase. A review." *Analyst* **116**: 881-890.

[107] Ward, M. and Delawski, E. (1991). "Radial mass sensitivity of the quartz crystal microbalance in liquid media." *Analytical Chemistry* **63**: 886-890.

[108] Schumacher, R., Gordon, J. G. and Melroy, O. (1987). "Observation of morphological relaxation of copper and silver electrodes in solution using a quartz microbalance." *Journal of Electroanalytical Chemistry* **216**: 127-135.

[109] Schumacher, R., Borges, G. and Kanazawa, K. K. (1985). "The quartz microbalance: A sensitive tool to probe surface reconstructions on gold electrodes in liquids." *Surface Science Letters* **163**: L621-L626.

[110] Schumacher, R. (1990). "The quartz microbalance: A novel approach to the in-situ investigation of interfacial phenomena at the solid/liquid junction." *Angewandte Chemie International edition in English* **29** (4): 329-438.

[111] Beck, R., Pitterman, U. and Weil, K. G. (1992). "Influence of the surface microstructure on the coupling between a quartz oscillator and a liquid." *Journal of the Electrochemical Society* **139** (2): 453-461.

[112] Yang, M., Thompson, M. and Duncan-Hewitt, W. C. (1993). "Interfacial properties and the response of the thickness-shear mode acoustic sensor in liquids." *Langmuir* **9** (3): 802-811.

[113] Martin, S. J., Frye, G. C., Ricco, A. J. and Senturia, S. D. (1993). "Effect of surface roughness on the response of thickness-shear mode resonators in liquids." *Analytical Chemistry* **65** (20): 2910-2922.

[114] Bruckenstein, S., Fensore, A., Li, Z. and Hillman, A. R. (1994). "Dual quartz crystal microbalance using a submerged reference crystal. Effect of surface roughness and liquid properties." *Journal of Electroanalytical Chemistry* **370** (1-2): 189-195.

[115] Daikhin, L. and Urbakh, M. (1997). "Influence of surface roughness on the quartz crystal microbalance response in a solution. New configuration for QCM studies." *Faraday discuss* **107**: 000-000.

[116] Urbakh, M. and Daikhin, L. (1998). "Surface morphology and the quartz crystal microbalance response in liquids." *Colloids and Surfaces A: Physicochemical and Engineering Aspects* **134** (1-2): 75-84.

[117] Daikhin, L., Gileadi, E., Katz, G., Tsionsky, V., Urbakh, M. and Zagidulin, D. (2002). "Influence of roughness on the admittance of the quartz crystal microbalance immersed in liquids." *Analytical Chemistry* **74** (3): 554-561.

[118] Martin, S. J. (1997). "Closing remarks." *Faraday discussions* **107**: 463-476.

[119] Rajakovic, L. V., Cavic-Vlasak, B. A., Ghaemmaghami, V., Kallury, K. M. R., Kipling, A. L. and Thompson, M. (1991). "Mediation of acoustic energy transmission from acoustic wave sensors to the liquid phase by interfacial viscosity." *Analytical Chemistry* **63**: 615-621.

[120] Duncan-Hewitt, W. C. and Thompson, M. (1992). "Four-layer theory for the acoustic shear wave sensor in liquids incorporating interfacial slip and liquid structure." *Analytical Chemistry* **64**: 94-105.

[121] Ghafouri, S. and Thompson, M. (2000). "Interfacial properties and the response of the transverse acoustic wave device in electrolytes." *Electroanalysis* **12** (5): 326-336.

[122] Thompson, M., Nisman, R., Hayward, G. L., Sindi, H., Stevenson, A. C. and Lowe, C. R. (2000). "Surface energy and the response of transverse acoustic wave devices in liquids." *Analyst* **125** (9): 1525-1528.

[123] EerNisse, E. P. (1984). "Stress effects in quartz crystal microbalances". in *"Applications of piezoelectric quartz crystal micobalances"*. C. Lu and A. W. Czanderna. Oxford, Elsevier. **7**: 125-194.

[124] Heusler, K., Grzegorzewski, A., Jäckel, L. and Pietrucha, J. (1988). "Measurement of mass and surface stress at one electrode of a quartz oscillator." *Berichte der Bunsengellschaft fur Physikalische Chemie* **92**: 1218-1225.

[125] Lucklum, R., Behling, C., Cernosek, R. W. and Martin, S. J. (1997). "Determination of complex shear modulus with thickness shear mode resonators." *Journal of physics D: Applied Physics* **30**: 346-356.

[126] Martin, S. J., Bandey, H. L., Cernosek, R. W., Hillman, A. R. and Brown, M. J. (2000). "Equivalent-circuit model for the thickness-shear mode resonator with a viscoelastic film near film resonance." *Analytical Chemistry* **72** (1): 141-149.

[127] Höök, F., Rodahl, M., Keller, C., Glasmästar, K., Fredriksson, C., Dahlqvist, P. and Kasemo, B. (1999). *"The dissipative QCM-D Technique: Interfacial phenomena and sensor applications for proteins, biomembranes, living cells and polymers."*. Proceedings of Joint Meeting of European Frequency and Time Forum and the 1999 IEEE International Frequency Control Symposium, Besancon, France, IEEE.

[128] Su, H. B. and Thompson, M. (1995). "Kinetics of interfacial nucleic-acid hybridization studied by acoustic network analysis." *Biosensors & Bioelectronics* **10** (3-4): 329-340.

[129] Calvo, E. J. and Etchenique, R. J. (1997). "Electrochemical quartz crystal impedance study of redox hydrogel mediators for amperometric enzyme electrodes." *Analytical chemistry* **69** (23): 4833-4841.

[130] Bandey, H. L., Hillman, A. R., Brown, M. J. and Martin, S. J. (1997). "Viscoelastic characterization of electroactive polymer films at the electrode/solution interface." *Faraday Discussions* **107**: 105-121.

[131] Reason, M., Teesdale-Spittle, P., Latham, R., Dawson, G., Porteous, P. and Smith, G. (2001). "A TSM sensor investigation of low crystallinity cellulose films." *International Journal of Pharmaceutics* **222** (1): 121-128.

[132] Crane, R. and Fischer, G. (1979). "Analysis of a quartz crystal microbalance with coatings of finite viscosty." *Journal of Physics D: Applied Physics* **12**: 2010-2026.

[133] Rosenbaum, J. (1988). *"Bulk acoustic wave theory and devices"*. Boston, Artech house.

[134] Wang, J., Yu, J.-d., Yong, Y.-K. and Imai, T. (2000). "A new theory for electroded piezoelectric plates and its finite element application for the forced vibrations of quartz resonators." *International Journal of soloids and structures* **37**: 5653-5673.

[135] Dye, D. (1926). "The piezoelectric quartz resonator and its equivalent electrical circuit." *Proceedings of the Physics Society* **38**: 399-458.

[136] Butterworth, S. (1915). "On electrically-maintained vibrations." *Proceedings of the Physics Society* **27**: 410-424.

[137] van Dyke, K. (1922). "The piezo-electric circuit and it's equivalent circuit." *Proceedings I.R.E.* **10** (83): 742-764.

[138] Bottom, V. E. (1982). *"Introduction to Quartz Crystal Unit Design"*. New York, Van Nostrand Reinhold Company.

[139] Hillman, A. R., Jackson, A. and Martin, S. J. (2001). "The problem of uniqueness of fit for viscoelastic films on thickness-shear mode resonator surfaces." *Analytical Chemistry* **73** (3): 540-549.

[140] Rodahl, M., Höök, F., Fredriksson, C., Keller, C., Krozer, A., Brzezinski, P., Voinova, M. and Kasemo, B. (1997). "Simultaneous frequency and dissipation factor QCM measurements of biomolecular adsorption and cell adhension." *Faraday discuss* **107**: 000-000.

[141] http:\\www.q-sense.com

[142] (1994). *"Crystal product data book"*. Crewkerne, International Quartz Devices Limited.

[143] Ha, T. H., Kim, D. K., Choi, M. U. and Kim, K. (2000). "Influence of poly(ethylenimine) on the monolayer of oleic acid at the air/water interface." *Journal of Colloid and Interface Science* **226** (1): 98-104.

[144] Okahata, Y. and Ebara, Y. (1992). "Observation of phospholipase A_2 activity towards the hydrolysis of phospholipid Langmuir-Blodgett films deposited on a quartz crystal microbalnce." *J. Chem. Soc. Chem. Commun.*: 116-117.

[145] Okahata, Y., En-na, G. and Ebato, H. (1990). "Synthetic chemoreceptive membranes. Sensing bitter or odorous substances on a synthetic lipid multibilayer film by using quartz-crystal microbalances and electric responses." *Analytical Chemistry* **62** (14): 1431-1438.

[146] Okahata, Y. and Ebato, H. (1991). "Absorption behaviours of surfactant molecules on a lipid-coated quartz-crystal microbalance. An alternative to eye-irritant tests." *Analytical Chemistry* **63**: 203-207.

[147] Ding, L., Li, J. H., Dong, S. J. and Wang, E. K. (1996). "Supported phospholipid membranes: Comparison among different deposition methods for a phospholipid monolayer." *Journal of Electroanalytical Chemistry* **416** (1-2): 105-112.

[148] Schierbaum, K. D., Weiss, T., Thoden van Velzen, E. U., Engbersen, J. F. J., Reinhoudt, D. N. and Gopel, W. (1994). "Molecular recognition by self assembled monolayers of cavitand receptors." *Science* **265**: 1413-1415.

[149] Matsuura, K., Ebara, Y. and Okahata, Y. (1996). "Guest selective adsorption from the gas phase onto a functional self-assembled monolayer on a super-sensitive quartz-crystal microbalance." *Thin Solid Films* **273**: 61-65.

[150] Walter, A. (1990). "Membrane solubilization with and reconstitution from surfactant solutions: a comparision of phosphatidylserine and phosphatidylcholine interactions with octyl glucoside." *Mol. Cell. Biochem.* **99**: 117-123.

[151] Giles, C. H., Forrester, S. D. and Roberts, G. G. (1990). "Historical Introduction". in *"Langmuir-Blodgett Films"*. G. Roberts. New York, Plenum Press: 1-15.

[152] Petty, M. C. (1996). *"Langmuir-Blodgett films. An introduction"*. Cambridge, Cambridge University Press.

[153] Okahata, Y., Kimura, K. and Ariga, K. (1989). "Detection of the phase transition of Langmuir-Blodgett films on a quartz crystal microbalance in a aqueous phase." *Journal of the American Chemical Society* **111** (26): 9190-9194.

[154] Okahata, Y. and Ebato, H. (1989). "Application of a quartz crystal microbalance for detection of phase transitions in liquid crystal and lipid multibilayers." *Analytical Chemistry* **61** (19): 2185-2188.

[155] Wotton, P. K., Mollgaard, B., Hadgraft, J. and Hoelgaard, A. (1985). "Vehicle effect on topical drug delivery. III. Effect of Azone on the cutaneous permeation of metronidazole and propylene glycol." *International journal of pharmaceutics* **24**: 19-26.

[156] Ramsden, J. (2003). "Development of a TSM biosensor for the determination of DNA-drug interactions: A novel method to assist drug development." (Thesis for *School of Pharmacy and Pharmaceutical Sciences*: De Montfort University, Leicester.

[157] Yao, S., Li, W., Su, X., zuo, X. and Wei, W. (1999). "A sensitive and specific method for isoniazid determination based on selective adsorption using an isoniazid ion-selective piezoelectric sensor." *Talanta* **50**: 469-480.

[158] Ebara, Y., Ebato, H., Ariga, K. and Yoshio., O. (1994). "Interactions of calcium ions with phospholipid membranes. Studies on pi-A isoththerms and electrochemical and quartz-crystal microbalance measurements." *Langmuir* **10** (7): 2267-2271.

[159] Ding, L., Li, J. H., Wang, E. K. and Dong, S. J. (1997). "K+ sensors based on supported alkanethiol/phospholipid bilayers." *Thin Solid Films* **293** (1-2): 153-158.

[160] Okahata, Y., Ebara, Y. and Sato, T. (1995). "The quartz-crystal-microbalance study of protein binding on lipid monolayers at the air-water interface." *Mrs Bulletin* **20**: 52-56.

[161] Ebara, Y. and Okahata, Y. (1993). "In situ surface detecting technique by using a quartz crystal microbalance. Interactions behaviors of protiens onto a phospholipid monolayer at the air water interface." *Langmuir* **9** (2): 574-576.

[162] Rodahl, M., Hook, F., Fredriksson, C., Keller, C., Krozer, A., Brzezinski, P., Voinova, M. and Kasemo, B. (1997). "Simultaneous frequency and dissipation factor QCM measurements of bimolecular adsorption and cell adhesion." *Faraday Discussions* **107**: 229-246.

[163] Höök, F., Rodahl, M., Keller, C., Glasmästar, K., Fredriksson, C., Dahlqvist, P. and Kasemo, B. (1999). *"The dissipative QCM-D Technique: Interfacial phenomena and sensor applications for proteins, biomembranes, living cells and polymers."*. Proceedings of Joint Meeting of European Frequency and Time Forum and the 1999 IEEE International Frequency Control Symposium, Besancon, France, IEEE.

[164] Okahata, Y. and Ye, X. (1989). "Molecular selective associations of cyclodextrins with lipid or cholesterol multibilayers cast on a piezoelectric crystal." *Journal of chemical society,chemical community*: 1147-1149.

[165] Okahata, Y., Ebato, H. and Ye, X. (1988). "Molecular selective adsorption on a multibilayer-coated piezoeletric crystal." *J. Chem. Soc., Chem. Commun*: 1037-1038.

[166] Okahata, Y., Ebato, H. and Taguchi, K. (1987). "Specific adsorption of bitter substances on lipid bilayer-coated piezoelectric crystals." *Journal of chemical society, chemical community*: 1363-1365.

[167] Okahata, Y. and Shimizu, O. (1987). "Olfactory reception on a multibilayer coated piezoelectric crystal in a gas phase." *Langmuir* **3**: 1171-1172.

[168] Abe, T. and Esashi, M. (2000). "One-chip multichannel quartz crystal microbalance (QCM) fabrication by Deep RIE." *Sensors and actuators* **82**: 139-143.